uOttawa

L'Université canadienne
Canada's university

FACULTÉ DES ÉTUDES SUPÉRIEURES ET POSTDOCTORALES

uOttawa

L'Université canadienne
Canada's university

FACULTY OF GRADUATE AND POSTDOCTORAL STUDIES

Hassan Zeineddine
AUTEUR DE LA THÈSE / AUTHOR OF THESIS

Ph.D. (Computer Science)
GRADE / DEGREE

School of Information Technology and Engineering
FACULTÉ, ÉCOLE, DÉPARTEMENT / FACULTY, SCHOOL, DEPARTMENT

Least Constraining Time-slot Allocation in GMPLS Optical TDM Networks and Optimization of Optical Buffering

TITRE DE LA THÈSE / TITLE OF THESIS

G. Bochmann
DIRECTEUR (DIRECTRICE) DE LA THÈSE / THESIS SUPERVISOR

CO-DIRECTEUR (CO-DIRECTRICE) DE LA THÈSE / THESIS CO-SUPERVISOR

EXAMINATEURS (EXAMINATRICES) DE LA THÈSE / THESIS EXAMINERS

M. Barbeau

T. Hall

A. Boukerche

T. Szymanski

Gary W. Slater
Le Doyen de la Faculté des études supérieures et postdoctorales / Dean of the Faculty of Graduate and Postdoctoral Studies

Least Constraining Time-Slot Allocation in GMPLS Optical TDM Networks and Optimization of Optical Buffering

Hassan Zeineddine

Thesis submitted to the
Faculty of Graduate and Postdoctoral Studies
in partial fulfillment of the requirements
for the PhD degree in

Computer Science

Ottawa-Carleton Institute for Computer Science
School of Information Technology and Engineering
Faculty of Engineering
University of Ottawa

Your file Votre référence
ISBN: 978-0-494-61235-4
Our file Notre référence
ISBN: 978-0-494-61235-4

Abstract

Optical Time Division Multiplexing (OTDM) in optical networks is a bandwidth sharing technique that organizes access to a shared wavelength in equal time-slots organized in repeated frames. In this case, a transmission channel can be established at the time-slot level instead of using the full wavelength. The main advantage of this technique is to allow several low speed communication channels to coexist on the same high speed optical wavelength, and hence to make effective use of the enormous bandwidth available on a single wavelength. On the other hand, the major problem with OTDM is the time slot continuity constraint in an OTDM channel, which is similar to the wavelength continuity in a WDM channel. Due to this constraint, time slot contentions can exist in the network if proper scheduling and slot reservation techniques are not employed. Basically, the adopted time slots must be free on all links throughout the communication route in order to successfully reserve a communication channel. In addition, to mitigate the effect of slot continuity constraint on bandwidth utilization, appropriate time slot buffering (or interchanging) is often employed. Previous work assumed the deployment of Optical Time-Slot Interchangers (OTSI) to solve the contention problems regardless of their industrial feasibility. In addition, other work considered very basic reservation schemes to achieve proper scheduling, such as the First Fit (FF), Random Fit (RF), and Least Loaded (LL) schemes. In this thesis, we propose a new time-slot reservation scheme for OTDM networks without buffering to significantly improve the performance and eliminate the buffering overhead. It is the Least Constraining (LC) slot reservation scheme which allocates resources having the lowest possible constraints on other resources in the network. In addition, we define a distributed scheme to deploy the LC approach in GMPLS networks, and prove that the same performance level can be maintained by a distributed signaling protocol. Finally, we propose an optimized optical buffering technique to achieve close to optimum performance when the LC reservation approach is not used. It helps in building effective time slot synchronization devices used between adjacent node pairs.

Table of Contents

LIST OF FIGURES

LIST OF TABLES

ACRONYM

CRA	*Conflict Resolution Algorithm*
CR-DP	*Constraint-Based Routing LDP*
CRSL	*Common Route-Slots List*
ESP	*Expanded Shortest-Path*
FDL	*Fiber Delay Line*
FF	*First Fit*
GMPLS	*Generalized Multi-Protocol Label Switching*
IS-IS	*Intermediate System to Intermediate System*
LAN	*Local Area Network*
LC	*Least Constraint*
LDP	*Label Distribution Protocol*
LER	*Labeled Edge Router*
LIL	*Links Info List*
LL	*Least Loaded*
LSAL	*Link-Slot Availability List*
LSIL	*Link-Slots Info List*
LSP	*Label Switched Path*
LSR	*Label Switched Router*
MAN	*Metropolitan Area Network*
MCS	*Minimum-Cost Search*
MPLS	*Multi-Protocol Label Switching*
OBS	*Optical Burst Switching*
OPS	*Optical Packet Switching*
OSPF	*Open Shortest Path First*
OTSI	*Optical Time-Slot Interchanger*
PIM	*Parallel Iterative Matching*
POTSI	*Passive Optical-Time Slot Interchanger*
POTSI-LR	*Limited Range Optical-Time Slot Interchanger*
QBvN	*Quick Birkhoff-von Neumann*
RF	*Random Fit*
RSCL	*Route-Slot Constraint List*
RSVP	*Resource Reservation Protocol*
RSVP-TE	*RSVP with Traffic Engineering*
RWTA	*Routing, Wavelength and Time-slot Assignment*
SABCA	*Slot Assignment Based on Capacity Allocation*
SABPA	*Slot Assignment Based on Packet Arrival*
TDM	*Time Division Mutliplexing*
TWIN	*Time-domain Wavelength Interleaved Networking*
TWIN-WR	*TWIN with Wavelength Reuse*
WAN	*Wide Area Network*
WDM	*Wavelength Division Multiplexing*

ACKNOWLEDGMENTS

"And We have enjoined upon man concerning his parents - His mother beareth him in weakness upon weakness, and his weaning is in two years - Give thanks unto Me and unto thy parents. Unto Me is the journeying." (Quraan 31\14). الشكر لك يا ربه

This written thesis is the harvest of many years of research and investigations. I definitely would not be writing the acknowledgements paragraph without the support of my supervisor Dr. Gregor v. Bochmann. I am extremely blessed to work with such a shrewd thinker and critical observer who enriched this work with his valuable comments and guidance. I would also like to thank my thesis committee members for their time spent reading and discussing this work.

My indescribable gratitude is to my Mom (hajja Mariam) and Dad (hajj Fadl) for seeding the stamina for knowledge in me. They are my reason for being and hence I owe them my accomplishments in life including this work.

All thanks goes to my beloved wife Manal. Her patience and support throughout my years of study were priceless. No matter what I do in return would not equally reward her. I know that her understanding and help were unconditional; however, maybe if I do the dishes for a few days, I could settle the score!! I should not forget to thank my two little daughters Aya and Zeinab for being my joy and stress busters.

I would also like to thank my parent in-laws for making life easier on me with their much appreciated help in various aspects of my day to day living.

Finally, I express my gratitude to each and every member of my family and in-laws for their encouragements and faith in me. In addition, I shall thank all my friends for their support.

1. Introduction

With the massive deployment of Wavelength Division Multiplexing (WDM) systems [Ramaswami2002], researchers have shown increased interests in studying the question of wavelength sharing. As the transmission capacity over a single wavelength is in the order of *10* Gigabits per second (Gbs), the resulting bandwidth has exceeded the aggregated traffic load of many source nodes. Thus, dedicating one wavelength for a single end-to-end connection with low load is like shipping a small envelop with an empty plane; that is., only a slim share of the bandwidth is being utilized while the rest remains untapped. To maximize bandwidth utilization, researchers worked under three major research streams focused on wavelength sharing: Optical Packet Switching (OPS), Optical Burst Switching (OBS), and Optical Time Division Multiplexing (OTDM).

Optical packet switching is achieved in an optical network by switching optical traffic units (packets) in the optical layer without opto-electronic conversion [Blumenthal1994, Yao2000, Pattayina2000]. Each packet must carry its addressing information in a header. Intermediate nodes are supposed to read the header, decide the next node in the corresponding route, and configure its cross-connect switch accordingly in a relatively short period of time. They should also be capable of storing contending packets in optical buffers. In fact, the header processing speed and optical buffering are two major challenges facing the realization of OPS. No matter how fast the header processing speed gets, it remains bound to the electronic speed; and hence, it is way too slow compared to the optical speed. In addition, optical buffering is still immature to handle randomized access. It seems that the road is still long before reaching the OPS goal.

While waiting for a breakthrough in OPS, Optical Burst Switching [Turner1999, Qiao1999, Vokkarane2003] seems to offer an interim solution. With OBS, a burst of traffic containing several packets is aggregated electronically at the source node before being sent optically in the network. It is an attempt to benefit from electronic buffering at the source before sending traffic through the optical network. In addition, the packet header is

replaced with a control header that travels ahead of time on a separate control channel. The control header is used to reserve resources on intermediate switches for a limited period, enough to forward the corresponding traffic burst. If a network resource happens to be busy or faulty, the burst is dropped. Clearly, a major disadvantage of OBS is the steep increase in packet loss as the traffic load gets higher. Several enhancements were introduced to reduce contention and improve loss ratio. Deflection routing, wavelength conversion, and optical buffering are the main contention resolution techniques [Maach2004].

Another candidate for filling the time gap between now and the emergence of OPS is Optical Time Division Multiplexing (OTDM) [Liew2003]. It reduces the granularity of traffic segments traveling in the network, maximizes bandwidth utilization, and reduces contention by proper scheduling. OTDM allows several connections to coexist on the same wavelength in a repeating frame of N time slots. Similar to the wavelength continuity constraint in wavelength routed networks, time slot continuity is essential in OTDM networks. To mitigate the effect of the slot continuity constraint on bandwidth utilization, appropriate time slot buffering (or interchanging) is described in the literature.

1.1. Problem Statement

Most of the optical time slot allocation schemes found in the literature are based on the First Fit or Random Fit allocation schemes [Zang1999, Zang2000, Huang2000, Liew2003, Maach2004, Yates2004, Wen2005, Yang2007a, Yang2007b]. Just one single work [Wen2005] adopted the Least Loaded scheme. In this thesis, we propose a new bandwidth allocation scheme to improve network performance in OTDM networks to a level close to optimum. We also define a distributed scheme for practical deployment of the new solution in a GMPLS network while maintaining the same improvement of performance. Although, the proposed solution should eliminate the need for optical buffering as it yields close to optimal performance, we also propose a new optimized optical buffering technique and related switch architecture.

1.2. Motivation and objectives

Motivated by the goal to find a slot allocation solution in OTDM networks that improves performance to a level close to optimum, we designed a scheme that reserves bandwidth resources having the least constraints on other dependent resources. It is what we call the Least Constraining (LC) slot allocation technique, where the slot constraint is measured by the number of available transmission channels on the fixed routes that can use this slot at a given point in time. In addition, influenced by the GMPLS protocol for optical networks [Colle2003, RFC3945], we define a distributed scheme to deploy the LC slot allocation technique in GMPLS networks. We focus on the resource state update aspect of the distributed scheme as it is a key factor for network scalability and compatibility with GMPLS. Although, the LC allocation approach should eliminate the need for buffering as a means to enhance performance, we propose an optimized buffering technique and corresponding switch architecture in optical TDM networks. We also describe the possible usage of the optimized buffering technique to synchronize transmission between two adjacent nodes (connected by a direct link).

1.3. List of Contributions

We identify the following items as the main contributions discussed in this thesis:

1. The Least Constraining Slot Allocation Scheme – which provides a performance close to the optimal performance achieved with full buffering at each node – in Chapter 3.
2. The Distributed Least Constraining Slot Allocation Scheme – an approach to deploy the LC scheme in a GMPLS environment while maintaining close to optimum performance – in Chapter 4.
3. Several variations of the LC scheme and their comparison – to identify the variant that achieves the best performance – in Chapter 5.

4. Limited Range Passive Optical Time Slot Interchanger – a novel optimized optical buffering technique which provides the same performance achieved with traditional OTSI – in Chapter 6.
5. Shared Passive OTSI architecture – a novel OTDM switch architecture based on a pool of shared OTSIs instead of a dedicated OTSI per input line as known in the literature – described in Chapter 6.
6. Interleaved Passive OTSI in OTDM networks – a novel proposal to interleave OTSIs among network nodes instead of deploying these buffering devices at each node – in Chapter 6.
7. Effective slot synchronization technique based on the Passive OTSI architecture – a new solution for the synchronization problem between two adjacent nodes in an OTDM network – in Chapter 6.

1.4. Outline

The thesis is made of 7 chapters and is structured as follows:

- Chapter 1 is the introduction.
- Chapter 2 provides a literature review of the technologies being investigated or adopted, namely OTDM network components, time slot reservation schemes, and GMPLS.
- Chapter 3 introduces the novel Least Constraining Slot Allocation scheme, which achieves a performance close to the optimal performance achieved with full buffering at each node. Simulation results, backed by analytical discussion, are used to measure the network performance under various topologies and different routing approaches.
- Chapter 4 discusses the deployment of the LC scheme in a GMPLS network. It describes a distributed algorithm for resource reservation; however, the focus is on minimizing the rate of status updates, which has a major impact on scalability and compatibility with GMPLS.
- Chapter 5 lists and compares 3 different variations of the original LC approach. It identifies the variation that achieves the best network performance.

- Chapter 6 proposes an optimized optical time slot interchanging technique based on the Passive OTSI architecture described in a previous work [Maach2004]. It studies the effect of reducing the range and number of OTSIs in the network in terms of performance. In addition, it describes the effective usage of Passive OTSI as synchronizing devices between two adjacent nodes in an OTDM network.
- Chapter 7 concludes the thesis by summarizing the characteristics and achieved results of each contribution. It also discusses potential future extensions to investigate some topics that are not covered in this work.

2. Background

In this chapter, we review the major aspects of OTDM with special emphasis on slot scheduling schemes. The content is organized in the following order: OTDM networks, OTDM switch architectures, optical time slot interchangers, slot reservation schemes, and a brief introduction to MPLS.

2.1. OTDM Network Architecture

As we briefly described in the introduction, the OTDM technique multiplexes low rate traffic streams in frames of N time slots over a high speed wavelength. I.e., up to N different streams can be carried over a single wavelength. Each stream is assigned one time slot in a frame over a given wavelength. Note that a connection can use multiple streams [Liew2003]. The stream bandwidth in the network is $\frac{1}{N}$ of the wavelength bandwidth. For example, if a frame is made of *1000* time slots and the wavelength speed is *10* Gbps, then the stream bandwidth is *10* Mbps. Figure (2.1) is a graphical example of an optical TDM network.

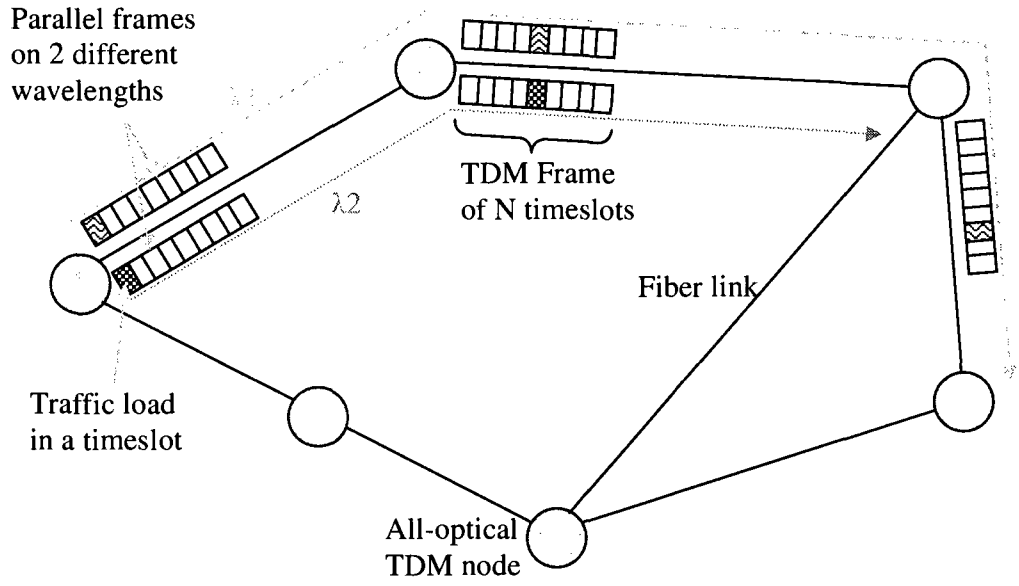

Figure 2.1: Example of an OTDM mesh network

OTDM networks fall under two major categories, mesh and star. In an OTDM mesh network, every node is equipped with an optical cross-connect that maps inputs to outputs according to a defined schedule. The schedule is updated according to the employed slot reservation scheme. It reflects the switching pattern for a time slot period, when traffic segments entering the switch are switched to the corresponding output. It is essential that all traffic segments within a slot period reach the cross-connect right at the beginning of a new time slot. In addition, the cross-connect must transition to the next state right before the start of a new time slot.

To achieve synchronization between segments arrival and switch state during a time slot, several solutions were introduced in the literature: 1- clock alignment plus precise fiber cut, and 2- use of input synchronizers.

For the first approach, all nodal clocks are synchronized to advance simultaneously from one slot to another. This can be achieved by broadcasting a clock signal from a central station to all nodes so that they can adjust their clock accordingly. In addition, all fibers

between adjacent nodes must be carefully cut to round up the propagation delay to the nearest integer in order to attain slot boundary alignment. In this case, a transmitted traffic segment is always guaranteed to reach the next cross-connect on a route at the start of a time slot. A slight slot misalignment might arise due to inaccurate fiber cutting, minor clock difference, or changing propagation delays due to temperature changes. This imperfection can be solved by defining an offset period as a guard time at each slot as shown in Figure (2.2). In addition to slot misalignment, the guard time must account for the cross-connect reconfiguration time when transitioning from one slot to another. The remaining part of a time slot would be the effective bandwidth that carries the traffic segments. For example, if the maximum tolerated error in fiber cutting is 10m and the switch reconfiguration time is $0.05\mu s$ the guard time must be $10/(2 \times 10^{8})$s + 0.05μs = 0.05μs + 0.05μs = 0.1μs, which is 1% of a 10μs time slot. To eliminate the configuration time from the formula, a switch architecture with two parallel-planes is required. When one switching plane is handling traffic, the other would be reconfiguring to be ready for traffic at the next time slot, and vice versa. Note that the slot time must be larger or equal to the reconfiguration time.

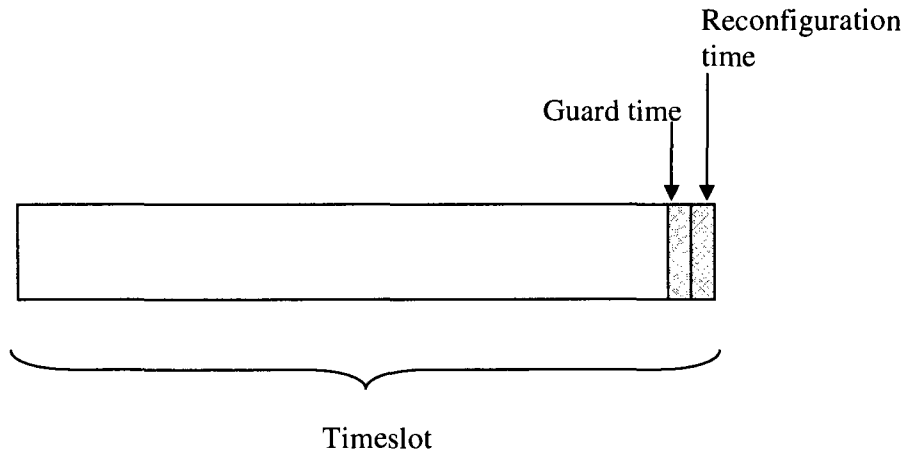

Figure 2.2: Time slot's graphical description

As for the second synchronization approach, special all-optical devices known as synchronizers are deployed at every switch's input [Ramamirtham2003]. A synchronizer delays incoming traffic by a pre-calculated period to offset the lag caused by clocks difference and propagation delays. Details are described in Section 2.3.

A Photonic Slot Routing mesh network is one of the OTDM network architectures described in the literature [Zang2000] and [Zang1999]. In this approach, packets going to the same destination and traveling on different wavelengths during a common time slot are treated as an integral unit at intermediate switches. In this case, there is no need to de-multiplex and multiplex wavelengths at intermediate nodes along the route to its destination. Multiplexing and de-multiplexing are only required when the packet is submitted or received. In addition, intermediate nodes can transmit traffic to a given destination node D on a free wavelength λ during a photonic slot t if the traffic unit in t is headed to node D.

In [Widjaja2004], the Time-domain Wavelength Interleaved Networking (TWIN) was introduced. The TWIN architecture provides time-shared connectivity using static switches and dynamic tunable transmitters. Each node is assigned a unique wavelength on which it would receive incoming traffic. In addition, all nodes are pre-configured to switch every wavelength to its assigned node. See Figure (2.3) for details. In this case, if a node S has to send traffic to node D, it tunes its transmitter to the wavelength assigned to D, and starts transmitting at a given time slot. Dynamic signaling and fast switching are not required to reconfigure intermediate nodes since all intermediate resources are statically allocated to lead the traffic to node D. The major limitation with this architecture is scalability. A network cannot include a number of nodes that exceeds the available number of supported wavelengths. In addition, a wavelength bandwidth is not efficiently utilized especially when a destination is not receiving traffic from any source.

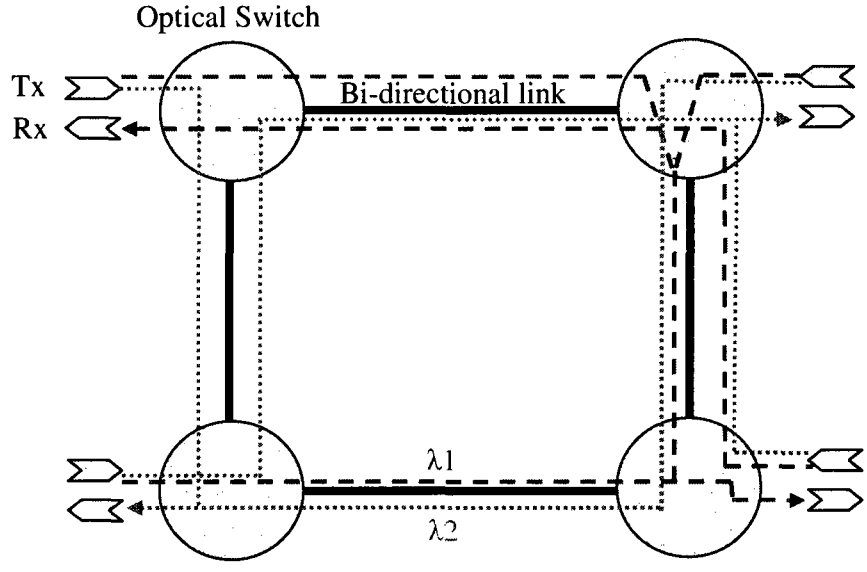

Figure 2.3: An optical network based on the TWIN architecture

To support larger networks and make better use of the bandwidth, an enhanced version of TWIN with wavelength reuse (TWIN-WR) was proposed in [Nuzman2006]. Basically, TWIN-WR suggests re-using a wavelength in network areas where it is not utilized. The authors described the basic TWIN connection between two nodes without wavelength reuse as single hop although these nodes might be interconnected by several links. Their concept of a hop is a direct line of light between two nodes without opto-electronic or optical switching. On the other hand, they see a TWIN-WR connection as a sequence of one or more basic TWIN connections between a source destination pair, i.e. a multi-hop connection. Nuzman et al. assumed a form of traffic relay is in place at each node to achieve bridging between hops. With this, they were able to support a network of N nodes with roughly $\sqrt{N}$ wavelengths.

In [Bochmann2004], an OTDM star network was proposed. In this network, the core node has an active all-optical cross-connect that is configured at each time slot based on a given schedule. Edge nodes are connected to the core, and equipped with transceivers to send and receive traffic segments through the core. A graphical example is shown is Figure (2.4). In

this network, accurate clock synchronization is easily attainable by careful coordination between the edge nodes and the core node. Basically, the edge node clock must be shifted to complement the propagation delay from the edge to the core so that all traffic segments reaching the core are aligned at the frame boundaries.

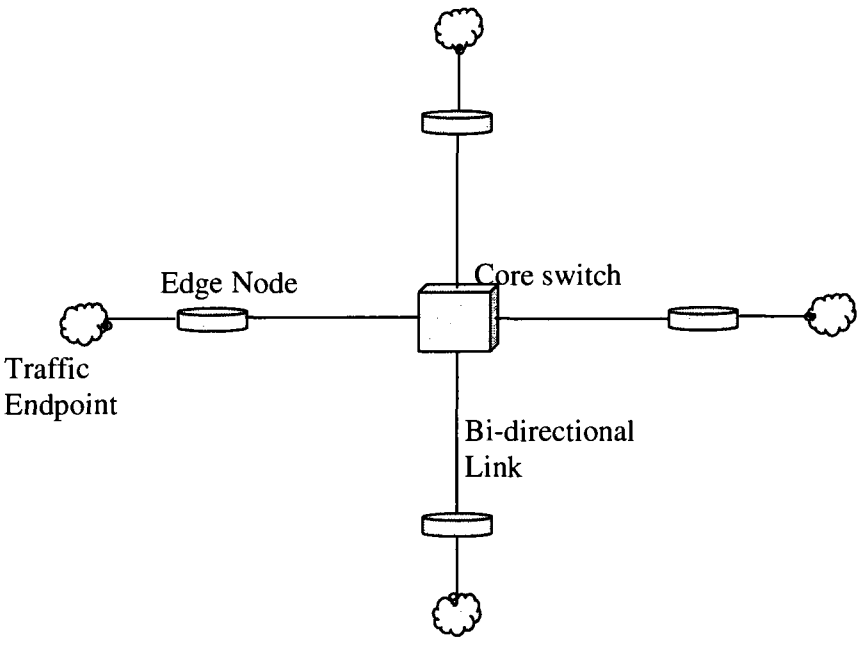

Figure 2.4: All-optical star network architecture

2.2. OTDM Node Architecture

The core component in an OTDM node is its optical cross-connect switch. Since the switch internal architecture is beyond the scope of our thesis, we describe its functionality from a black box perspective. An M x N optical cross-connect switch has M inputs and N outputs. It maps inputs to outputs; and the resulting pattern is called the switch state. A switch state can be fixed (static scheduling) or staggering (dynamic scheduling). Static scheduling is a by-product of static bandwidth allocation where the same switch state is maintained for an entire network session. On the other hand, dynamic scheduling is required to achieve dynamic bandwidth allocation where the switch state must change over the life time of a network session. State variation is essential in achieving time sharing of a link or

wavelength bandwidth. OPS, OBS, and OTDM are applications of time sharing. With OPS and OBS, the switch state is supposed to change at varying time intervals depending on the arriving packet and burst sizes. Meanwhile with OTDM, the switch state changes at a regular time interval equal to the time slot duration.

The switch state is controlled by an electronic management component called Controller. The controller maintains the scheduling information and clock synchronization, and handles all the essential signaling with adjacent nodes. It communicates with the cross-connect and other components through special interface units.

Additional components can be added at the input or output of a cross-connect switch to maximize network performance such as the Optical Time Slot Interchangers (OTSI) and the time slot Synchronizer (SYNC). We go through the OTSI architecture in detail in the following section. For now, we define OTSI as an all-optical device that takes an OTDM frame as input and permutes the time slot contents within the defined frame. They are employed to avoid contention resulting from traffic segments arriving from different inputs and heading to the same output at the same time slot. In the literature, OTSIs have always been used at the input side [Ramamirtham2003] of the switch until we proposed placing them at the output side [Maach2004]. Our proposal eliminates the blocking caused by traffic segments arriving at two consecutive time slots on the same input and that need to be switched to two different outputs, but at the same time slot.

A Synchronizer is always placed at the input side of a switch and delays an incoming optical signal by a fraction of a time slot. It aligns the incoming traffic segments to the switch's time slot boundaries. The Synchronizer's delay should vary based on the incoming link propagation delay. It achieves this functionality by repeatedly switching the incoming signal to fiber loops of various lengths before outputting that signal to the cross-connect switch. It is in that sense similar to the OTSI architecture that we review in the following section. For an example of OTDM switch architecture, see Figure (2.5). Note that the de-multiplexers at the input side are embedded inside the OTSI devices.

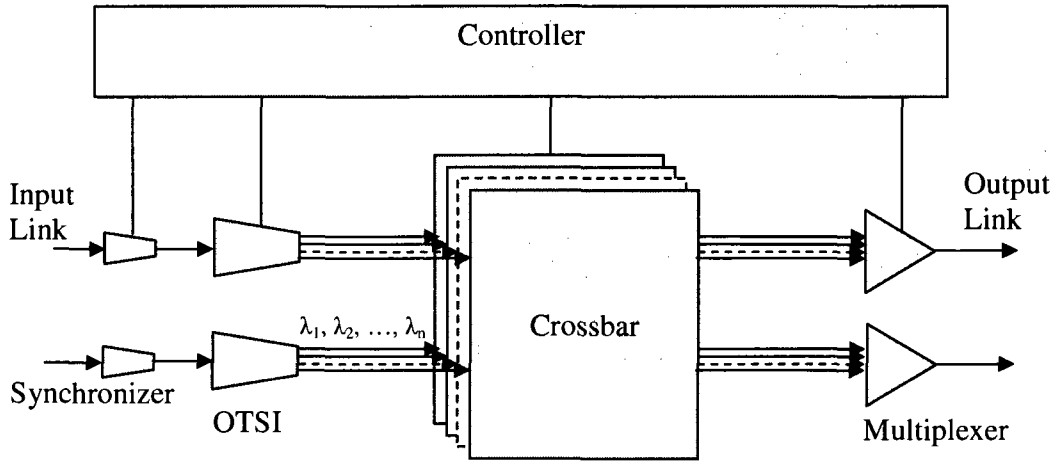

Figure 2.5: An OTDM switch architecture

2.3. Architecture of Optical Time Slot Interchangers

The OTSI was investigated in the literature as a possible solution for time slot contention [Ramamirtham2003, Maach2004, Wang2006]. An OTSI serves as an optical component that switches between time slots. The OTSI is made of an optical crossbar and a number of variable size fiber delay lines (FDL). Each FDL starts from and ends at the optical crossbar; it delays an optical signal by multiples of time slots. When a traffic segment in a time slot enters an OTSI, it gets circulated through an appropriate selection of delay lines, before exiting the interchanger in another time slot.

The three basic characteristics that would affect the cost and performance of an OTSI are the size of its internal crossbar, the total length of delay lines, and the number of switching operations to achieve one slot interchanging task. In [Ramamirtham2003], the authors compared the characteristics of several types of OTSIs based on the crossbar size, fiber

length, and number of switching operations. Table (2.1) features the result of this comparison.

OTSIs are classified under two categories: blocking and non-blocking. A non-blocking OTSI, having a crossbar size of $N+1 \times N+1$, is made of N delay lines, each of a length corresponding to *one* time slot. To delay a traffic segment arriving on time slot j by a period of d time slots, the traffic at slot j gets re-circulated/switched d times in the j^{th} delay line before being switched out. To reduce the number of required switching operations to just 2, an OTSI made of $N-1$ delay lines of sizes $1, 2, \ldots, N-1$, respectively, can be adopted; see Figure (2.6). A more practical approach, which cuts on fiber length, is to use a set of delay lines of sizes $1, 2, \ldots, A$, with another set of lines of sizes $2A, 3A, \ldots, (B-1)A$, where A and B are integer values. In the last two approaches, the number of switching operations was reduced to a maximum of *three* at the expense of a longer fiber length. A re-arrangeably non-blocking OTSI, made of *two* sets of fiber lines of size $1, 2, 4, \ldots, N/4$, and a single fiber line of size $N/2$, minimizes the crossbar size and total fiber length in the non-blocking category. As a further improvement, a blocking OTSI, made of $N/2$ fiber lines of sizes $1, 2, \ldots, N/2$, reduces the fiber length and crossbar size to $N/2$ and $log_2N \times log_2N$, respectively. Note that an OTSI device is non-blocking based on the following definition: a non-blocking interchanger is always capable of delaying two different time slots i and j by d_i and d_j as long as $i + d_i \neq j + d_j$.

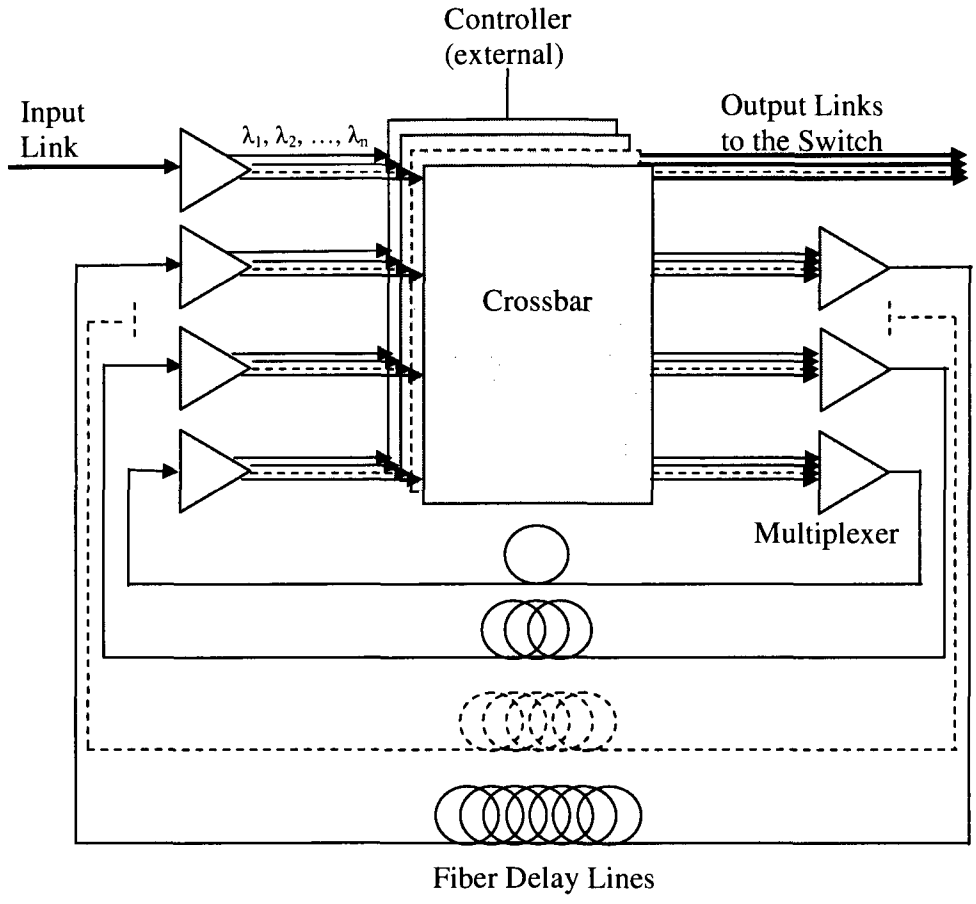

Figure 2.6: Internal architecture of a 1,2, ..., N-1 OTSI

In [Maach2004], we proposed the Passive OTSI (POTSI), which is made of a multi-input queue of N sequentially connected fiber delay lines, and an optical crossbar connected to the N inputs of the queue; see Figure (2.7). The delay imposed by every FDL is exactly equal to one time slot period. To delay a traffic segment by a period of d time slots, the crossbar directs the traffic to the d^{th} FDL in the multi-input queue; from that point, traffic flows passively through d FDLs before reaching the output point of the queue. In this case, a traffic segment experiences a delay in the POTSI equal to $d \times T$, where T is the time slot period. The total length of the delay lines employed in the passive interchanger is a factor of N, and the number of needed switching per time slot is *one*. Furthermore, the size of the optical crossbar is $1 \times N$. A major concern with this architecture is the insertion loss caused by the coupling of the optical signal at each delay unit. To work around such

limitation, we need to interleave a few amplifiers among the FDLs depending on the loss ratio of optical couplers and fiber lines.

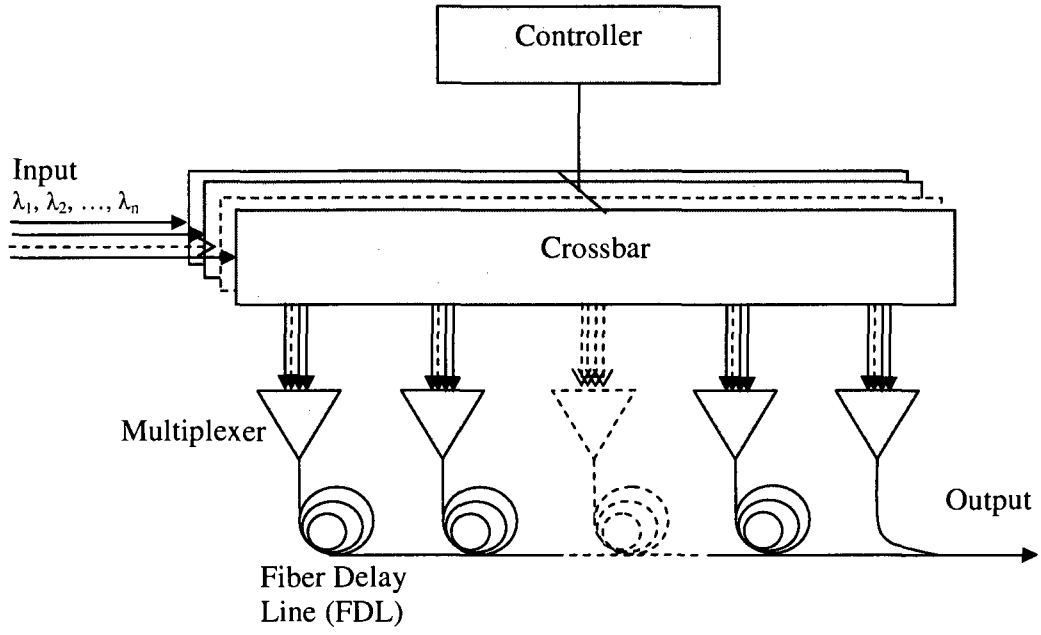

Figure 2.7: Internal architecture of a Passive OTSI

As shown in Table (2.1), it is evident that the POTSI provides the best number of switching operations, crossbar size and total fiber length.

OTSI Design described by number and size of FDLs	Crossbar Size	Fiber Length	Switching operations
N FDLs of size 1	$N+1 \times N+1$	N	N
$N-1$ FDLs of size $1, 2, \ldots, N-1$	$N \times N$	$N^2/2$	2
$2\sqrt{N}-1$ FDLs of size $1, \ldots, A, 2A, \ldots, (B-1)A$	$2\sqrt{N}-1 \times 2\sqrt{N}-1$	$N\sqrt{N}/2$	3
$2 \log_2 N$ FDLs of size $2 \times (1, 2, 4, \ldots, N/4), N/2$	$2 \log_2 N \times 2 \log_2 N$	$(3N/2) - 2$	$2(\log_2 N) - 1$
$\log_2 N$ FDLs of size $1, 2, 4, \ldots, N/2$	$\log_2 N \times \log_2 N$	$N-1$	Variable (3 for $N = 256$)

N-1 FDLs of size *1* (POTSI)	*1* × *N-1*	*N*	*1*

Table 2.1: Characteristics of various OTSI architectures

2.4 Optical Time Slot Reservation schemes

With the advent of OTDM technology, the question for optimized time slot reservation schemes emerged as an interesting research topic. The goal is to reduce buffering at intermediate nodes and improve network performance. Always under the assumption that time slot reservation is nothing but a fine granularity wavelength allocation, researchers gave lesser weight to the buffering in favor of network performance. This assumption holds true when considering either an optical TDM network with opto-electronic interfaces or an all-optical TDM network synchronized on frame boundaries. With frame boundary synchronization, each time slot can be treated as a unique wavelength at a finer granularity. As discussed earlier in section 2.1, careful clock alignment between core and edge nodes would achieve frame boundary synchronization in a star network. However, this type of synchronization in a mesh network requires expensive Synchronizers which have lengthy fiber delay lines at every input. Alternatively, slot boundary synchronization can be more feasible in mesh networks since it requires shorter delay lines opening the door for investigating appropriate slot reservation schemes.

2.4.1. Optical Time Slot Reservation Based on Frame Boundary Synchronization

In [Subramaniam2000], Subramaniam et al. studied the problem of assigning time slots and wavelengths to a given static set of multi-rate sessions in ring topologies. Their objective was to maximize throughput by minimizing the maximum length of a TDM

frame. They proved that the off-line single-rate session scheduling problem is equivalent to the off-line wavelength assignment problem, and hence obtained bounds on frame length similar to the bounds on the number of wavelengths. The authors concluded: "When the slots of a session have to be contiguous and on a single wavelength, we proved that our assignment scheme achieves a frame size that is at most three times the optimal size. On the other hand, when a session's slots need not be contiguous or on a single wavelength, then the scheduling algorithm achieves twice the optimal frame size." [Subramaniam2000]

In [Yates1999], Yates et al. stated that a network of W wavelengths and N time slots per frame is exactly equivalent to a wavelength routed network of $W \times N$ time slots with no TDM. They utilized the first-fit time slot (FFT) scheme as an enhancement over the random fit time slot (RFT) scheme. The main purpose of their paper was to examine the relative importance of wavelength conversion and time-slot interchange in reducing blocking, or increasing utilization, in the network. The authors relied on simulations and analysis in investigating these cases. They concluded that a TDM network with OTSI and WR network with wavelength conversion produce equivalent performance.

In [Huang2000], Huang et al. proposed a RWTA scheme based on a greedy approach. The algorithm tends to find a path with higher available bandwidth and less hops between a source destination pairs. It takes as input the list of connection requests, sorts it in ascending order based on the required bandwidth in terms of time slots, and finds paths for each slot in every request in the sorted list. A selected path P for a given slot must have the highest ratio F_p/h_p where F_p is the number of available free slots on P, and h_p is the number of hops in P. Afterwards, the first available time slot is chosen along the path. The clear limitation with this algorithm is its needs to know all connection requests at the start. In addition, this scheme works when the required bandwidth is known in advance as in time slotted OBS. The authors compare their work against a plain first-fit wavelength assignment scheme with no TDM. Obviously, they reported improvement in blocking probability mainly because of the time sharing of wavelengths.

In [Liu2005a], Liu et al. compared three slot scheduling algorithms in agile all-optical star networks: Round Robin Allocation, Parallel Iterative Matching (PIM), and Adapted PIM.

The Round robin allocation is based on a simple fixed configuration at the core switch. In a star network of N nodes, an edge node has the right to send traffic to the other $N-1$ edge nodes on different $N-1$ slots. No signaling is required in this case since the core switch is set to a predetermined configuration. However, the round robin method is bandwidth inefficient in the case of non-uniform traffic.

The PIM scheme is based on a random matching of input and output. Each unmatched input sends a request to every output for which it has traffic. If an unmatched output receives requests from multiple inputs, it randomly accepts and responds to one of these requests. If an input receives multiple responses from different outputs, it randomly chooses one output. PIM suffers from unfair resource allocations since it randomly allocates resources to arriving requests regardless of the traffic load.

The Adapted PIM scheme [Vinokurov2005] is an approach to mitigate the unfair allocation of resources. Unlike the regular PIM, an unmatched request is stored in a priority queue at the central controller instead of being repeatedly sent. This request would have priority over newly arriving requests in the next scheduling iteration. The longer the request stays in the priority queue due to repeated denial, the higher its priority gets. As for the delays associated with this approach, the authors proved by means of simulation that a grant is delayed for a small duration as compared to the propagation delay.

In [Saberi2004], Saberi and Coates developed the minimum-cost search frame scheduling algorithm (MCS). The algorithm takes a traffic demand matrix as input where each entry (i, j) represents the requested number of time slots in the next frame from source node i to destination node j. It then assigns the appropriate wavelengths and time slots for each source destination pair in the matrix. To reduce the signaling overhead and switch reconfiguration overhead when shifting from one frame to another, the algorithm ensures that scheduling is only modified for new requests and does not alter the mapping of

persistent connections. It also tries to schedule slots in a pattern that reduces the switching operations, and hence reduces power consumption. It favors the scheduling of most traffic segments between a given source-destination pair in contiguous time slots. It is noted that the proposed MCS scheme does not achieve optimal bandwidth utilization since it does not consider a global allocation approach. Instead, it loops through the traffic demand matrix entries and tries to allocate one slot per entry; after reaching the last entry, it starts the round robin allocation all over again. This method achieves fair slot assignment for each pair.

In [Liu2005b], Liu et al. conducted a comparison between the slot-by-slot scheduling noted in the Adapted PIM approach and the frame-by-frame scheduling noted in the MCS approach. They concluded: "For distances larger than this break-even value (approximately *600* km), frame-by-frame scheduling produces marginally smaller end-to-end delay than slot-by-slot scheduling. Thus frame-by frame is suitable for WANs. The reverse is true for smaller distances typical of MANs where the slot-by-slot protocol yields smaller delay values." [Liu2005b]

In [Peng2006], Peng et al. developed the Quick Birkhoff-von Neumann (QBvN) Decomposition Algorithm as a time slot allocation scheme in an all-optical star network. The time complexity of the proposed algorithm is in the order of $N \times n$ where N is the number of nodes and n is the number of time slots in a frame. The authors extend their scheme to provide guaranteed scheduling with configuration overhead; they called it the extended work QBvN-cover. They provide a bound on the number of generated switch configurations to speed up performance of the core switch. Under continuous bit rate traffic, the authors reported superior delay performance in comparison with other similar heuristics in the literature.

2.4.2. Optical Time Slot Reservation Based on Slot Boundary Synchronization

In [Wen2005], Wen et al. studied the connection-assignment problem for a TDM wavelength-routed network. They divided the problem into three independent sub-problems: routing, wavelength allocation, and time slot assignment. They relied on the shortest path routing algorithm with a new link cost function called least resistance weight function, which depends on the wavelength utilization and number of hops, to derive routes. The authors chose the least loaded wavelength (LLW) scheme to allocate a wavelength between a source-destination pairs. A wavelength load on a given link is the number of used time slots in that wavelength. Consequently, the wavelength load on a path is its maximum load encountered on a link along the derived route. For time slot assignment on a selected wavelength, the authors also chose the least loaded time slot (LLT) scheme to assign time slots between a source-destination pairs. A time slot load is the number of fibers on which the time slot is occupied at a given multi-fibers link. Consequently, the load of a time slot sequence on a path corresponds to the maximum time slot load in the sequence. They compared the LLT scheme with the first-fit time slot (FFT) scheme. FFT assigns the first encountered sequence of slots along a path. It has low computational overhead and requires no global knowledge of time slot loads in the network. By means of simulations, Wen et al. concluded that LLT has substantially outperformed FFT at all load levels. Their justification of this conclusion is that "LLT tends to spread out the traffic evenly among all slots and efficiently prevents overloading of individual slots, increasing the chances for the multi-rate sessions to acquire the requested number of slots." [Wen2005]

In [Zang1999] and [Zang2000], Zang et al. studied two slot assignment approaches in photonic slot routed network: Slot Assignment Based on Packet Arrivals (SABPA) and Slot Assignment Based on Capacity Allocation (SABCA). In SABPA, when a node has traffic to transmit to a destination D, it chooses a partially filled traffic unit heading to D during a given time slot and transmits traffic on one of the free wavelengths. If no time slot

scheduled to that destination is found to carry the required traffic load, an empty slot is reserved based on a first-fit approach. To achieve fairness in bandwidth allocation, the authors proposed SABCA. With this approach, each source destination pair has a predefined quota of the bandwidth along the links of the transmission route. The quotas are derived based on the traffic loads for all source destination pairs. Clearly, SABCA outperformed SABPA in terms of minimizing contention, maximizing throughput and maintaining fairness as Zang et al. concluded.

In [Chen2004], Chen et al. studied the problem of routing and time slot assignment in O-TDM networks. They proposed the expanded shortest-path (ESP) routing scheme that maximizes the performance of an optical network and minimizes the delay in optical buffers. For this purpose, they consider the buffer cost along with the link cost when deriving a path between a source destination pair. The buffer cost is based on the buffer holding time. It depends actually on the adopted slot assignment scheme which is designed to minimize the buffer delay time for a given call. The major drawback of ESP over Dijkstra's shortest path is its complexity which increases from $O(m^2)$ to $O(m^2n^2)$ where n is the frame size and m is the number of nodes. To reduce the complexity, they put a limit D on the buffer size where $D < n$. Hence they achieved a better complexity figure which is in the order $O(m^2D^2)$. They reported improved performance and better delay time when comparing their approach with the first-fit approach.

In [Siew2006], Siew et al. proposed a simple Conflict Resolution Algorithm (CRA) as a slot allocation scheme for the TWIN architecture. To allocate a time slot, the CRA algorithm finds a free time slot at the source node S and a corresponding free time slot at the destination node D. The time slot at D is derived by referring to the total delay between S and D. If a free pair of slots is not found, the algorithm moves to the next free slot at the source and repeats the same process until a match is found. If no match is found, the allocation attempt fails. The CRA scheme in TWIN networks resembles the first-fit allocation in a star network; and hence, its worst-case complexity is $O(2N)$.

In [Liew2003], Liew et al. adopted a simple RWTA scheme in their slotted OBS network simulations based on the First-Fit approach. They concluded that the slotted WDM achieved high network utilization in comparison to wavelength routing.

2.4.3. Optical Time Slot Reservation with QoS consideration

In [Maach2004], we proposed a slot reservation scheme that depends solely on the available link capacity regardless of the slot matching problem at intermediate nodes. We solved the slot matching problem by assuming that every output link and every node has a full range OTSI. To serve a request of m slots between a source destination pair, the algorithm starts with the shortest path P_0 and reserves k_0 available slots where $k_0 \leq m$. If $k_0 = m$, the request is considered fully accepted. If $k_0 < m$, the algorithm proceeds to the second shortest path P_1 and reserves k_1 available slots where $k_0 + k_1 \leq m$. It keeps trying until it reserves k_n slots over path P_n, where $k_0 + k_1 + \cdots + k_n = m$. If all essential paths are checked and some of the requested slots are still not served, those slots are considered blocked and the request is considered partially accepted. After simulating the proposed approach, we reported better network performance in comparison with the first-fit shortest path approach. It is worthwhile noting that all the performance gain is attributed to the use of full-range OTSIs and the alternative path approach.

In [Hafid2005a], Hafid et al. proposed a new advance reservation scheme in slotted optical networks. In this scheme, a call request must include the start time and duration beside the required bandwidth (in term of time slots count). If the request cannot be satisfied due to bandwidth shortage within the required time frame, the source will be offered other alternatives. After a negotiation session, the source node picks the alternative that best suites its request. Advance reservation provides the user with more choices than the simple accept/reject choice. This solution is geared more towards quality of service improvement than bandwidth efficiency.

2.4.4. Distributed Optical Time Slot Reservation

A time slot reservation scheme can be distributed or centralized. In a centralized scheme, one node is designated to host a network manager that is responsible for allocating and releasing bandwidth based on arriving requests. If a node chooses to communicate with another node in the network, it sends a request to the manager. The manager tries to allocate free resources on a route between both nodes to satisfy the communication request. If the attempt is successful, the manager sends to source node a confirmation with the essential transmission coordinates. Otherwise, it sends a failed response. All the schemes described above are based on a centralized approach. In this section, we cover the distribute schemes. In a distribute scheme, every node participates in the reservation process in one way or another. There is no single node that does it all. The effort and network knowledge must be split among all network nodes.

In [Yuan1996], Yuan et al. studied two categories of distributed resource reservation protocols in wavelength-routed and OTDM networks: Forward and Backward Reservation protocols. With forward reservation protocols, four types of messages are used:

- Reservation Message (RES): It is a reservation request that includes a unique connection identifier, and a bit map that keeps track of virtual channels (i.e. wavelengths or time slots) that can be used to satisfy the connection request.
- Acknowledgment Message (ACK): It is a confirmation response that includes the connection identifier and a channel field reflecting the selected virtual channel.
- Negative Acknowledgment Message (NACK): It is a failure response that includes the connection identifier
- Release Message (REL): It is a connection release request that includes the connection identifier.

Under the forward reservation scheme, a source node composes a RES with a bit map reflecting the availability of virtual channels and sends it to the next node on the route. An intermediate node receives the RES and updates the bit map based on the availability of the corresponding virtual channels, and passes the updated RES to the next node. The same process is repeated until the RES message reaches the destination node. As the RES is passed from one node to another along the route, the available virtual channels are locked. If no corresponding virtual channel is available at a given node, a NACK is sent back to the source node and the RES is dropped. As the NACK message propagates back to the source along the same route, the available virtual channels are unlocked. If the RES reaches the destination node successfully, the destination sends an ACK to the source with the selected virtual channel. As the ACK message propagates back to the source along the same route, the selected virtual channel is reserved and all the other available channels are unlocked. After the reception of an ACK, a source node can start transmitting traffic through the selected virtual channel. When the source finishes transmitting, it sends a REL message to tear down the connection and release the reserved resources. Figure (2.8) shows two forward reservation use cases: a) failed attempt and b) successful attempt.

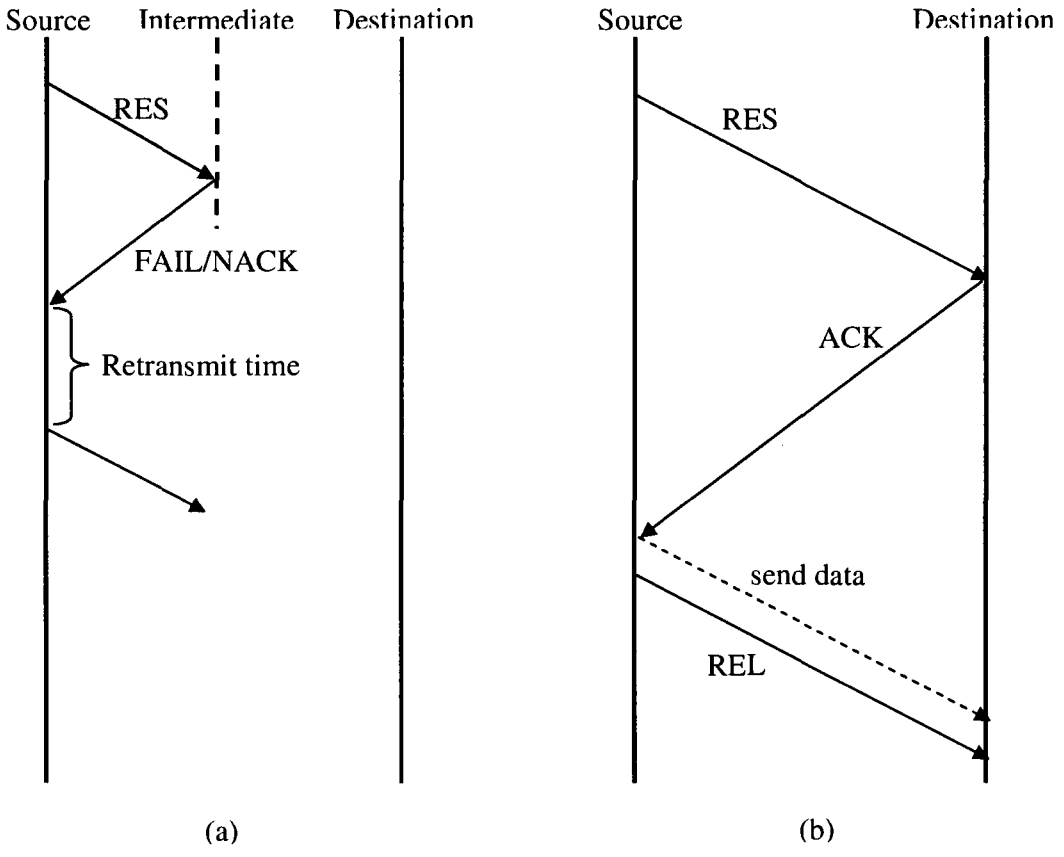

Figure 2.8: Forward reservation use cases

The authors describe 4 variations of the forward reservation protocol: aggressive forward reservation with dropping (AFD), aggressive forward reservation with holding (AFH), conservative forward reservation with dropping (CFD), conservative forward reservation with holding (CFH). A scheme with a holding characteristic allows an intermediate node to hold a failing RES message for a pre-defined period of time; otherwise, it has a dropping characteristic. If some corresponding virtual channels become available within the pre-defined holding time, the RES is updated and sent forward; otherwise, a NACK is sent backward. On the other hand, an aggressive scheme requires that intermediate nodes lock all the available virtual channels along the path of a RES message. In this case, success is guaranteed if any virtual channel is identified. Alternatively, the conservative scheme

requires that intermediate nodes lock a single virtual channel. In this case, success is guaranteed only if the designated virtual channel is available on all links.

With backward reservation protocols, five types of messages are used:

- Probe Message (PROB): it is an information gathering message that has a bit map reflecting the availability of virtual channels (i.e. wavelengths or time slots).
- Reservation Message (RES): It is similar to the RES message described in the forwarding scheme, except that it travels backward as it is described next.
- Fail message (FAIL): It is used to unlock virtual channels locked by RES in case of failure in establishing a connection.
- Negative Acknowledgment Message (NACK): It is used to inform the source node of a reservation failure.
- Release Message (REL): It is a connection release request that includes the connection identifier.

Under a backward reservation scheme, a source node composes a PROB with a bit map reflecting the availability of virtual channels and sends it to the next node on the route. An intermediate node receives the PROB and updates the bit map based on the availability of the corresponding virtual channels, and passes the updated PROB to the next node. The same process is repeated until the PROB message reaches the destination node. Unlike the forward reservation scheme, the available virtual channels are not locked as the PROB is passed from one node to another along the route. If no corresponding virtual channel is available at a given node, a NACK is sent back to the source node and the PROB is dropped. If the PROB reaches the destination successfully, the destination node sends a RES to the source with a bit map reflecting a selected subset of the PROB bit map. As the RES message propagates back to the source along the same route, each intermediate node checks the availability of selected virtual channels, updates the RES bit map accordingly, and locks the available ones. If no virtual channel is available at a given point, a NACK is sent to the source and a FAIL is sent to the destination to unlock the already locked resourced. The same process is repeated until the RES message reaches the source node. If the RES reaches the source node successfully, the source sends an ACK to the destination with the selected virtual channel. As the ACK message propagates to the destination along

the same route, the selected virtual channel is reserved and all the other available channels are unlocked. Note that a source node can start transmitting traffic through the selected virtual channel right after the reception of an ACK. When the source finishes transmitting, it sends a REL message to tear down the connection and release the reserved resources. Figure (2.9) shows three backward reservation use cases: a) failed attempt during a probing pass, b) failed attempt during a reservation pass and c) successful attempt.

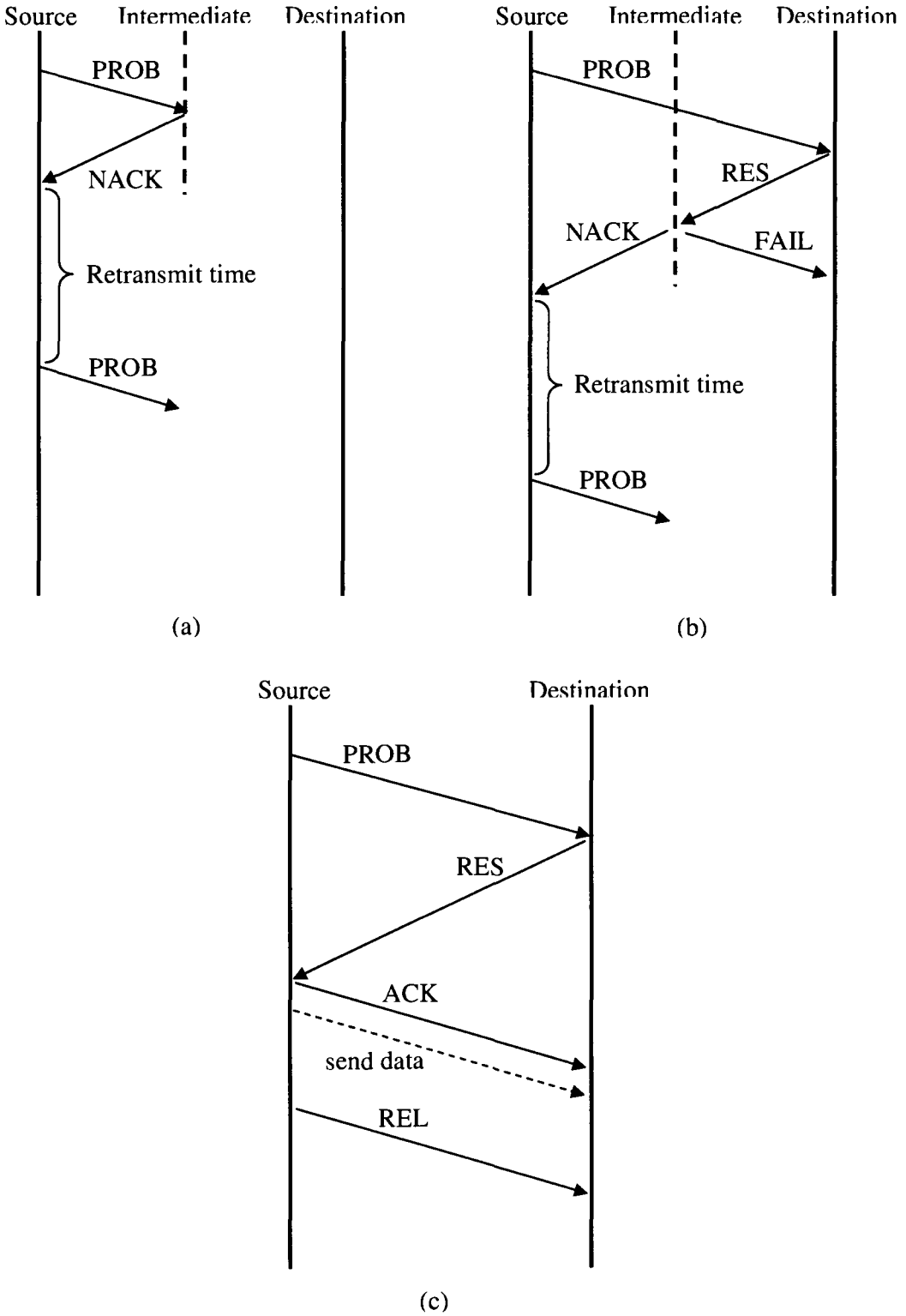

Figure 2.9: Backward reservation use case

Similar to the variation of the forward reservation, the authors describe 4 variations of the backward reservation protocol: aggressive backward reservation with dropping (ABD), aggressive backward reservation with holding (ABH), conservative backward reservation with dropping (CBD), conservative backward reservation with holding (CBH). A backward scheme with a holding characteristic shares similar functionalities with its counterpart in the forward reservation side; however, it allows an intermediate node to hold only a failing RES message, but not a PROB, for a pre-defined period of time; otherwise it has a dropping characteristic. In addition, in case of failure, a NACK is sent to the source; and, a FAIL is sent to the destination. Similarly, the aggressive and conservative approaches resemble their forward reservation counterparts, but in the opposite direction. Note that if a conservative reservation scheme is adopted, the ACK message is not necessary.

As a result of their study, Yuan et al. reported that the conservative schemes outperformed the aggressive scheme; and, the backward schemes outperformed the forward schemes under the same aggressiveness level. They noted that the conservative forward scheme has higher throughput than the aggressive backward scheme. In addition, when the wavelength number is reasonably large, the holding characteristic improves the performance for all schemes except for the conservative forward scheme. They also found that the message size has a large effect on the performance of a protocol. The message size reflects the amount of information loaded on a given message. For example, the size of a RES message depends on the size of the associated bit map reflecting the virtual channel availabilities; i.e., the larger the number of virtual channels is, the higher the message size gets. Using small messages, better performance was noticed with conservative schemes in comparison with their aggressive counterparts. On the other hand, large messages boosted the performance of backward schemes in comparison with their forward scheme counterparts. Generally, a backward scheme always outperformed a forward scheme when all other characteristics are alike.

In [Yuan1997], Yuan et al. repeated the same study in their previous work [Yuan1996] but with additional characteristics such as network size, re-transmission rate and control

network speed. They reported that the backward schemes provided better performance when the message size is small and when the network size is large. When the message size is large or the network size is small, all the protocols showed similar performance. The authors added: "The speed of the control network affects the performance of the protocols greatly." [Yuan1996] As another variation, the author considered an optimized conservative approach. They reported that choosing an optimal virtual channel bit map, covering a subset of the network channels, in the RES message improved performance by about *100%* in the forward reservation schemes and *25%* in the backward schemes.

In [Mei1997], Mei and Qiao presented a similar study to what Yuan et al. did in [Yuan1996], but used different nomenclatures to describe the various schemes. They reported similar results in general. The major differentiators in their study are the consideration of Path Multiplexing (PM) versus Link Multiplexing (LM), and primary path versus alternative paths routing with CBH (CBH-PRIME and CBH-ALT). PM denotes the usage of the same wavelength across the entire path. LM denotes the possibility of using different wavelengths across the path (i.e. wavelength conversion) [Qiao1997]. They showed that CBH-ALT with LM improves the throughput over the best forward reservation scheme under LM (which is CFD) by *10%*; while CBH-PRIME did not provide a significant improvement. On the other hand, CBH-PRIME with PM improved throughput over the best forward reservation scheme under PM (which is AFD) by *10%*; while CBH-ALT did not improve the performance further.

In [Hafid2005b], Hafid et al. extended the advance reservation scheme in [Hafid2005a] to serve inter-domain networks. In their solution, each network has a central Advance Reservation Manager (ARM) responsible for the internal reservation process. For inter-domain scheduling, when every network's ARM handles the internal scheduling task, it appends its proposal to a list and forwards it to the next ARM on the route. At the destination ARM, the resulting list of proposals is sent backward to the source ARM. The source ARM forwards the list to the user in order to select the best proposal. After selecting a proposal, a confirmation message is propagated forward to the destination in order to reserve the appropriate resources. The authors did not evaluate the inter-ARM

signaling in terms of bandwidth utilization and efficiency. However, we can easily see that the proposed signaling scheme is bandwidth inefficient due to its three ways messaging, and the growing list of proposals appended to the message. Figure (2.10) shows four ARMs communication scenarios: a) successful reservation, b) negotiation failure, c) failure due to insufficient resources at the destination, and d) failure due to insufficient resources at an intermediate ARM.

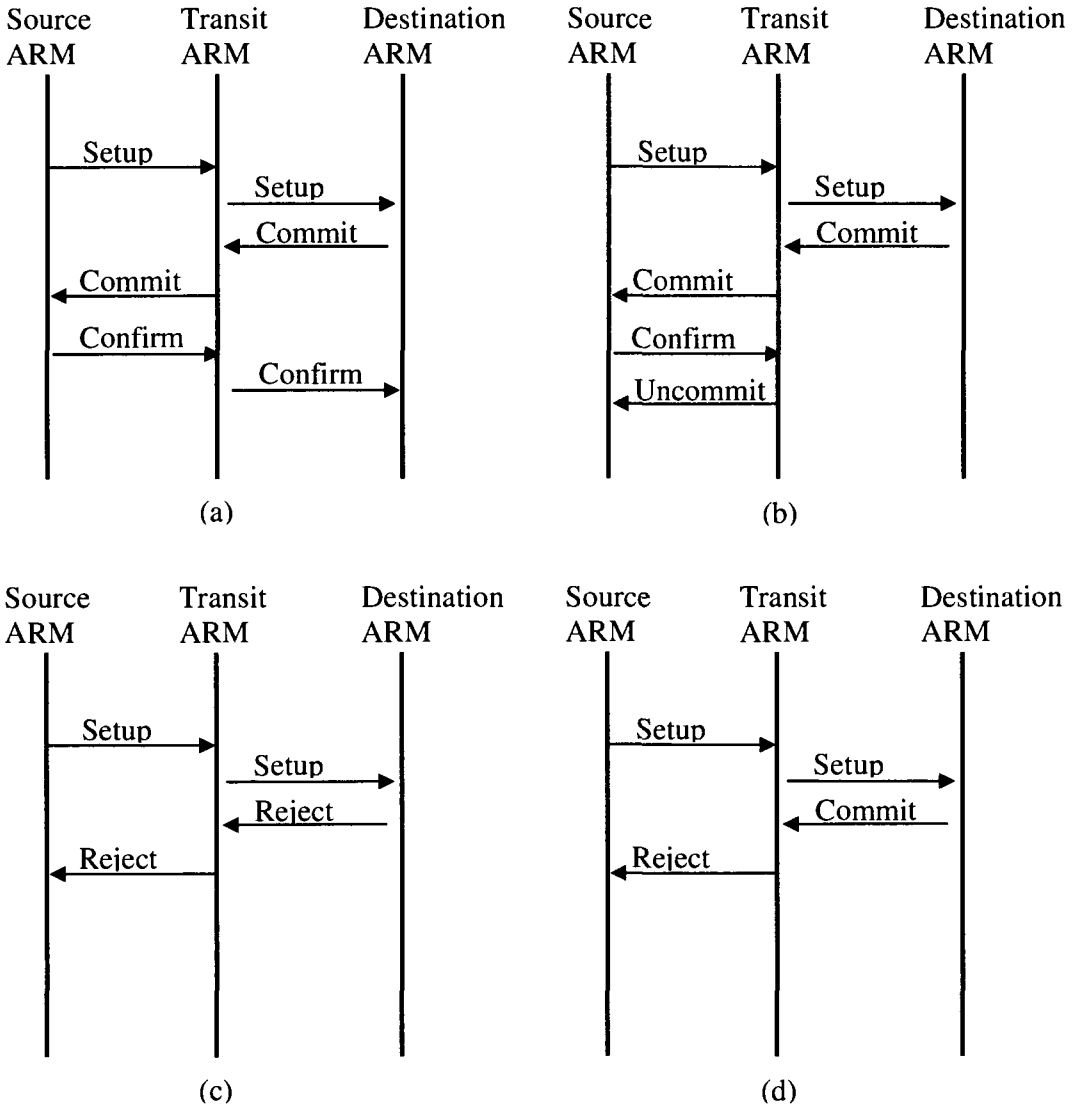

Figure 2.10: ARM communication use cases

In [Yang2007a], Yang et al. compares the performance of four distributed RWTA algorithms in a bidirectional ring network. In each algorithm, they only vary the wavelength allocation scheme and use shortest path routing and first-fit time slot reservation. The four wavelength allocation schemes that they utilized are: the First Fit, Random, Most Loaded and Least Loaded wavelength. They assume no global knowledge in the network, where each node only has local knowledge about the resources on its outgoing links. To achieve bandwidth reservation in this environment, backward reservation is required. Essential information about resources at every node along the path must be collected in a forward message travelling from the source to the destination. When the destination receives this forward travelling message, it chooses the appropriate resources and sends a backward message towards the source. It is the typical backward reservation approach described earlier in this section.

In [Yang2007b], Yang et al, investigated the forward reservation scheme assuming global knowledge at each node. Due to the need for extensive signaling to maintain this global knowledge, the authors resorted to the well-known technique of periodic resource update [Shaikh2001, Shen2004, Shen2006]. They studied the effect of varying the update interval under two different reservation schemes, First Fit and Random. They found that the Random scheme outperformed the First Fit at all levels of periodic updates. They justify this observation by saying: "FF tends to pack wavelengths/time slots according to a fixed order. When traffic load is very light, the stale global information is more likely to cause FF to make incorrect routing, wavelength and time slot assignment decisions than RR, which in turn may cause more blocking for FF than RR."

2.5. Multi-Protocol Label Switching

Over the years, Multi-Protocol Label Switching (MPLS) [RFC3031] has evolved to be the dominant packet-switched protocol in the telecommunication field. From an OSI perspective, MPLS fits between the layer 2 (Data Link) and layer 3 (Network). An MPLS network serves as a transparent medium for any traffic type, such as IP, ATM, Frame

Relay and Ethernet. With the insertion of a 4-bytes shim header, which includes a label, any traffic segment, regardless of its origin and size, can be routed through an MPLS network towards its destination. In this sense, MPLS wins over ATM when it comes to bandwidth efficiency and adaptability since ATM uses a 5-bytes header for every 48 bytes of data. In addition, exhaustive segmentation and assembly are required to adapt to other protocols. On the other hand, MPLS is a perfect solution for IP-based traffic as it helps in carrying IP traffic past the IP network boundaries in a feasible way. It just inserts the relatively small shim header without the need to dissect the routed IP packet.

2.5.1. MPLS Header

The MPLS shim header is made of the following parts, as shown in Figure (2.11):

- Label: 20 bits carrying a label value.
- CoS: 3 bits defining Quality of service parameters.
- S (Stack Field): 1 bit defining that the current label is the last in the stack
- TTL: 8 bits reflecting the time to live

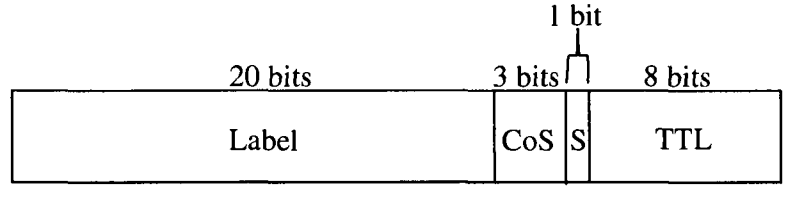

Figure 2.11: MPLS Header

2.5.2. Resource Allocation in MPLS

An MPLS network is made of Labeled Edge Routers (LER) and Labeled Switch Routers (LSR). The LER nodes are the first and last nodes through which a traffic segment should pass when routed in an MPLS network. These are the entry and exit points where the label

is inserted into, and stripped from, the traffic segment. On the other hand, the LSR nodes forward the segment to its destination based on the carried label. To route traffic over an MPLS network, a Labeled Switched Path (LSP) must be established between two LER points, and might pass through several LSR nodes depending on the routing and quality of service parameters. The ingress LER initiates a label request message and forwards it to the egress LER through the appropriate route. Upon receipt of the request, the egress LER returns a label via a label mapping message. Each individual LSR along the reverse route updates its forwarding table accordingly and redefine the label for the upstream LSR or LER. Figure (2.12) represents a graphical example of the reservation process. The Label Distribution Protocol (LDP) [RFC3036, RFC3212] and the Resource Reservation Protocol (RSVP) [RFC2205, RFC3209] are the most common protocols that are adopted in MPLS for LSP reservation.

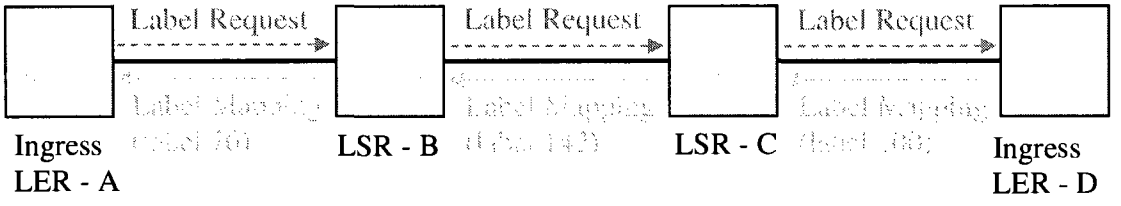

Figure 2.12: MPLS reservation process

2.5.3. Resource Update in MPLS

In MPLS, each node has a database keeping track of various network resource information and status. The nodes exchange resource information via update messages based on the Open Shortest Path First (OSPF) [RFC2328, RFC3630] or Intermediate System to Intermediate System (IS-IS) protocols [RFC1629]. Status update in MPLS happens on a periodic basis rather than immediately after a change, usually at a interval between 5 sec and 30 min [RFC2328, RFC4316]. Hence, the nodal database might not reflect the true status of a network in the period between two update sessions. However, the benefits of saving the bandwidth overhead and the signaling cost associated with exhaustive

immediate updates justify the inconvenience of having a slightly outdated database.

2.5.4. Generalized MPLS

To employ MPLS in an optical network, some enhancements were necessary to the MPLS protocol suites. The RSVP and LDP protocol were adjusted to support signaling and creation of optical channels [RFC4974, RFC3472]. In addition, OSPF and IS-IS were extended to carry updates on optical resources status such as bandwidth availability and local constraints [RFC4203, RFC4205]. These enhancements were the essence behind the emergence of the Generalized MPLS (GMPLS) [Banerjee2001, Lang2004, RFC3471], which is meant to apply MPLS in optical networks. With GMPLS, the label or LSP can be a time slot, a wavelength, or a full fiber. In addition, hierarchical LSPs are supported in the context of GMPLS. A hierarchy of LSPs is formed when one LSP is tunneled inside another existing LSP. For example, a fiber-level LSP could exist between two nodes and yet could be carrying different wavelength-level LSPs serving various source-destination node pairs. See Figure (2.13) for a graphical illustration.

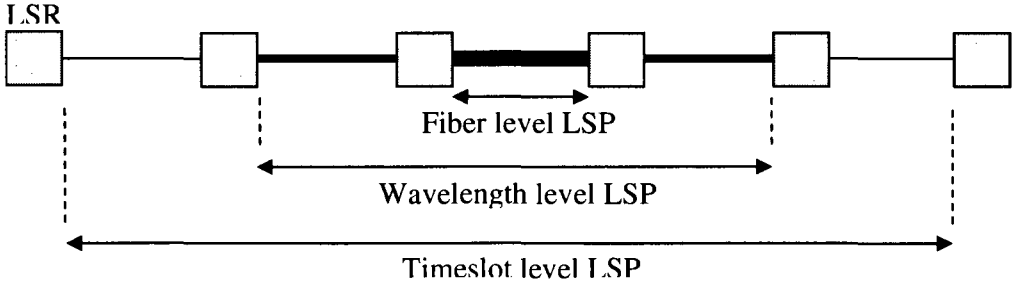

Figure 2.13: Hierarchical LSPs in GMPLS

3. Least Constraining Slot Allocation

3.1. Problem Definition

As discussed in the review chapter, some research papers [Chen2004, Liew2003, Siew2006, Wen2005, Zang1999, Zang2000] assumed time slot boundaries synchronization instead of frame. However, that comes with the price of loosing frame alignment, and hence the benefit of adopting wavelength allocation schemes as possible solutions for the time slot reservation problem. Thus, finding an effective time slot reservation scheme in an optical network, where transmission is synchronized on slot and not frame boundaries, becomes a vital question.

In this chapter, we propose a novel time slot reservation schemes in all-optical TDM mesh network without buffers at nodes, where transmission is synchronized on slot boundaries. With the introduction of this scheme, we aim to reduce call blocking to a close to optimum rate achieved with buffering. We consider that the reservation of a slot imposes constraint on the network measured by the number of transmission channels on the fixed routes that might use the slot at a given point in time. The scheme selects the least constraining slots on the route, hence the name "least constraining" (LC) slot. We use the FF approach with full time slot interchanging capability as a benchmark to measure our results. It has been proven that employing full wavelength interchanging yields optimum results with fixed routing [Zeineddine1998]. This is true because blocking would not occur unless one of the links along the fixed route is saturated. In addition, we compare the performance of the LC approach to the LL approach in a multi-fiber environment. We also investigate how LC behaves in a star network synchronized on slot boundaries.

3.2. LC Allocation approach

3.2.1. Basic Concepts

Before describing the basic steps of the LC approach, we should clarify the nomenclature used in this chapter to provide a better understanding of the presented concepts. Route, route-slot and link-slot are essential concepts used in describing the LC approach.

Assuming fixed alternative routing, a network route is a predetermined series of unidirectional links interconnected through intermediate nodes from a given source node to a given destination node. We say that two routes intersect if they have at least one link in common. A node transmits data into a link in the form of repeating frames of N equal time slots. Due to the link propagation delay, frame alignment is not preserved along the route. However, slot boundary synchronization is assumed. Considering link AB from node A to node B, data transmitted during a given time slot at egress node A might be received during a different time slot at ingress node B. Thus, a time slot is better identified with reference to a link; we use the term link-slot AB_x to describe time slot x on link AB. There is no need to mention the corresponding wavelength since only one wavelength plane is considered in this study; basically, the LC approach is designed to operate at a sub-wavelength level and is independent of the number of employed wavelengths. Formally speaking, a link-slot is a time slot on a link with reference to the frame of its egress node. In general, a transmitted data from source node S to destination node D travels through different links along a fixed route, and hence occupies a series of different link-slots. For instance, if A and B are two intermediate nodes between S and D, a series of link-slots would be described as $SA_x AB_y BD_z$. Knowing the delay of each link, an intermediate link-slot UV_j corresponds to a source link-slot SA_i according to the general rule $j = (i + d_{SU}) \bmod N$, where d_{SU} is the total delay of all links from node S to node U. Thus, knowing the fixed route between a source-destination pair and all associated link delays, one can easily derive the entire series of link-slots when given a starting link-slot. In this case, we can describe the series $SA_x AB_y$

BD_z in a simple notation $\overline{SD}_x$, which we call a route-slot. The upper bar is essential to differentiate between link-slot and route-slot. A route-slot $\overline{SD}_x$ is considered available if all its constituent link-slots are available; otherwise, $\overline{SD}_x$ is unavailable. In a single fiber environment, a link-slot is available if it is not reserved. On the other hand, in a multi-fiber case, a link-slot is available if it is free at least on one of the link fibers. To make our approach generic enough, we develop it based on a multi-fiber environment, and apply it to a single-fiber network as a special case.

The exercise of allocating resources, for a communication request, from node S to D is to find and reserve an available route-slot $\overline{SD}_x$ along a given fixed route.

3.2.2. Basic Definitions

3.2.2.1. Resource Availabilities

If a link-slot XY_j is part of a route-slot $\overline{SD}_i$, we write:

$$XY_j \text{ in } \overline{SD}_i, \text{ which implies that } j = (i + d_{SX}) \bmod N. \tag{3.1}$$

Considering M fibers per link, we define the link-slot availability A_{XY_j}, an integer between 0 and M, to be the number of fibers on which XY_j is free. If A_{XY_j} is equal to zero, then XY_j is unavailable. Furthermore, we define the availability $A_{\overline{SD}_i}$ of a route-slot to be equal to the minimum availability A_{XY_j} among its constituent link-slots,

$$A_{\overline{SD}_i} = \underset{XY_j \text{ in } \overline{SD}_i}{MIN} \left(A_{XY_j} \right). \tag{3.2}$$

A route-slot's availability could be identical to the availabilities of several constituent link-slots. This could happen when several link-slots have the same minimum availability. We define the count of link-slots who share the same availability with their container route-slot as the availability-matching-count:

$$E_{\overline{SD_i}} = \sum_{XY_j \, in \, \overline{SD_i}} Equal(\mathrm{A}_{\overline{SD_i}}, \mathrm{A}_{XY_j}) \qquad where \; Equal(a,b) = \begin{cases} 0, if \; a \neq b \\ 1, if \; a = b \end{cases} \qquad (3.3)$$

3.2.2.2. Intersecting Route-Slot Sets

Knowing the set of fixed alternative routes that can be used for each source-destination pair, we derive the set Ω of all possible route-slots in the network. We define Ω_{XY_j} to be a subset of Ω consisting of all route-slots that contain link-slot XY_j.

$$\Omega_{XY_j} = \left\{ \overline{SD_i} \in \Omega \;\; | \; XY_j \; in \; \overline{SD_i} \;\; \right\}. \qquad (3.4)$$

We further define Ω'_{XY_j} to be a subset of Ω_{XY_j} consisting of all route-slots whose availabilities are equal to A_{XY_j}.

$$\Omega'_{XY_j} = \left\{ \overline{SD}_i \in \Omega_{XY_j} \;\; | \;\; \mathrm{A}_{\overline{SD_i}} = \mathrm{A}_{XY_j} \right\} \quad . \qquad (3.5)$$

The purpose of Ω'_{XY_j} is to identify all route-slots whose availabilities are decremented when the link-slot XY_i is reserved.

In addition, we define Ω''_{XY_j} to be a subset of Ω'_{XY_j} consisting of all route-slots whose availability-matching-counts are equal to 1:

$$\Omega''_{XY_j} = \left\{ \overline{SD}_i \in \Omega'_{XY_j} \mid E_{\overline{SD}_i} = 1 \right\} \tag{3.6}$$

The purpose of Ω''_{XY_j} is to identify all route-slots whose availabilities are incremented when the link-slot XY_i is released.

3.2.2.3. Resource Constraint

We designate the constraint of link-slot XY_i to be the sum of the availabilities of all route-slots belonging to Ω_{XY_j}.

$$C_{XY_j} = \sum_{\overline{SD}_i \in \Omega_{XY_j}} A_{\overline{SD}_i} . \tag{3.7}$$

In a single fiber environment, $A_{\overline{SD}_i}$ becomes a binary variable showing whether the route-slot is available (1) or not (0); and hence, C_{XY_j} would reflect the number of available route-slots containing XY_j. In other words, it indicates the number of routes that can potentially use the designated link-slot.

Last, we define the constraint of a route-slot to be equal to the total constraint of all its constituent link-slots:

$$C_{\overline{SD}_i} = \sum_{XY_j \, in \, \overline{SD}_i} C_{XY_j} . \tag{3.8}$$

To clearly understand the relationship between the constraint of a route-slot and the availabilities of the intersecting route-slots, we expand Equation 3.8 with 3.7:

$$C_{\overline{SD}_i} = \sum_{XY_j \, in \, \overline{SD}_i} \sum_{\overline{ZP}_n \in \Omega_{XY_j}} A_{\overline{ZP}_n} \tag{3.9}$$

In addition, to describe the relationship between the constraint of a route-slot and the link-slots that define the availabilities of the intersecting route-slots, we expand further with Equation 3.2, we get:

$$C_{\overline{SD_i}} = \sum_{XY_j \, in \, \overline{SD_i}} \sum_{\overline{ZP_n} \in \Omega_{XY_j}} \underline{MIN}_{UV_j \, in \, \overline{ZP_n}} \left(A_{UV_j} \right) \tag{3.10}$$

3.2.3. Allocation Principle

Equation 3.7 shows that the constraint of a route-slot reflects the total availability of all route-slots that intersects with it in one of its links. Thus, the route-slot's constraint is an indicator of the number of available route-slots that could use one of its constituent link-slots. It is evident that reserving a route-slot which has the least impact on other available route-slots keeps more available resources in the network, hence improves the blocking rate for subsequent communication requests. Here, the impact on other available route-slots is measured by the constraint. Thus, the route-slot that has the lowest constraint $C_{\overline{SD_i}}$ would be the best choice on a given route between *S* and *D*. In this case, only a minimal number of route-slots in the network could become unavailable when serving a given call.

3.2.4. Constraint Update

After identifying the best route-slot, all constituent link-slots are reserved. Consequently, the constraint of each link-slot in each route-slot in Ω'_{XY_i} is modified according to the algorithm, shown in Figure (3.1).

```
foreach XY_j in SD_i do {
    C_XY_j := C_XY_j - 1
    foreach RT_n ∈ Ω'_XY_j do
        if RT_n ≠ SD_i
            foreach UV_k in RT_n do
                C_UV_k := C_UV_k - 1
    ReserveLinkSlot(XY_j)
}
```

Figure 3.1: Constraint update algorithm

By definition (4), Ω'_{XY_j} contains all route-slots whose availabilities are decremented due to a reservation of XY_j. For instance, when reserving XY_j in a single fiber environment, all route-slots in Ω'_{XY_j} become unavailable, and accordingly, their availabilities flip from 1 to 0. Therefore, the constraint of their constituent link-slots must be decremented since a link-slot constraint is the sum of the availability of the intersecting route-slots.

Finally, a similar algorithm is repeated when freeing resources, but the set Ω'' is used instead of Ω', and the constraints are increased instead of decreased. See Figure (3.2). We use Ω'' because we are only interested in the route-slots whose availabilities will be increased after releasing the corresponding link slot. If a route-slot has multiple link-slots with the same minimum availability, increasing the availability in one of these link-slots should not affect the route-slot availability. Route-slot availability should increase only if the released link-slot is the only constituent link-slot that has the minimum availability.

```
foreach XY_j in SD_i do {
    C_UV_k := C_UV_k + 1
    foreach RT_n ∈ Ω'_XY_j do
        if RT_n ≠ SD_i
            foreach UV_k in RT_n do
                C_UV_k := C_UV_k + 1
    FreeLinkSlot(XY_j)
}
```

Figure 3.2: Constraint update algorithm

3.2.5. Illustrative Example

In the network of Figure (3.3), a circle defines a node, and an arrow represents a unidirectional single fiber link during a particular link-slot. Next to each arrow is an underlined delay value in slot unit. The dashed area represents network segments where no communication is possible from/to EG_{10} and GF_5 due to unavailability of matching link-slots.

Considering a transmission request from node E to node F, we should find an available route-slot that has the lowest constraint on route EGF. We assume 3 available route-slots were identified, $\overline{EF_2}$, $\overline{EF_8}$, *and* $\overline{EF_{10}}$. Let us start with measuring the constraint of $\overline{EF_{10}}$ based on the logistics of Figure (3.3). By definition (6), the constraint of a route-slot is equal to the total constraint of all its constituent slots, $C_{\overline{EF_{10}}} = C_{EG_{10}} + C_{GF_5}$. Assuming a single fiber environment, we would benefit from identifying $\Omega'_{EG_{10}}$ to get the constraint of EG_{10}; $\Omega'_{EG_{10}} = \{\overline{AF_3}, \overline{AG_3}, \overline{BF_7}, \overline{BG_7}, \overline{CF_4}, \overline{CG_4}, \overline{DF_6}, \overline{DG_6}, \overline{EF_{10}}, \overline{EG_{10}}\}$. Since the availabilities are either 0 or 1 in a single fiber network, a route-slot being in $\Omega'_{EG_{10}}$ means that its availability is 1. Thus, $C_{EG_{10}}$ is given by $Size(\Omega'_{EG_{10}})$, which is 10. Similarly for

GF_5, we find $\Omega'_{GF_5} = \{\overline{AF_3}, \overline{BF_7}, \overline{CF_4}, \overline{DF_6}, \overline{EF_{10}}, \overline{GF_5}, \overline{HF_9}\}$ and $C_{GF_5} = 7$; and hence, $C_{\overline{EF_{10}}} = 10 + 7 = 17$. Repeating the same process for $\overline{EF_2}$ and $\overline{EF_8}$, which have different logistics not shown in Figure (3.3), we may find $C_{\overline{EF_2}} = 21$ and $C_{\overline{EF_8}} = 19$. As a result, $\overline{EF_{10}}$ has the lowest constraint and is chosen for reservation. We reserve the constituent link-slots EG_{10} and GF_5, and decrement the constraint of each link-slot found in each route-slot in $\Omega'_{EG_{10}}$ and Ω'_{GF_5}, except for $\overline{EF_{10}}$.

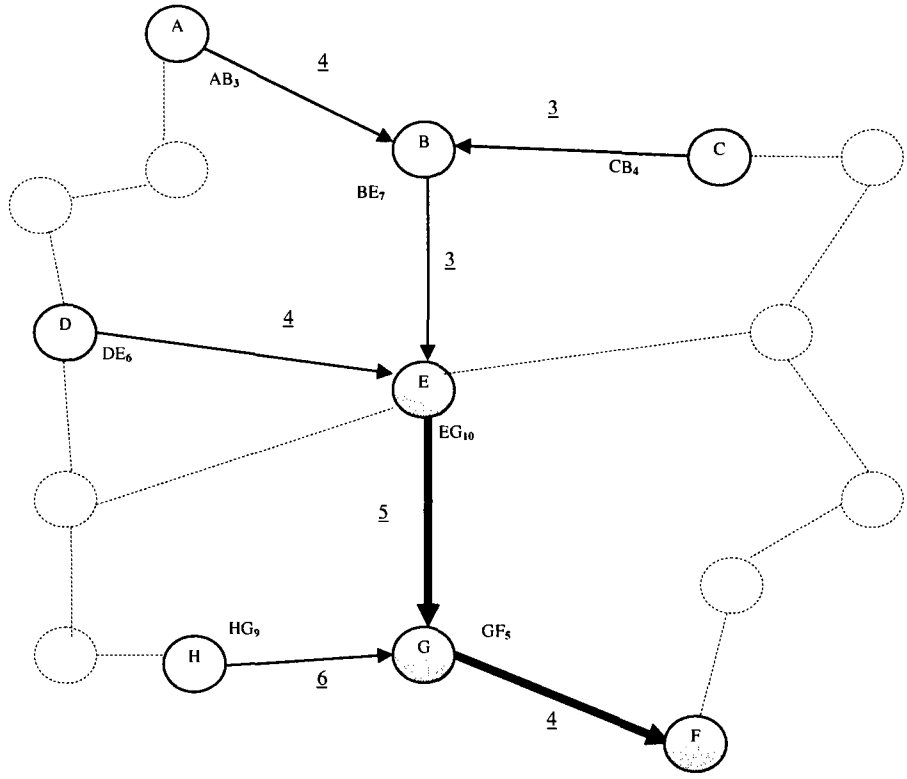

Figure 3.3: A route-slot ($\overline{EF_{10}}$) and its related link-slots

3.3. Simulation Results

In this section, we compare the performance of the LC approach against the FF scheme and FF with OTSI in a single fibre network, and also with LL in a multi-fibre network. In addition, we determine its effectiveness in ring and star topologies.

3.3.1. Simulation

The simulation experiments are based on the 14-node 21-link NSFNET network topology shown in Figure (3.4). We also used a 14-node ring and star topologies as shown in Figures (3.5) and (3.6). A link between two nodes consists of dual unidirectional fibres with a fixed capacity of 10 time slot channels per fibre. Fixed k-alternative paths routing is used to derive paths between all source destination pairs [Sukhni2008], where k in our simulation was defaulted to 1 unless noted otherwise. The first path between a source destination pair is the shortest; the n^{th} one is the shortest path that does not have any link-intersection with the other *n-1* paths. Each path serves up to 10 concurrent connections at the granularity of a transmission channel, i.e. one time slot per link along the path. Each simulation is repeated for 30 runs; each run goes until 100,000 calls are attempted. Calls arrive according to a Poisson process, and lasts for an exponentially distributed period. The simulation results concerning blocking probabilities have confidence intervals similar to those shown in Figure 3.7 where the 95% confidence intervals are plotted.

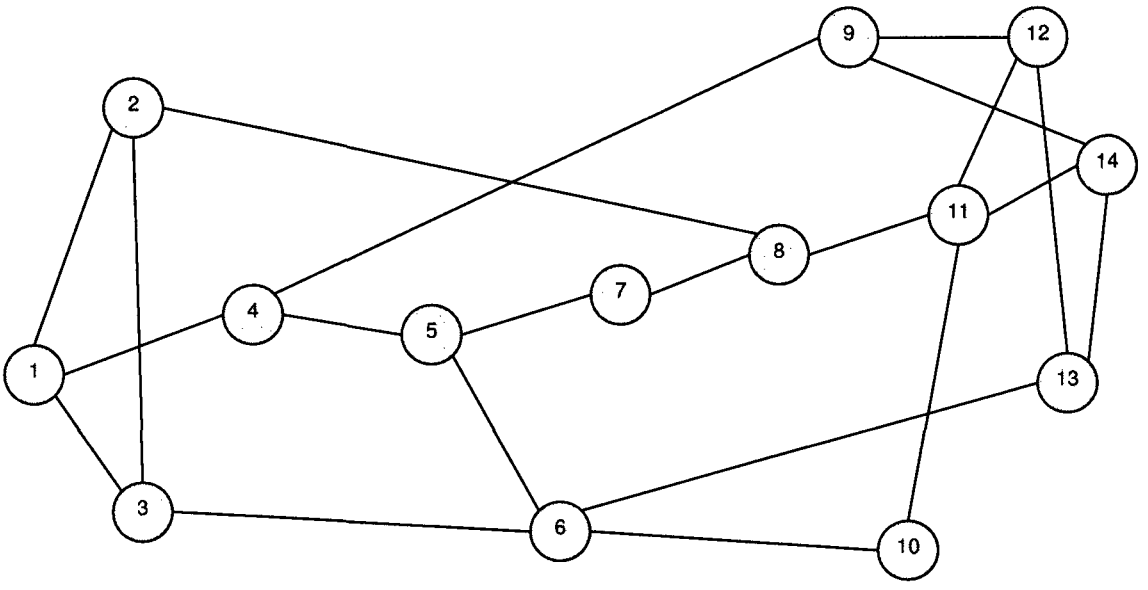

Figure 3.4: NSFNET topology

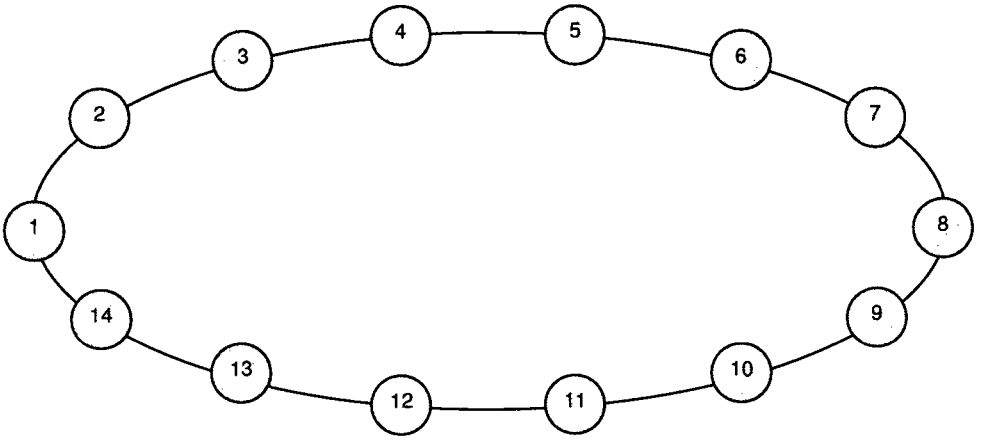

Figure 3.5: A 14-node ring topology

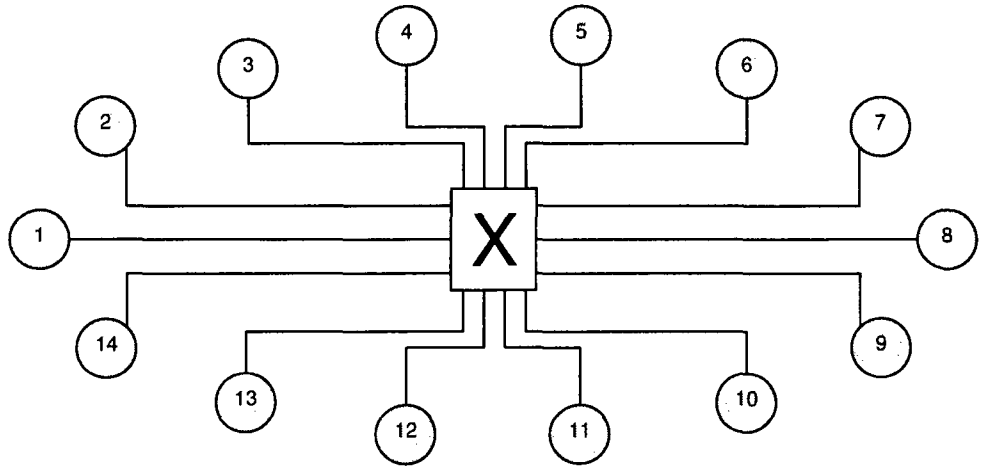

Figure 3.6: A 14-node star topology

We study our scheme under two different traffic distributions among source-destination pairs, uniform and non-uniform. In the uniform traffic case, every pair is chosen at random with equal constraint and hence having the same traffic load in Erlang (mean arrival rate × mean holding time). In the non-uniform case, source-destination pairs have different constraints to achieve non-uniform traffic distribution. Traffic quotas are non-uniformly distributed among 8 random groups of source-destination pairs. Each one of these groups is assigned a different percentage of the network traffic load. For example, assume that 3% of random SD pairs are assigned 30% of the load; this translates, in a network of 200 SD node pairs, to 6 random SD pairs each having 5 percent chance of generating traffic calls. Here is the table that the simulation follows in randomly distributing the traffic load in the network:

SD Node Group (% of total SD pairs)	Traffic Load (% of network load)
3	30
3	20
5	15
10	10

10	08
20	07
20	06
29	04

Tab. 3.1: Non-Uniform Traffic Distribution Map

3.3.2. Observations

Figure (3.7) shows the improvement in blocking probability that the LC approach achieves in comparison to the FF approach. The LC approach, under uniform traffic distribution, provides a performance gain almost identical to the case of using optical time slot interchangers with the FF approach. It is worthwhile noting that with the use of interchangers all blocked calls, in our simulation, happened due to link saturation along the fixed route. Hence, the performance results of employing OTSIs are the optimum any reservation scheme can achieve under a fixed routing approach. Thus, the LC approach achieves close to optimum performance.

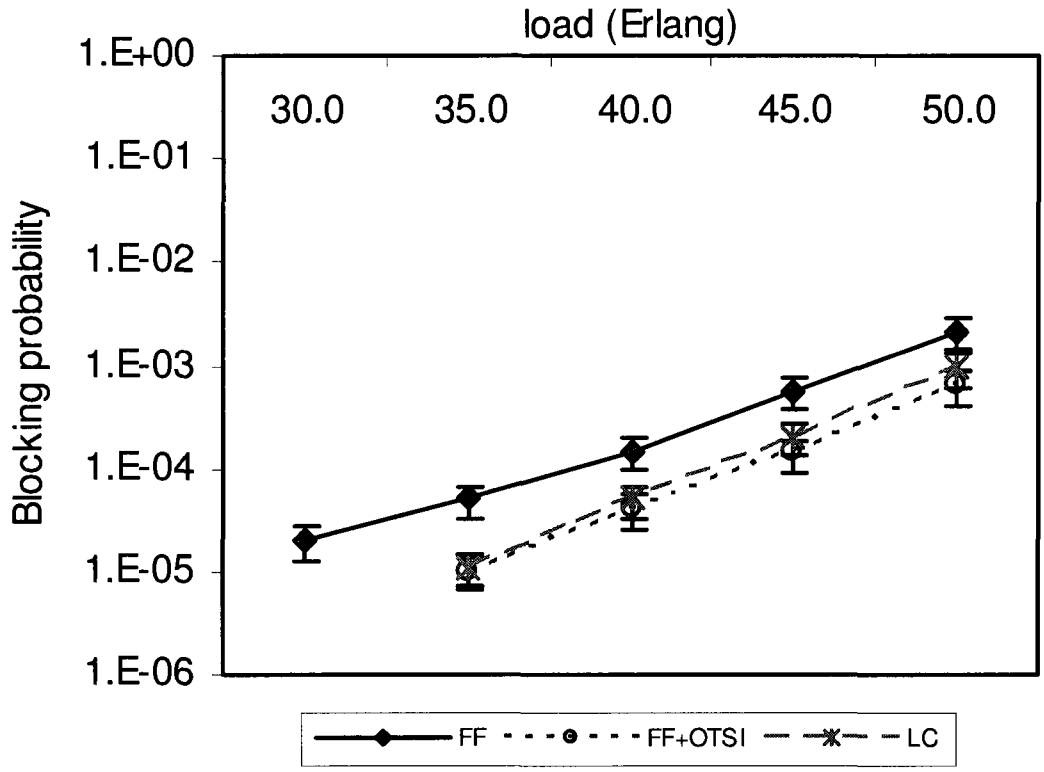

Figure 3.7: LC vs. FF with uniform traffic

Figure (3.8) reflects the results of applying non-uniform traffic distribution among source destination node pairs. The blocking rate in all cases was higher than what was achieved under uniform traffic distribution. However, the LC approach maintained its optimal performance as compared to the FF approach with OTSI. The charts show that LC and FF with OTSI yielded identical performance. The reason for this is the randomness in distributing calls among source destination pairs at each simulation run. Considering two routes under similar loads, the route that intersects with more other routes would make more impact on network performance. This route is considered more critical than the other. Take for example one simulation run for the FF approach with OTSI. If a large number of critical routes get a high percentage of the load, the performance tends to go below average. Now, consider a simulation run with the LC approach. If a similar number of less critical routes get the same high load percentage, performance tends to be above average.

Due to random load distributions, simulation runs produced numbers below and above average in both cases, LC and FF with OTSI. However, after 30 runs of each case, performance averages out to the same level as shown in Figure (3.8).

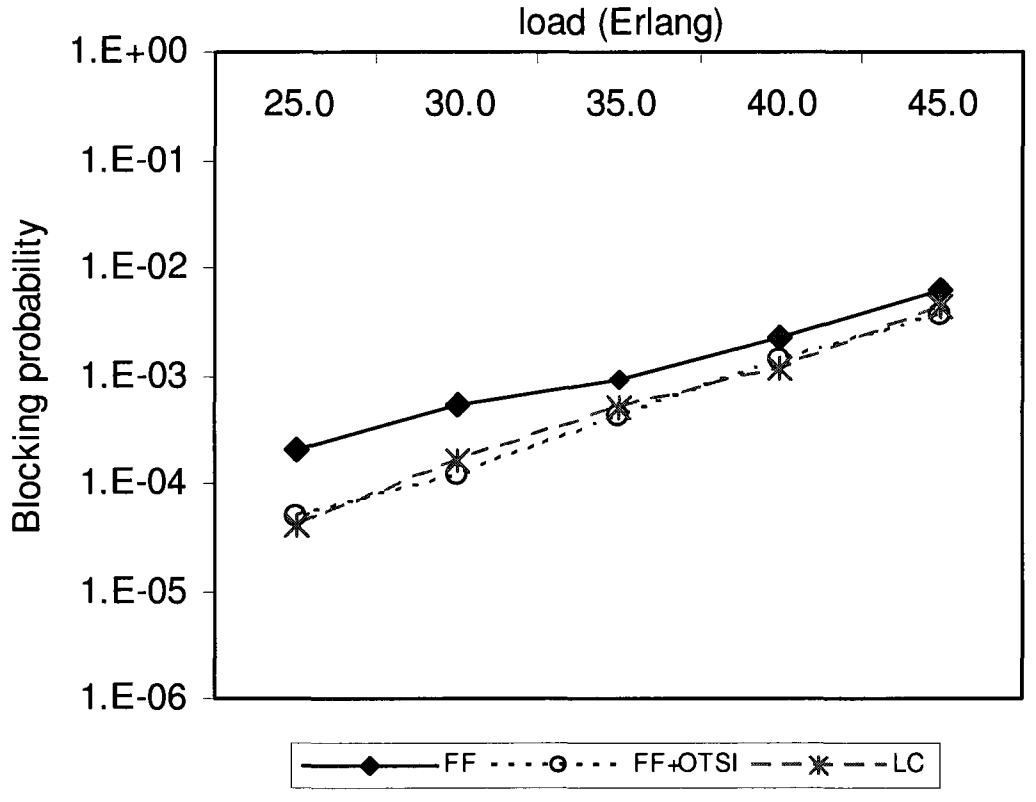

Figure 3.8: LC vs FF with non-uniform traffic

Figure (3.9) shows that the LC approach provided better performance results than the LL approach when applied to a multi-fibers network consisting of 3 fibers per link. It outperformed LL at every load level. In addition, the LC approach can be applied to single and multi-fiber environments; on the other hand, the LL approach collapses to an FF approach in single fiber networks, and hence loses its benefit.

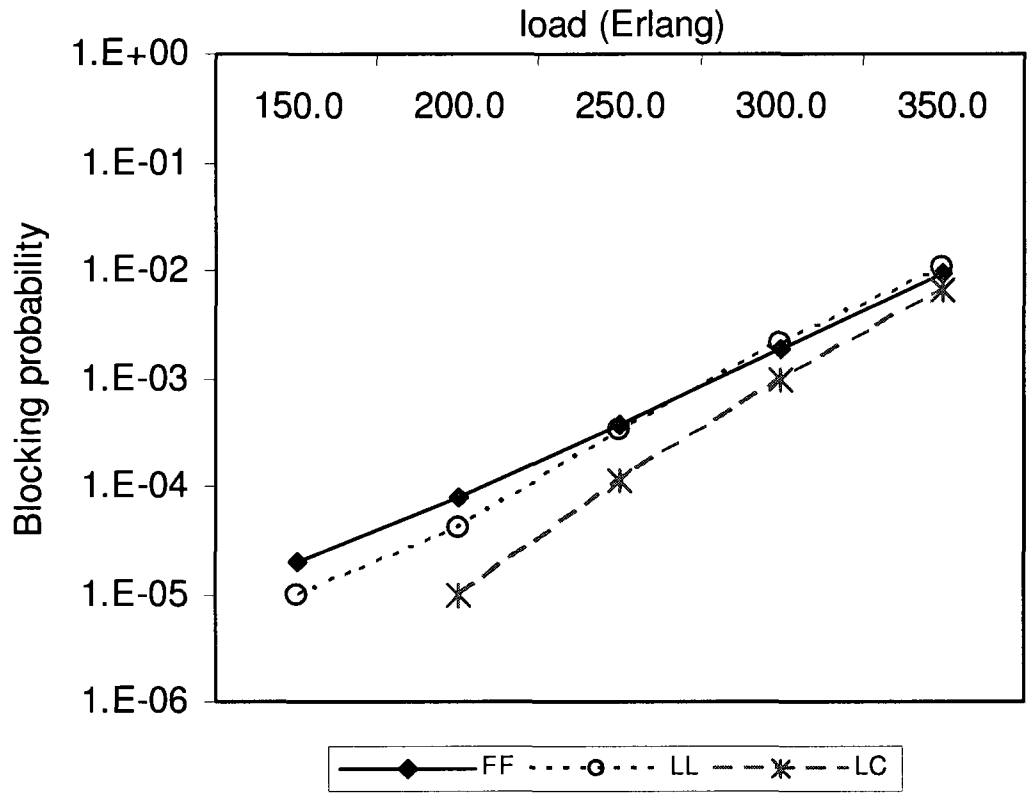

Figure 3.9: Comparing LC to LL in multi-fiber networks (3 fibers per link)

In all the simulation runs, the default number of routes per source-destination pairs was always 1. Figure (3.10) represents the performance of the LC approach when 2 alternative routes are employed. It shows that the same performance trend is achieved regardless of the number of alternative routes adopted between a source-destination pair. In fact, incrementing the number of routes has no effect other than increasing the size of Ω, and hence having larger resource constraints.

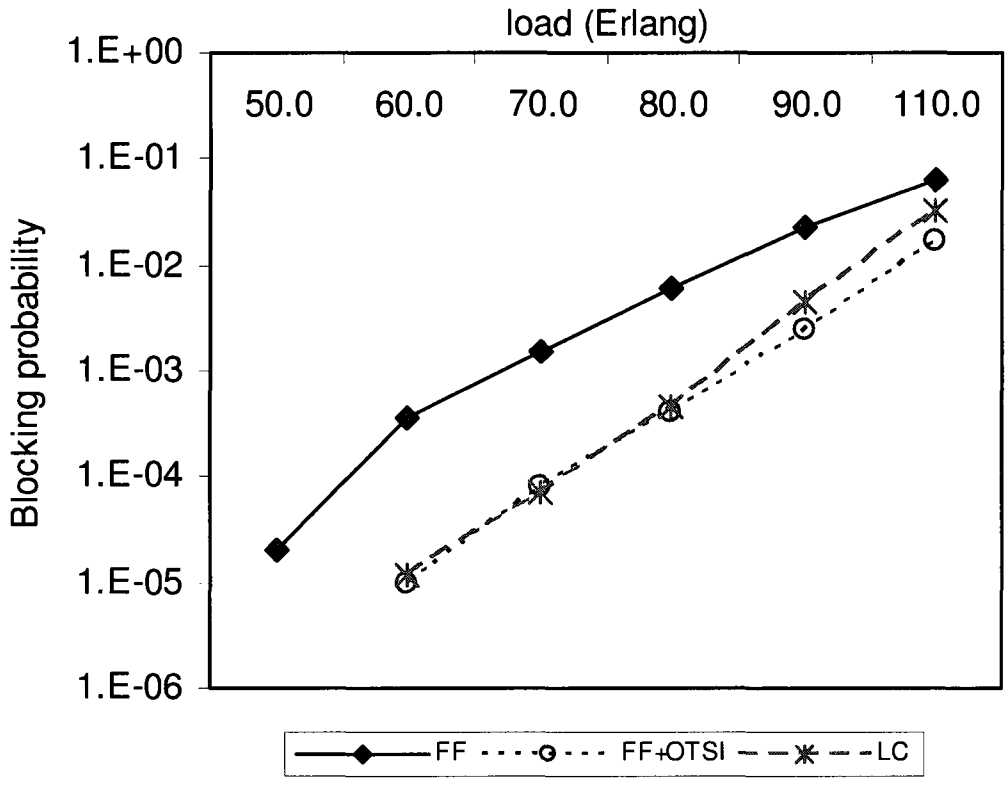

Figure 3.10: LC vs FF with 2 alternative-paths routing

Figure (3.11) shows the performance of the LC approach in a 14-node ring network topology. The performance trend resembles the results of the mesh network shown in Figure (3.7). The difference in blocking rate between Figure (3.11) and (3.7) for the same load level is due to the reduced number of links between the ring and mesh topologies. A 14-node ring has 13 links compared to the 21-link NSFNET topology. In addition, the average hop count is 3.8 in the 14-node ring compared to 2.3 in the NSFNET topology.

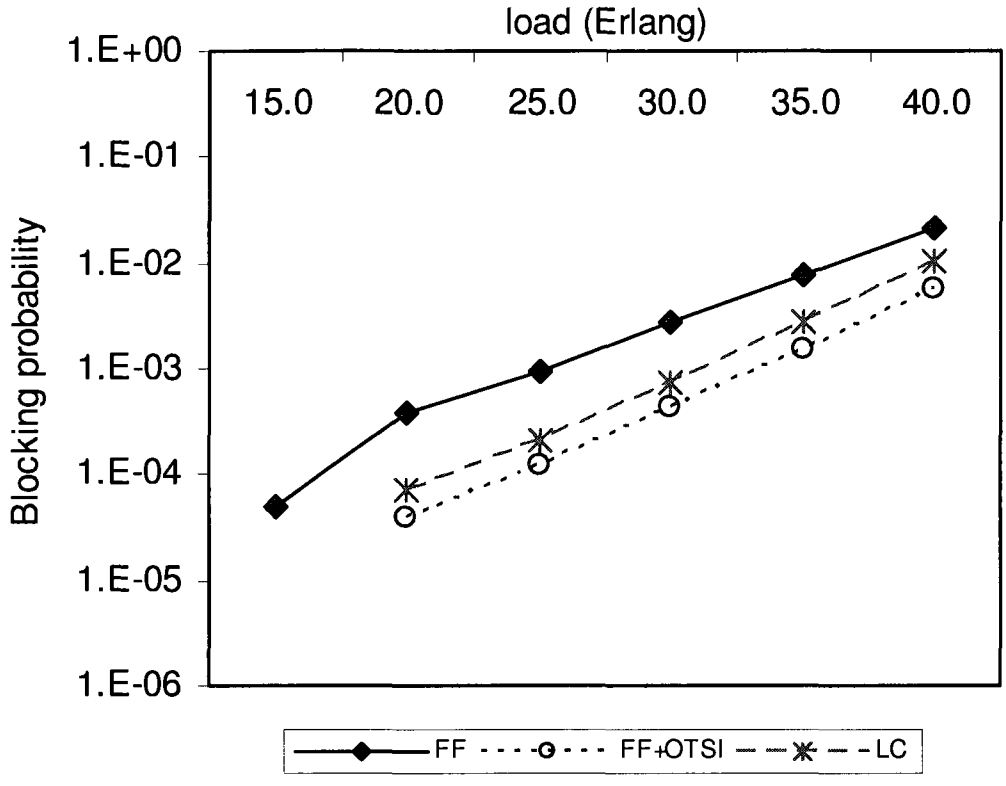

Figure 3.11: LC performance in 14-node ring network

Figure (3.12) shows the performance of the LC approach in a star network topology. It provides identical results to the FF approach. This result is expected since all links in a star have the same number of intersecting 2-hops routes; hence, all link-slot constraints were initially equal. In addition, when a reservation is made on a link-slot, corresponding link-slots in all other links get equally updated. Thus, the LC approach collapses to an FF approach in a star topology since the constraint scheme would have no impact.

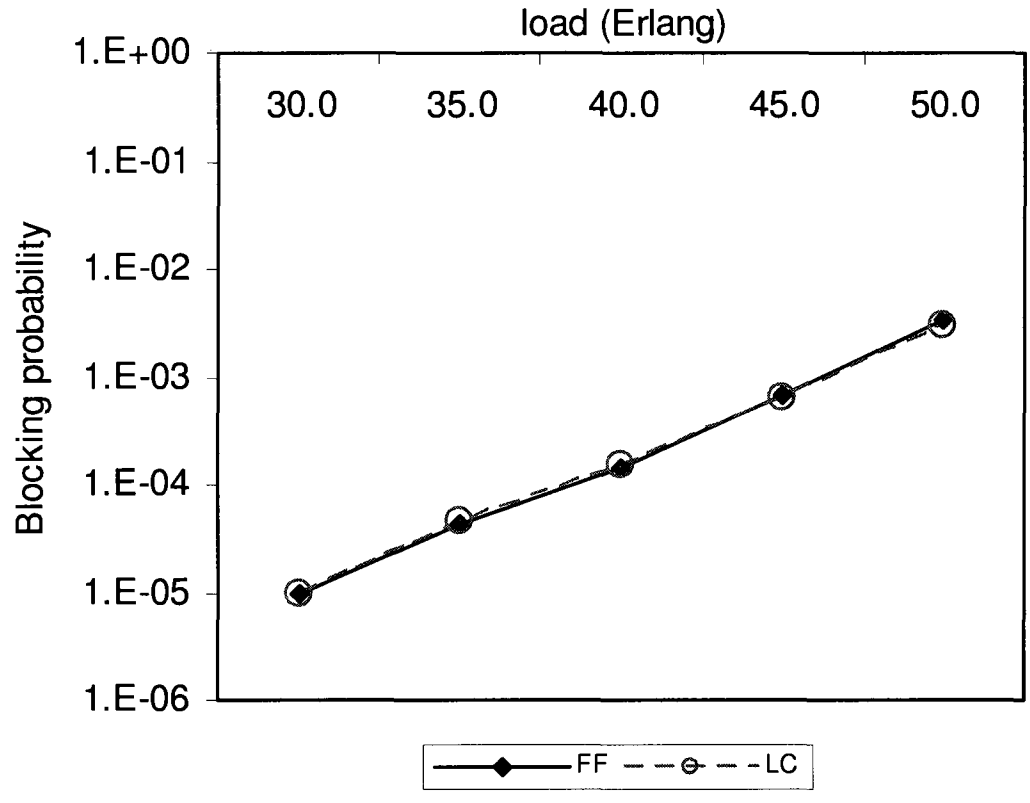

Figure 3.12: Measuring LC in a star network

Figure (3.13) shows two charts of the LC approach performance with non-uniform traffic distribution in NSF network. One of the charts represents the normal LC approach; and, the other shows the results of a modified version of the LC approach where the constraint of a link-slot is based on the intersecting route-slots availabilities multiplied by their corresponding routes load percentage ρ_{SD} according to the following Equation: $C_{XY_j} = \sum_{SD_i \in \Omega_{XY_j}} \left(A_{\overline{SD_i}} \times \rho_{SD} \right)$. For example with a non-uniform traffic distribution, if route SD serves 5 percent of the network traffic load, ρ_{SD} is then equal to 5. The charts clearly shows that considering the traffic loads of interesting routes when calculating resource constraints has no impact on the performance of the LC approach. In that sense, we say that the resource constraint in LC approach is load independent. As an elaboration, all link-

slots on a given link are equally loaded although the load distribution in the network is not uniform. The average load for a link-slot XY_j is $\rho_{XY_j} = \frac{\sum_{SD \in \Lambda_{XY}} \rho_{SD}}{N \times |\Lambda_{XY}|}$, where Λ_{XY} is the set of routes passing through link *XY*. Therefore, including the load in the link-slot constraint calculation does not add any value.

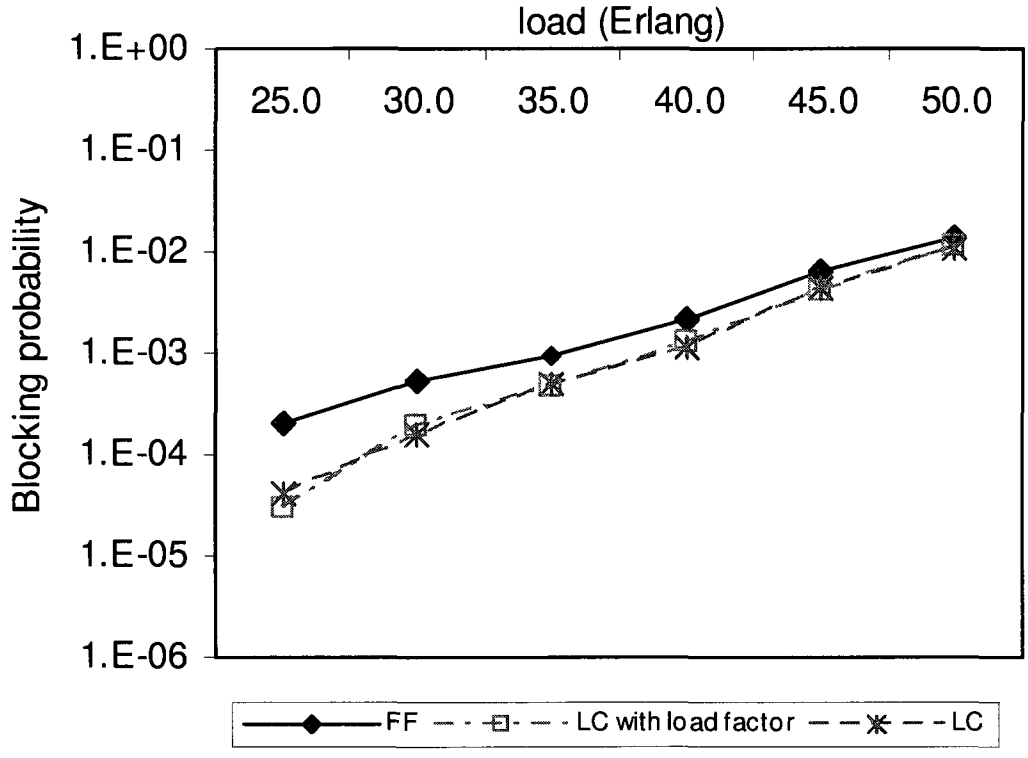

Figure 3.13: LC performance after factoring the load in the resource constraints

3.4. Analytical Discussion

In this section, we develop an equation for the blocking probability of the LC approach as a factor of the blocking probability of the FF approach. Our intention behind this informal

analysis is to add some clarity and assurance to the simulation results. It is imperative to say that this analysis is approximate. Most of the derived equations are approximations based on the assumption of uniform traffic distributions between all pairs of nodes and of a network architecture where all links are equally loaded. Over the course of our analytical discussion, we rely on the following basic definitions:

Symbol	Description
n	*Number of nodes*
l	*Number of links*
f	*Number of fibers per link*
t	*Number of time slots per frame*
λ	*Poisson arrival mean*
σ	*Average holding time*
$d = \frac{l}{n}$	*Average nodal degree* *(number of links / number of nodes)*
$h = \frac{n}{2d}$	*Average hops count* *(max hops count / 2)*
$r = \frac{n \times (n-1) \times h}{l}$	*Average number of intersecting routes per link* *(sum of link counts in all routes / number of links)*
$e = \frac{\sigma}{\lambda}$	*Average number of active connections* *(average holding / mean arrival)*
$\mu = \frac{e \times h}{l \times t \times f}$	*Load factor* *(number of used time slots / total number of time slots)*

Tab. 3.1: Analysis Symbols

Knowing the number of reserved connections (given by e) in the network, the average link-slot constraint can be calculated as follows:

$$C_{XY_j} = C_{max} - C_{upd} \tag{3.11}$$

where C_{max} is the maximum constraint value a link-slot can have:

$$C_{max} = r \times f \tag{3.12}$$

and C_{upd} is the average reduction of the constraint due to updates resulting from the reservation of e connections:

$$C_{upd} = \frac{e \times h^2 \times r \times K}{l \times t} \tag{3.13}$$

The parameter K represents the probability of a route-slot's availability being equal to the reserved link-slot's availability. Note that a link-slot reservation should affect an intersecting route-slot's availability only if they have the same availability. In this case, the constraints of the constituent link-slots should be updated. A route-slot's availability is equal to a link-slot's availability if this link-slot has the lowest availability among all constituent link-slots. Thus, K is equal to the probability of a link-slot's availability being less than or equal to all link-slot's availabilities in a route of h hops.

$$K = \left[P_{(A_{XY_j} \le A_{UV_x})}\right]^{h-1} \tag{3.14}$$

Knowing the availability range $[0. .f]$ and assuming that the availability of a link-slot can be any value in that range with equal probability, the probability that a link-slot's availability is less or equal than the availability of another link-slot can be approximated as:

$$P_{(A_{XY_j} \le A_{UV_x})} = \frac{\sum_{z=1}^{f+1} z}{(f+1)^2} = \frac{f+2}{2\times(f+1)} \tag{3.15}$$

By definition, the link-slot constraint is the sum of the availabilities of all route-slots that intersect in it. Therefore, it indicates the number of possible connections that get blocked should the link-slot become unavailable. In other words, reserving a link-slot XY_i, having $A_{XY_j} = 1$, would consequently block an average of C_{XY_j} possible connections. Thus, the number of blocked connections, when the link-slot gets unavailable, is equal to the link-slot's constraint at the reservation time. Let B_{XY_j} be the average number of blocked connections as a result of consuming the last availability on a link-slot. If υ is the average number of link-slots that are unavailable in a uniformly loaded network, the network blocking probability can be described as follows:

$$P = \frac{\upsilon \times B_{XY_j}}{l \times t \times f} \tag{3.16}$$

If $P_{(FF)}$ and $P_{(LC)}$ are the blocking probabilities related to the FF and LC approaches, respectively, we derive:

$$P_{(LC)} = \frac{B_{XY_j}^{LC}}{B_{XY_j}^{FF}} \times P_{(FF)} \tag{3.17}$$

With the FF approach, there is no mandate to select the least constraining route-slot during the allocation process, as in the LC case; selection is rather arbitrary. Thus, the average number of blocked connections when reserving XY_j $B_{XY_j}^{FF}$ tends to be equal to the average link-slot constraint described in Equation (3.11). On the other hand, the LC approach

always favors the least constraining route-slots; and hence, $B_{XY_j}^{LC}$ tends to be below average according to the following formula:

$$B_{XY_j}^{LC} = \delta \times C_{XY_j} \quad , \quad where\ 0 < \delta \leq 1 \tag{3.18}$$

and, consequently

$$P_{(LC)} = \delta \times P_{(FF)}, \quad where\ 0 < \delta \leq 1 \tag{3.19}$$

To get an approximation of $B_{XY_j}^{LC}$, we need to understand the distribution of the constraint values in the network. A link-slot constraint can be between *0* and C_{max}. Figure (3.14) shows the distribution trend of constraint values amongst the link-slots in the network. Each chart represents the percentage trend of link-slots that have low, medium, and high constraints under a specific load level. In a non-loaded network, all link-slot constraints are equal to C_{max}; i.e. 100% of link-slots have high constraints. We know that the constraint of a reserved link-slots is reduced by $r \times K$; and consequently, the constraint of $(h-1) \times r \times K$ updated link-slots is reduced by 1. Thus, the constraint of a reserved link-slot is reduced at a much greater rate than an updated link-slot. In a low loaded multi-fiber network, the number of reserved link-slots given by $e \times h$ is low; however, the number of updated link-slots given by $e \times (h-1) \times r \times K$ is relatively high. Thus, the percentage of link-slots having low constraints is low, and the percentage of link-slots having medium constraints is relatively higher. This trend is different in a single-fiber network due to the narrower range of constraint values, where $C_{max} = r$. The average reduction rate in a single-fiber network is $\frac{r}{C_{upd}}$; while this rate is $\frac{r \times f}{C_{upd}}$ in the multi-fiber case. In addition, a reserved link-slot in a single-fiber network has *zero*-constraint since it has *zero*-availability which eventually blocks all intersecting route-slots. Thus, the percentage of link-slots having low constraints is much higher than those with medium constraints in a

low loaded single-fiber network. At average load, the percentages of link-slots with low, medium and high constraints are comparatively close in a multi-fiber network. However in an average loaded single-fiber network, the percentage of link-slots having low constraints gets relatively higher than those with medium constraints due to the higher reduction rate as compared to the multi-fiber case. At high load, the trend is similar in single and multi-fiber cases where the percentage of link-slots with low constraints is relatively high.

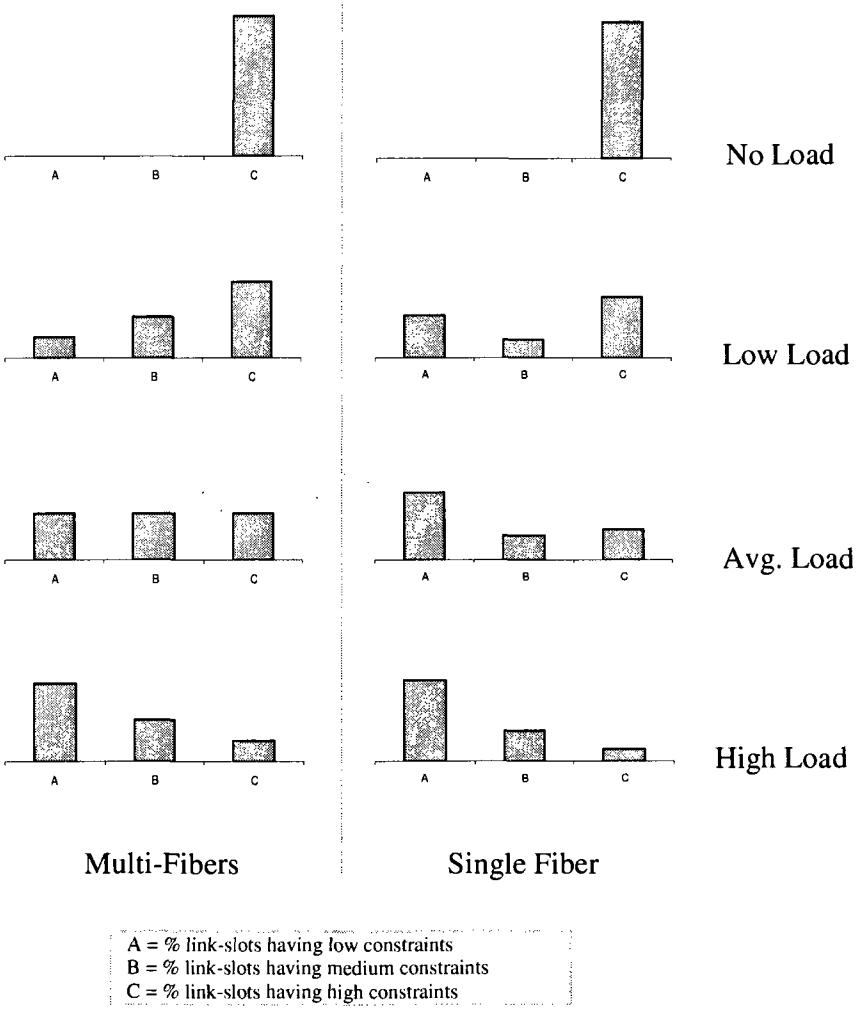

Figure 3.14: Percentage of link-slots having low, average, and high constraints

Based on the charted trends, we deduce that the value of $B_{XY_j}^{LC}$ is within a range between low and average constraints. It tends towards low constraints with high loads, and towards average constraints C_{XY_j} with low loads. In an average loaded multi-fibers network where the constraint values are uniformly distributed amongst link-slots, the average constraint is $C_{XY_j} = \frac{C_{max}}{2}$, and the average constraint below C_{XY_j} is $\frac{C_{XY_j}}{2}$. Link-slots with constraints between 1 and $\frac{C_{XY_j}}{2}$ are the least constraining and their average is $\frac{C_{XY_j}}{4}$. Thus, $B_{XY_j}^{LC} = \frac{1}{4} C_{XY_j}$ (i.e. $\delta = \frac{1}{4}$). At low load, C_{XY_j} is greater than $\frac{C_{max}}{2}$; in this case, δ needs to be slightly decreased to keep $B_{XY_j}^{LC}$ close to the low constraint values. On the other hand, C_{XY_j} is less than $\frac{C_{max}}{2}$ at high load; in this case, δ needs to be slightly increased to keep $B_{XY_j}^{LC}$ away from *zero* and close to the low constraint values. δ is adjusted by φ, where $-0.25 \le \varphi \le +0.75$. To generalize, we assume that $\frac{C_{XY_j}}{C_{max}} \le 0.75$ since the opposite is only possible at extremely low loads where virtually no blocking is noticed regardless of the allocation scheme. Based on these assumptions, we approximately define φ as follows:

$$\varphi = 0.5 - \frac{C_{XY_j}}{C_{max}} \tag{3.20}$$

and hence, δ for the multi-fibers case is defined as follows:

$$\delta = \frac{1}{4} + \varphi = \mu \times h \times \left(\frac{f+2}{2(f+1)} \right)^{h-1} - 0.25, \quad where \quad f > 1 \tag{3.21}$$

In a single-fiber network, δ is slightly different due to the constraint's higher reduction rate as compared to the multi-fiber case. Thus, we should redefine it as a special case. Starting with an average loaded single-fiber network, the average link-slot constraint C_{XY_j} is less than $\frac{C_{max}}{2}$ since the percentage of low constraint link-slots is higher than the medium constraint ones. In addition, we know that a substantial portion of the low constraint single-fiber network's link-slots have actually *zero*-constraints. Thus, $B_{XY_j}^{LC}$ cannot be between *0* and $\frac{C_{XY_j}}{2}$ as is the case of an average loaded multi-fiber networks. It should rather be between $\frac{C_{XY_j}}{2}$ and C_{XY_j}. As an approximation, we write $B_{XY_j}^{LC} = \frac{3}{4} C_{XY_j}$ (i.e. $\delta = \frac{3}{4}$). As with the multi-fiber case, δ needs to be shifted by φ' with lower and higher loads as described in the multi-fiber case, where $-0.75 \le \varphi' \le +0.25$. As a generalization, we write φ' = 2φ, assuming that $\varphi \le 0.125$. In fact, φ is greater than *0.125* only at extremely high loads, where the performance of the optimum allocation approach (FF+OTSI) converges to the performance of the FF approach. Knowing the initial value for δ and the scale φ, we derive $\delta_{P(LC)}$ for the single fiber case:

$$\delta = \frac{3}{4} + 2\varphi = 2 \times \mu \times h \times \left(\frac{f+2}{2(f+1)} \right)^{h-1} - 0.25, \quad where \quad f = 1 \tag{3.22}$$

Note that Equations (3.21) and (3.22) are approximations since they are based on the assumption of uniform traffic and equal traffic load for all links. In addition, the constraint values are assumed to be distributed based on the heuristic described in Figure (3.14). Thus, subsequent equations that include δ are informal approximation rather than formal equations.

As a unified definition for both single and multi-fiber cases, $P_{(LC)}$ can be described as follows:

$$P_{(LC)} = \left(\left\lfloor \frac{f+1}{f} \right\rfloor \times \mu \times h \times \left(\frac{f+2}{2(f+1)} \right)^{h-1} - 0.25 \right) \times P_{(FF)} \qquad (3.23)$$

Figure (3.15) shows a comparison between the analytical results and their simulation counterparts, relying on the same parameters adopted in the simulation of a multi-fiber network. In addition, Figure (3.16) represents the same comparison for the single-fiber case. Note that we used the simulation results for $P_{(FF)}$ instead of deriving them analytically for the sake of accurate comparison between the simulation and analytical results. In both graphs, the analytical results are close to the simulation's outputs, and reflect the same trend. The slight difference in performance results is attributed to the approximations we have made at various steps of this analytical study.

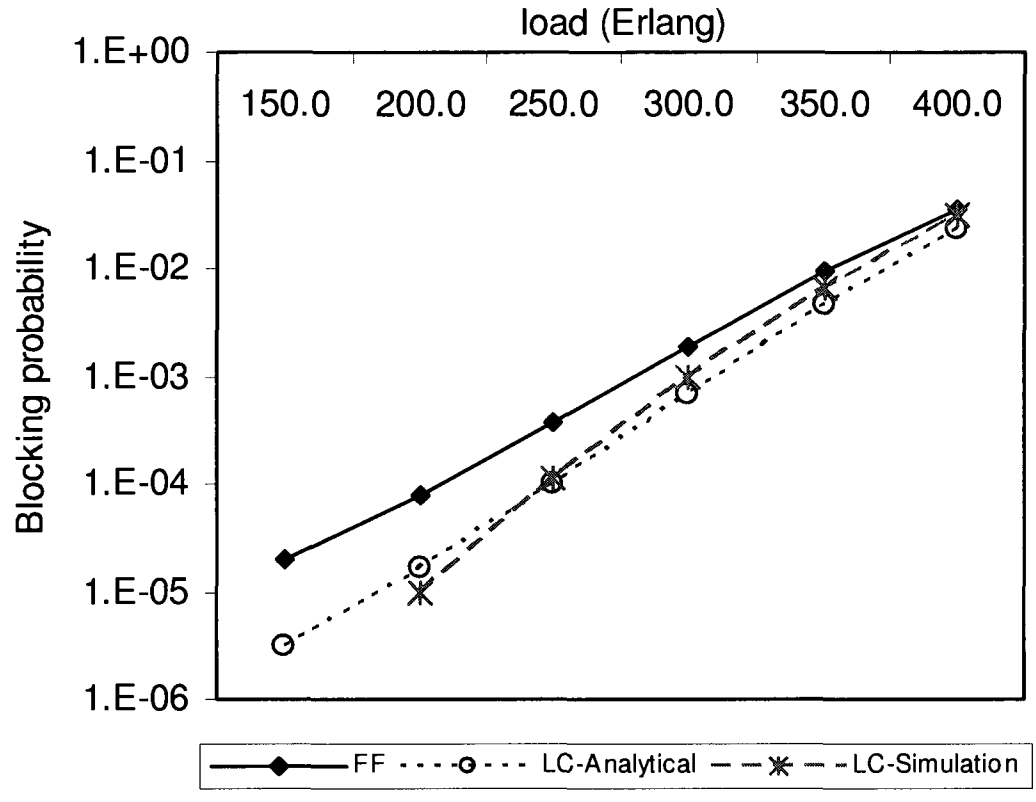

Figure 3.15: Analytical results of the LC approach in a multi-fiber network

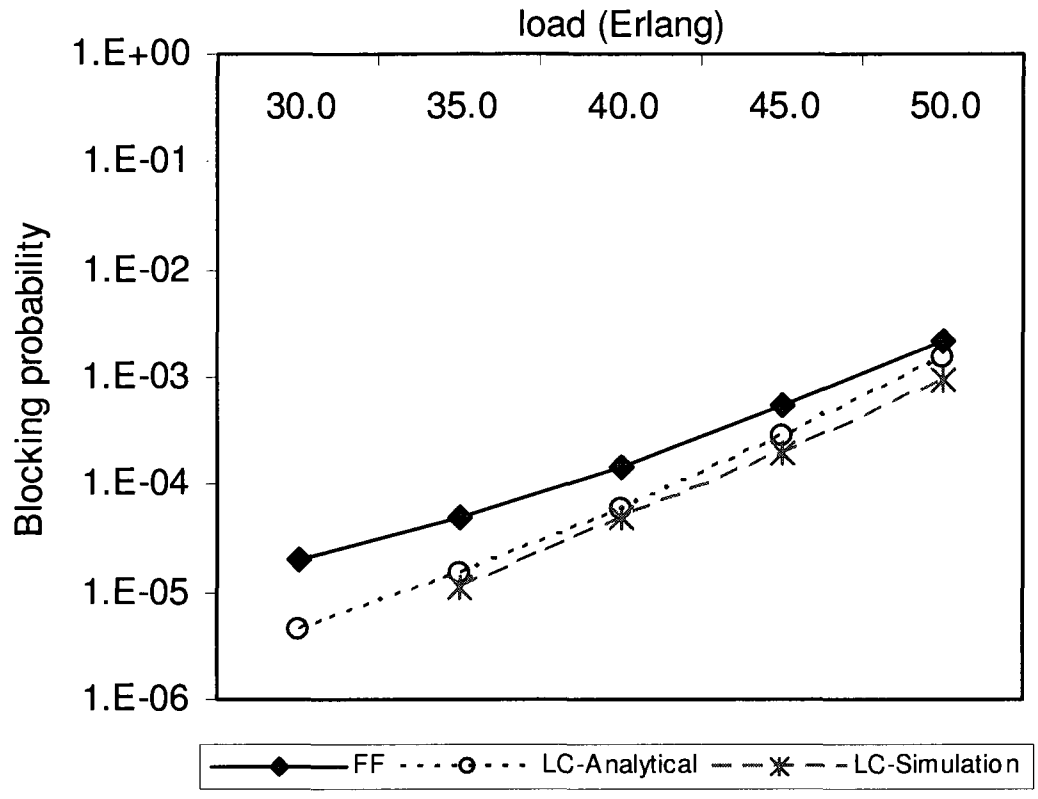

Figure 3.16: Analytical results of the LC approach in a single-fiber network

3.5. Conclusion

After proposing the least constraining slot reservation approach (LC) in all-optical TDM networks, we compared its performance to the first-fit (FF) approach, and FF with optical time slot interchangers (OTSI). The LC approach provides a performance gain close to the FF approach with OTSI. The result is consistent under uniform and non-uniform traffic distribution. In addition, we found that the LC approach outperformed the least loaded (LL) approach in multi-fiber environments. Thus, LC has an edge over LL, since the

former is not restricted to multi-fiber networks as is the latter. On the other hand, the LC approach did not show any performance improvement over the FF approach when considering a star topology synchronized on slot boundaries. The reason for this result can be attributed to equal slot constraints and fixed hop counts in the star topology. Finally, we tried a variation of the LC approach in which we included the load as a factor in the constraint calculation. We found that the load factor has no impact on the network performance. As an analytical elaboration, we defined the blocking probability of the LC approach as a ratio of blocking in the FF approach. These analytical results are close to the simulations. As a conclusion of this chapter, we say that the LC approach provides close to optimum performance in optical TDM networks with no buffering regardless of the load distribution or the number of employed fibers per link.

4. Distributed Algorithm for the Least Constraining Slot Allocation Scheme in a GMPLS Context

4.1. Introduction

In this chapter, we propose a distributed solution for the least constraining slot reservation scheme. Our aim is to employ LC in the context of Generalized MPLS [RFC3945]. The key components of a distributed bandwidth allocation scheme are the nodal database containing information about the status of the network, the reservation protocol, and the status update mechanism. A nodal database contains a subset of the centralized view having minimum information required to participate in a distributed bandwidth allocation process. The outcome of the distributed process should be identical to the output of the centralized scheme. Therefore, the data stored at each node must be carefully defined, exchanged and updated during the network life time. Exchanging minimum and adequate information among nodes during an allocation process is essential in making the right allocation decision with a low bandwidth overhead. Information exchange is required during the reservation and status update phases. During the reservation phase, the exchange is confined among the nodes existing along the considered route. On the other hand, status update information should be broadcast to a large group of nodes that should know about a particular status change. This group usually contains all nodes whose database should be updated as a result of a status change along a network route. Usually, the group of updated nodes is the entire network as with the OSPF link state update protocol employed in GMPLS.

Aiming to make the LC scheme applicable in the context of GMPLS, we should define a distributed algorithm that blends well with the GMPLS protocols. In GMPLS, each node has a database and exchanges link state information via update messages based on the Open Shortest Path First (OSPF) [RFC2328] or Intermediate System to Intermediate System (IS-IS) routing protocols [RFC1629]. For connection reservation, GMPLS uses the Resource Reservation Protocol with Traffic Engineering (RSVP-TE) [RFC3209] or the Constraint-Based Routing Label Distribution Protocol (CR-LDP) [RFC3212]. Both reservation protocols require two phases: the label request phase issued by the source node which is followed by the label response phase issued by the destination.

In this chapter, we define the nodal database and the basic parameters to be added to GMPLS' reservation and status update messages. Ideally, resource update should occur after each reservation. However, to comply with GMPLS periodic link state updates, we intend to reduce the LC resource status update rate to a level that matches GMPLS standards while maintaining close to optimum performance. In the following sections, we describe the elements of our distributed scheme and how it complies with GMPLS. Before concluding this chapter, we discuss the effect of reducing the rate of resource status updates on the network performance.

4.2. Distributed Approach

4.2.1. Node Database

Each node in a network employing the distributed LC approach maintains a database containing basic information essential for the decentralized reservation process. Basically, for each outgoing link *XY* at a node *X*, two lists must be maintained: Links Info List (LIL) and Link-Slots Info List (LSIL). LIL has entries for each link in the network that shares a route with *XY*. A LIL's entry corresponding to link *UV* has the following structure:

- Total delay *d* in time slot units between nodes *U* and *X*. If *U* is upstream from *X*, the delay is a positive integer; otherwise, the delay is negative.

- Common Route-Slots List (CRSL) containing entries for all route-slots that have link *XY* and *UV* in their paths. Each CRSL entry stores the following data:
    - Link-slot availability list (LSAL) indexed by link-slot. In general, the LSAL contains the availabilities for a selection of link-slots. In this context, it should contain the availabilities for the constituent link-slots

LSIL has an entry for each link-slot on *XY*, which contains the following data:

- Availability
- Constraint

As a graphical elaboration, Figure (4.1) represents the described nodal database in a hierarchical model.

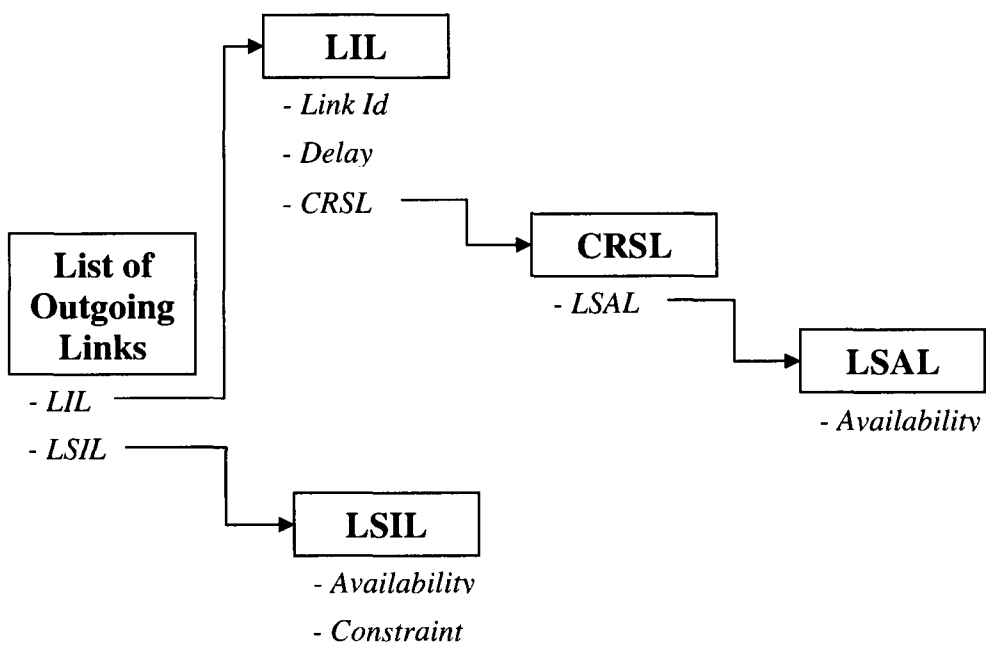

Figure 4.1: Nodal database hierarchy

4.2.2. Reservation process

Although the aim is to extend the existing RSVP-TE or CR-LDP protocols, we define a new set of messages that can be integrated later with the corresponding messages in these protocols just to avoid lengthy technical discussions that go beyond the scope of this work. The distributed LC approach uses the following messages during the slots reservation process:

- Request (REQ): it contains source and destination node ids, the cumulative delay, and a route-slot constraint list (RSCL) reflecting the constraints of all available route-slots. The content of the REQ can be integrated with the RSVP Path message.
- Response (REP): it contains source and destination node ids, a selected route-slot, the cumulative delay, and an LSAL. The LSAL in this context contains the availabilities of the constituent link-slots. These parameters can be integrated with RSVP Resv message.
- Release (REL): it contains the destination node id, and a link-slot. It can be integrated with the RSVP Resv Teardown message.
- Negative Acknowledgment (NACK): it is used to inform the source of a denied request. This acknowledgment can be realized by using an RSVP Path Error message.

During a reservation process, the following steps are performed:

1. The source node sends a REQ to the destination on a predetermined route. It initially sets the REQ RSCL parameters to the constraint values stored in the outgoing link's LSIL.
2. An intermediate node receives the request message, and performs the following steps before forwarding the received message to the next node on the route:
   i. Identify matching link-slots on the outgoing link by using the cumulative delay in the REQ.
   ii. Add the link-slot constraints in the outgoing link's LSIL to the corresponding route-slot constraints in the REQ RSCL.
   iii. Set the availability in each entry of the RSCL to the availability of its corresponding link-slot only if the latter value is less than the former.

iv. Add the corresponding delay *d* in the LIL to the cumulative delay in the REQ.

3. When a destination node receives the REQ, it sends a REP to the source node after setting the REP's route-slot field to the lowest weighed route-slot in the received REQ RSCL. It also sets the REP's cumulative delay to the REQ's cumulative delay.
4. When an intermediate node receives the REP, it does the following before forwarding the received REP to the next node on the reverse route to the source.
   i. Deduct the corresponding delay *d* in the LIL from the REP's cumulative delay.
   ii. Identify and lock the link-slot that matches the selected route-slot by referring to the cumulative delay.
   iii. Insert the availability of the corresponding link-slot into the REP LSAL

When the REP message reaches the source node, the node starts transmitting on the reserved route-slot. After completing the communication process, the source sends a REL message towards the destination to free all resources, which were locked for serving the communication request. The diagram in Figure (4.2) shows a use case of a reservation operation on a 3-hop route.

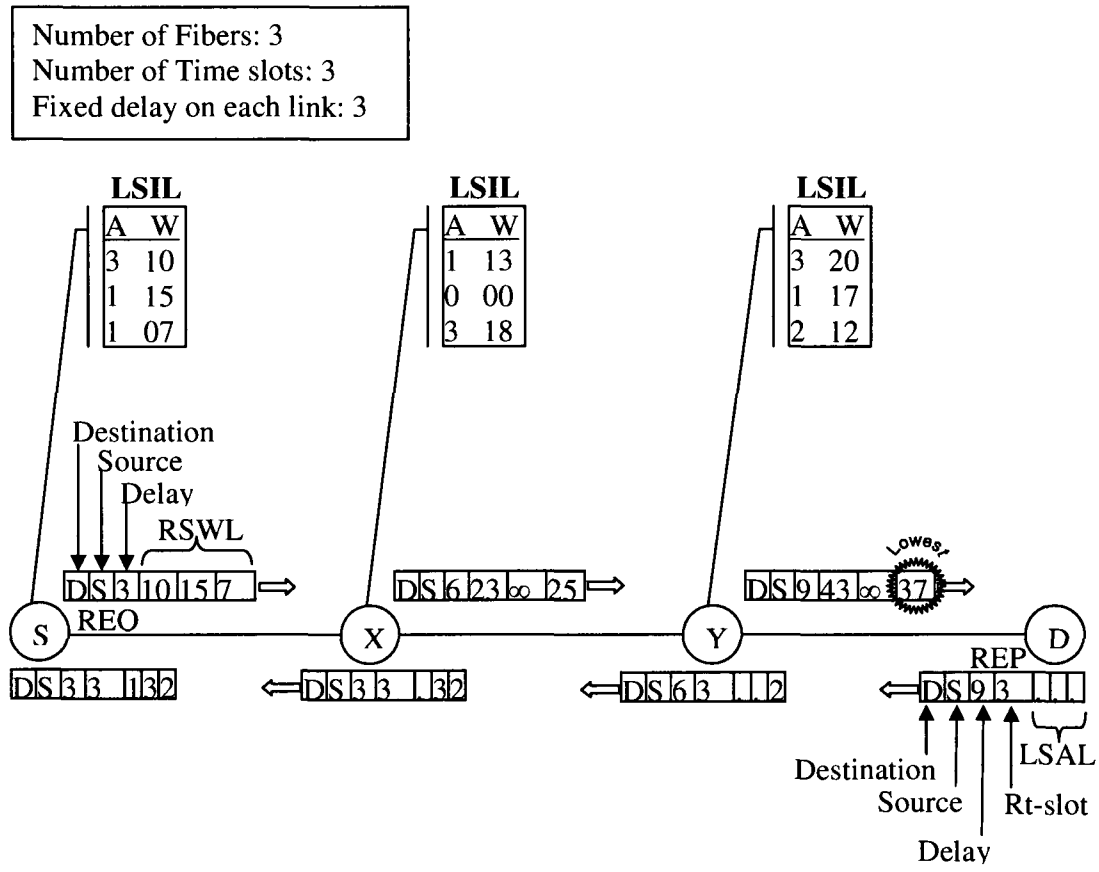

Figure 4.2: reservation use case

A request for communication can be rejected either during the REQ phase or the REP phase. If no matching resource is available during a REQ phase, the REQ message is dropped and a NACK is sent back to the source. In this case, the connection is considered blocked. On the other hand, if two REPs on two intersecting routes require the same available link-slot on the intersection link, the corresponding intermediate node locks this link-slot to the first arriving REP and drops the later one. It sends a NACK to the source of the dropped REP and a REL to its destination in order to free the locked resources. In this case, the connection is not considered blocked since the source node can retry with another REQ. Further details on the rejection scenarios during the REQ and REP phases can be found in [Yuan1996].

4.2.3. Resource Status Update

With every established or released connection, the constraints and availabilities of corresponding resources change across the network. Therefore, a resource status update scheme is required to keep the databases of all nodes up to date. An update scheme can be immediate or periodic. An immediate update is broadcasted by the source node when a route-slot is reserved or released. On the other hand, a periodic update is broadcast by all nodes at regular time intervals like the OSPF link state update mechanism. In both schemes, we employ an update message (UPD) similar to the OSPF Update message. However, we append an LSAL as an extra parameter.

During our work to simulate irregularities and errors in the centralized scheme, we explicitly forced our simulation algorithm to skip the immediate update for n successive calls and then to execute a periodic update operation before the $(n - 1)^{th}$ call. We noticed that network performance remained close to optimum for relatively large n. It basically means that one resource status update every t period of time could maintain close to optimum performance and significantly reduce the associated signaling cost. In addition, if t is greater or equal to 30 min, the update process can be integrated with the link state procedure of GMPLS.

4.2.3.1. Immediate Resource Status Update

The following steps occur during an immediate resource status update:

1. The source node notifies all nodes in the network about the reservation or release of link-slots by broadcasting a UPD message containing the LSAL that was contained in the received REP.
2. Each node receiving the notification performs the following steps for each reserved or released link-slot XY_i in the LSAL:
   i. Identify the outgoing link UV that shares a common route with link-slot XY_i if any, by referring to the locally stored LIL.

ii. Identify the corresponding local link-slot UV_j by using the total delay from the reserved link's upstream node X to this local node U.

iii. Identify the route-slot $\overline{SD_k}$ joining link-slot XY_i with the corresponding local link-slot UV_j. This can be achieved by referring to the locally stored CRSL.

iv. Depending on the notification type, update the constraint and availability as follows:

a. *Reservation Notification*: Indentify the route-slot availability $A_{\overline{SD_k}}$ which would be the minimum availability in the LSAL of the corresponding CRSL entry. First, if $A_{\overline{SD_k}}$ is equal to A_{XY_i}, deduct 1 from the constraint of the corresponding local link-slot UV_j. Second, deduct 1 from the availability of XY_i in the CRSL LSAL.

b. *Release Notification*: Indentify the route-slot availability $A_{\overline{SD_k}}$ which would be the minimum availability in the LSAL of the corresponding CRSL entry. If $A_{\overline{SD_k}}$ is equal to A_{XY_i}, check the CRSL LSAL for other slots that has the same availability. If no slots other than XY_i are identified, then add 1 to the constraint of the corresponding local link-slot UV_j.

4.2.3.2. Periodic Resource Status Update

In order to implement a periodic resource status update, the following steps are essential:

1. At a fixed time interval t, every node in the network compiles an LSAL and appends it to a UPD message before broadcasting it to the network. A compiled LSAL contains only link-slots availabilities whose values have changed since the previous notification.
3. Each node receiving the notification performs the following steps for each link-slot XY_i in the LSAL:

i. Process the first 3 steps of the immediate update case.

ii. Set the corresponding link-slot availability in the CRSL LSAL to the availability of the considered link-slot XY_i. Identify the new route-slot availability $A_{\overline{SD_k}}$ which

would be the minimum availability in the LSAL of the corresponding CRSL entry. Depending on the resulting change Δ between the old and new route-slot availability, the constraint of the corresponding local link-slot should change accordingly. If Δ is positive, increase the link-slot constraint by Δ; otherwise, decrease it by $|\Delta|$.

4.2.4. Backward vs. Forward Reservation

The described reservation protocol is a backward reservation scheme according to the criteria described in [Yuan1996]. We chose the backward approach because it is proven in [Yuan1996] that the backward scheme outperforms the forward scheme. In addition, it matches with the GMPLS backward reservation protocols. If we adopt the forward approach, all available resources should be locked during the REQ phase. They would be unlocked except for the reserved resources during the REP phase. Although, this mechanism would eliminate the problem of blocking during the REP phase, it increases blocking during the REQ phase as the locked resources on a given link would block any communication request on that link. On the other hand, a response might be blocked in the backward scheme only when another REP is quicker to reach a contended resource.

4.3. Simulation Results

In this section, we discuss the performance of the distributed LC approach under various status update rates. Our observations are based on simulation results following the same simulation guidelines as in Chapter 3.

Figure (4.3) shows the performance of the LC approach for different status update frequencies. Best performance is obtained for immediate updates, that is, an update after each call accepted or terminated. In the case that an update is only done after 100 000 new calls have been accepted by the network, we obtain what we call "degraded performance"; this performance is approximately one half of the best-performance level that is attained

with immediate updates. Performance remains at that degraded level even if we increase the update rate to once per 100 calls (arriving to the network). However, if the update rate is increased to once per 10 calls, we obtain best performance as in the case of immediate updates. Figure (4.4) shows similar results for non-uniform traffic.

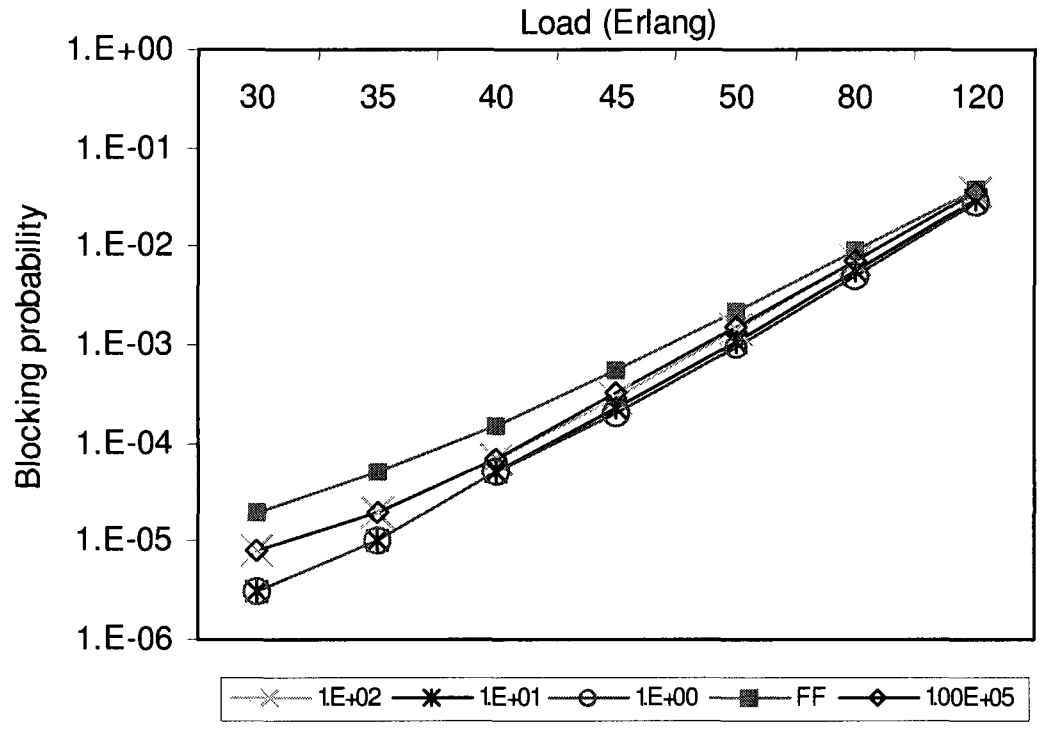

Figure 4.3: LC performance for different update rates (once per 1E+x calls) – with uniform traffic

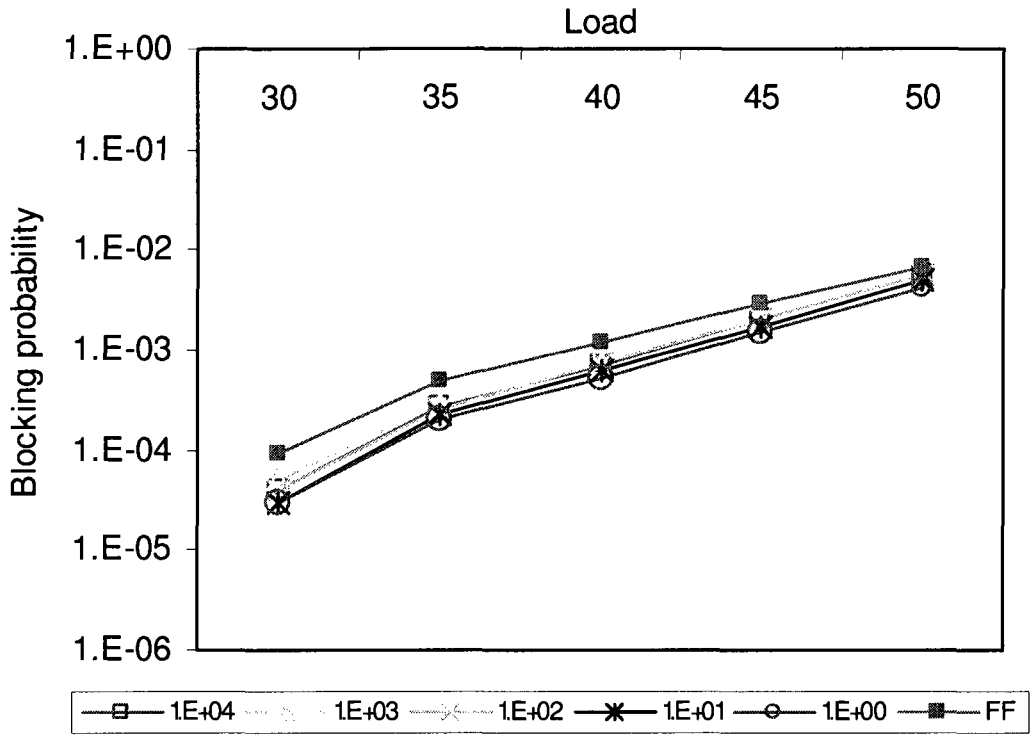

Figure 4.4: LC performance for different update rates (once per 1E+x calls) – with non-uniform traffic

Figure (4.5) is a chart that shows samples of blocking probability collected over several short periods of 10 calls each. To reduce statistical variations caused by sampling over short periods, the same simulation is repeated 10000 times with a high load of 120 Erlang. The employed status update rate is once per 500 calls after an initial period (not shown in the diagram) of immediate updates. We notice an initial transition period of gradual performance degradation reflected in the early samples. The transition is from the best-performance level to the degraded performance level. The first couple of samplings are close to the best performance rate of 0.027. If we average out the statistical variations after the transition period, the worst performance rate seems to stabilize at a fixed level of 0.035 on average. The chart also shows that subsequent (single) status updates (see vertical dotted lines) do not reproduce the best performance rate observed earlier.

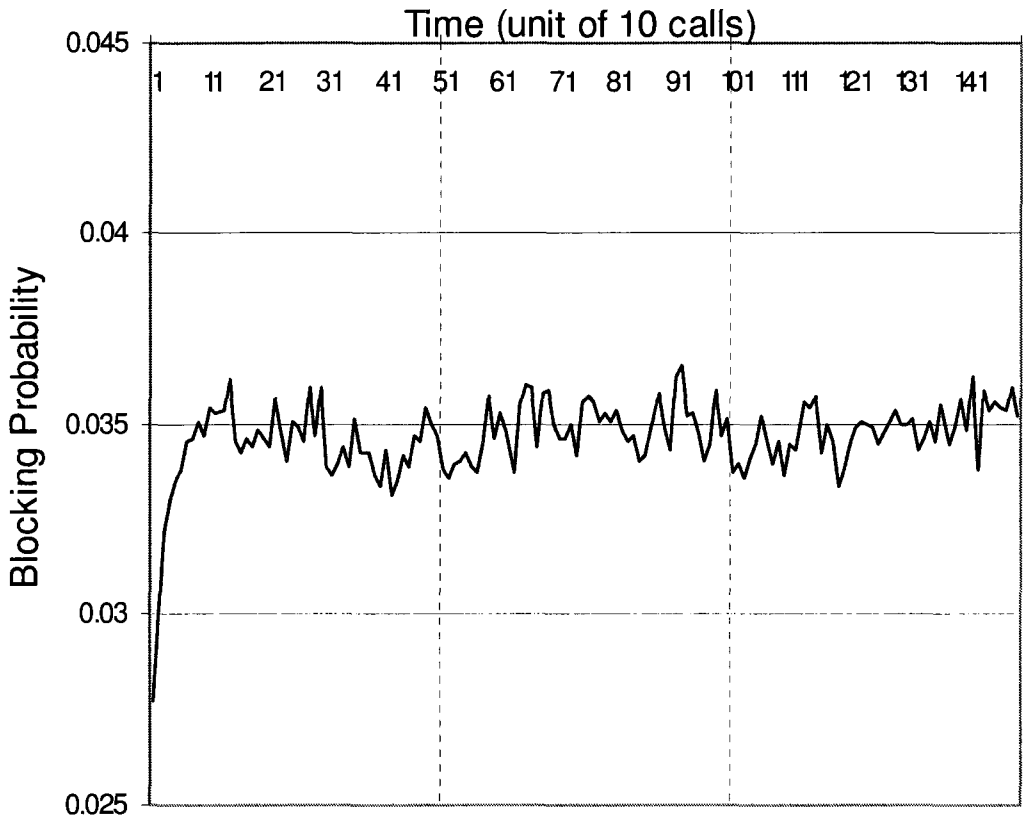

Figure 4.5: LC performance measured every 10 calls – load is 120 Erlang – (update rate is once every 500 calls)

To discuss these results further, we define the following:

- ω_τ: is the list of all recorded route-slots constraints in the network. The constraint values are based on link-slot constraints that are recorded in nodal databases.
- $\acute{\omega}_\tau$: is the list of all actual route-slots constraints in the network. The constraint values are based on actual link-slot constraints which are not recorded in nodal databases.
- *Low*(*SD*, ω_τ): is a function that returns the available route-slot on route *SD* that has the lowest constraint according to ω_τ.

In the case of immediate updates, ω_τ should always be equal to $\acute{\omega}_\tau$ at any time *t*; i.e. $\omega_\tau = \acute{\omega}_\tau$, and hence *Low*(*SD*, ω_τ) = *Low*(*SD*, $\acute{\omega}_\tau$) for all routes at any point in time. This equation is essential for a perfect route-slot allocation pattern and best network performance. Starting from a perfect LC allocation pattern and stopping all further updates, ω_τ and $\acute{\omega}_\tau$

would break ties after the first allocated or de-allocated call; and ω_τ is said to be outdated. However, the equation $Low(SD, \omega_\tau) = Low(SD, \acute{\omega}_\tau)$ might still hold for a majority of routes during the first few allocated or de-allocated calls. As long as this equation holds for the routes at which all subsequent calls arrive, the system would allocate the same route-slots that would be chosen in the case of immediate updates. Thus, the perfect LC route-slots allocation pattern in the network is maintained, and hence best performance is preserved. As soon as a call arrives at a route *SD* where $Low(SD, \omega_\tau) \neq Low(SD, \acute{\omega}_\tau)$, the resulting allocation pattern becomes imperfect; and hence performance starts to degrade. The length of the best performance period preceding the degraded performance is analyzed in Section 4.4. During the best performance period, the constraints in $\acute{\omega}_\tau$ will always be based on a perfect LC allocation pattern. As a result, if (single) updates occur at a period shorter than or equal to the best performance period, ω_τ will always be based on a perfect LC pattern; best performance is continually maintained. On the other hand, if (single) updates occur at a longer period, ω_τ will most likely be based on an imperfect allocation pattern leading to degradation of performance.

Regardless of the update rate, network performance is at the degraded level as long as the update interval is longer than the best-performance period. Note that if the route-slot allocation pattern becomes imperfect it reflects an imperfect $\acute{\omega}_\tau$. After an update, $\acute{\omega}_\tau$ gets copied to ω_t which would emphasize the pattern's imperfection. Thus, further updates emphasize rather than fix imperfection; and hence, the irrelevance of update rates to the performance degradation level is now clear.

Although the route-slot allocation pattern is imperfect, the performance level is still better than the performance level of the FF approach. Note that an outdated ω_τ still imposes an order that the system follows when allocating route-slots. This order is the result of the most recent LC update. It actually gives different priorities to the route-slots in all routes according to the constraints collected by the last update. Note that the resulting priority order for different routes is not arbitrary but rather synchronized based on the LC update. This synchronization between different routes is the essence behind the degraded performance level which is better than the worst case scenario of the FF approach. As an

analogy, a synchronized traffic light system based on an outdated traffic pattern would still manage traffic better than a chaotic arbitrary system.

Figure (4.6) shows the performance trend when moving from a period of no update to immediate updates. It is the opposite of what is shown in Figure (4.5) in order to understand the transition from degraded to best performance when re-invoking the immediate update scheme after a relatively long period of no updates. The results are based on the same test used for Figure (4.3), but we interleave a period of immediate updates equal to 500 arrivals starting after the 500^{th} arrived call. It clearly shows that network performance returns to best performance after a short transition period equal to the transition time between best and degraded performance level (~30 arrived calls).

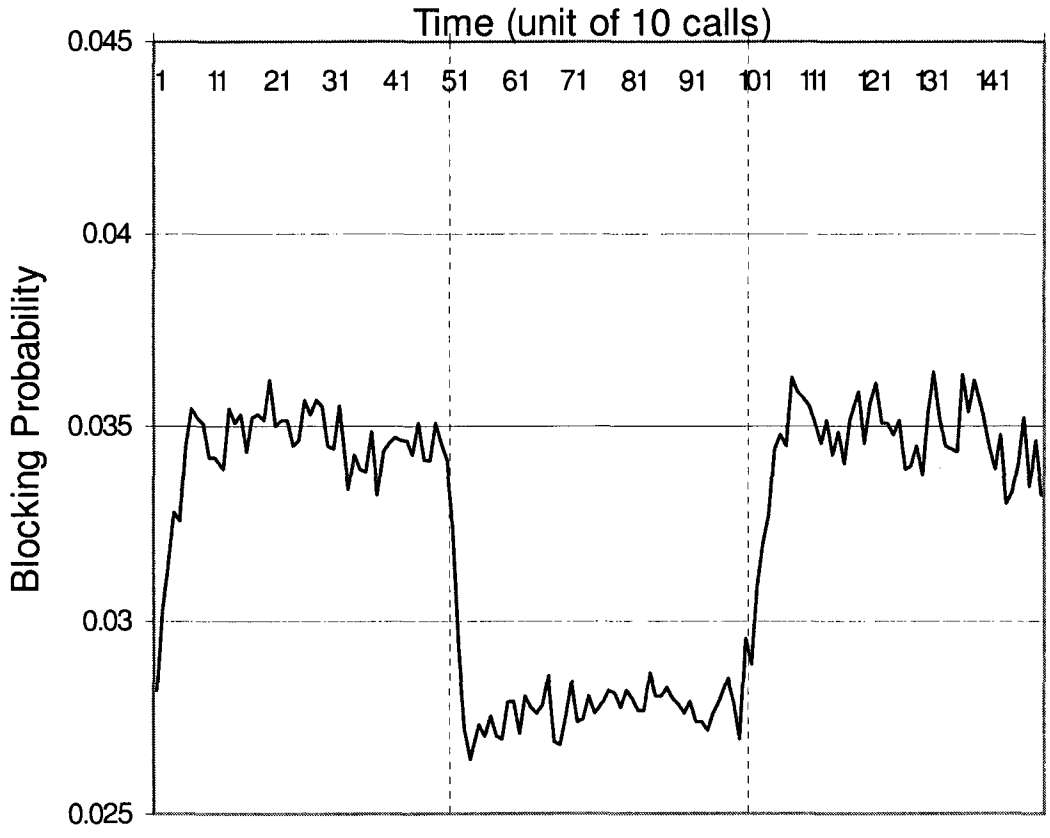

Figure 4.6: LC performance measured every 10 calls – load is 120 Erlang –(update rate is none for the first and last 500 calls, and immediate updates for the middle 500 calls)

Going back to Figure (4.5), the same performance trend is achieved under uniform and non-uniform traffic. However, in real life, the non-uniform traffic patterns may change over time throughout the network life time. For instance, the traffic pattern might differ between day and night, or winter and summer, in a given network. Therefore, we need to test the distributed LC approach in a network with non-uniform traffic distribution among source destination pairs, where the distribution pattern changes at a certain point in time. Figure (4.7.a) shows the results of a test, in which there is a shift from non-uniform traffic distribution pattern X to Y in the middle of the test during a period of no updates. The grayed area highlights the results under traffic pattern Y. The chart shows a severe deterioration in performance after a short period of brisk improvement right after the pattern's shift. When immediate updates are employed again after a period of 500 arrived calls, performance improves slightly. In addition, when updates stop after another period of 500 arrivals, performance deteriorates again to the same level just before the most recent immediate update phase. In fact, the severe performance deterioration is intrinsic to the new adopted traffic distribution pattern. Figure (4.7.c) shows the network performance when traffic pattern Y is adopted from start to finish using the same traffic load used in the test of Figure (4.7.a). It clearly shows that the blocking rate with the LC approach with no status update is equal to the performance level shown in section Y1 and Y3. Similarly, the blocking rate during immediate updates is equal to the performance level shown in sections Y2. Figure (4.7.b) also shows the related results for traffic pattern X. The spiky performance improvement, right at the cusp between the periods of the two traffic allocation patterns, exists because both patterns fill different areas of the network with different loads. When pattern Y takes over, it loads areas that aren't heavily used by pattern X; and hence, performance improves for a short period until these areas are loaded according to the new pattern. Therefore, changing the non-uniform traffic allocation pattern over the course of network operation has no impact on the performance level individually achieved by each traffic distribution pattern. This confirms our observation that the LC approach is load independent as we show in Figure (3.13) in Chapter 3.

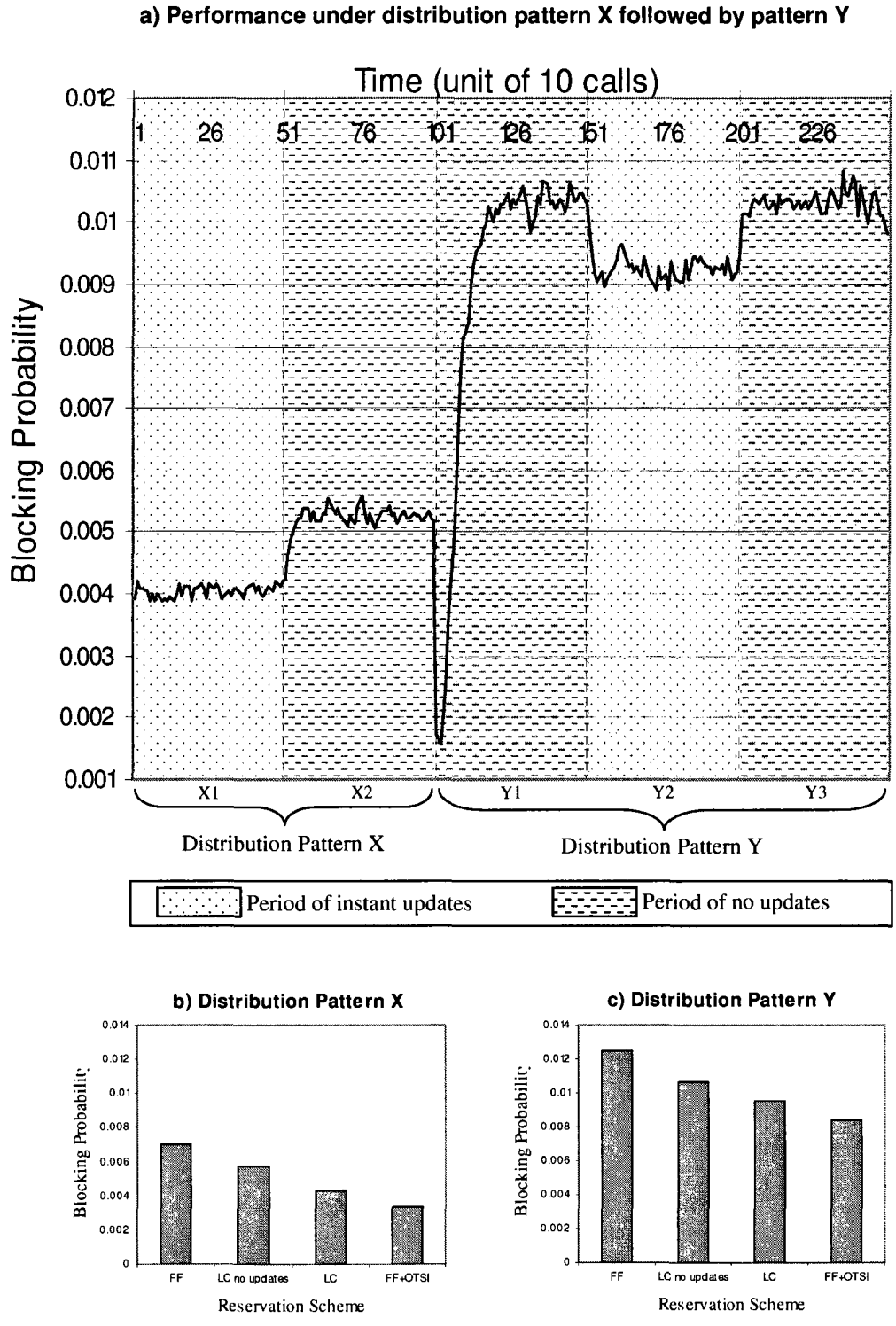

Figure 4.7: LC performance measured every 10 calls – load is 120 Erlang –(with two different traffic patterns)

In a multi-fibers environment, an imperfect route-slot allocations pattern can still produce a performance similar to what is obtained with a perfect pattern (see Figure 4.8). The improved performance of an imperfect pattern in a multi-fibers environment is mainly due to the additional number of fibers. Although P in a multi-fibers environment is smaller than in the single fiber case, it does not justify the difference in performance. Its effect will be limited to slightly increasing the perfection period. Regardless of this period, the pattern would eventually become imperfect after few calls without updates. However, the priority order that remains in effect still produces close to optimal performance as shown in Figure (4.8). Therefore, we conclude that network performance metrics resulting from imperfect and perfect allocation patterns converge as an effect of extra fibers.

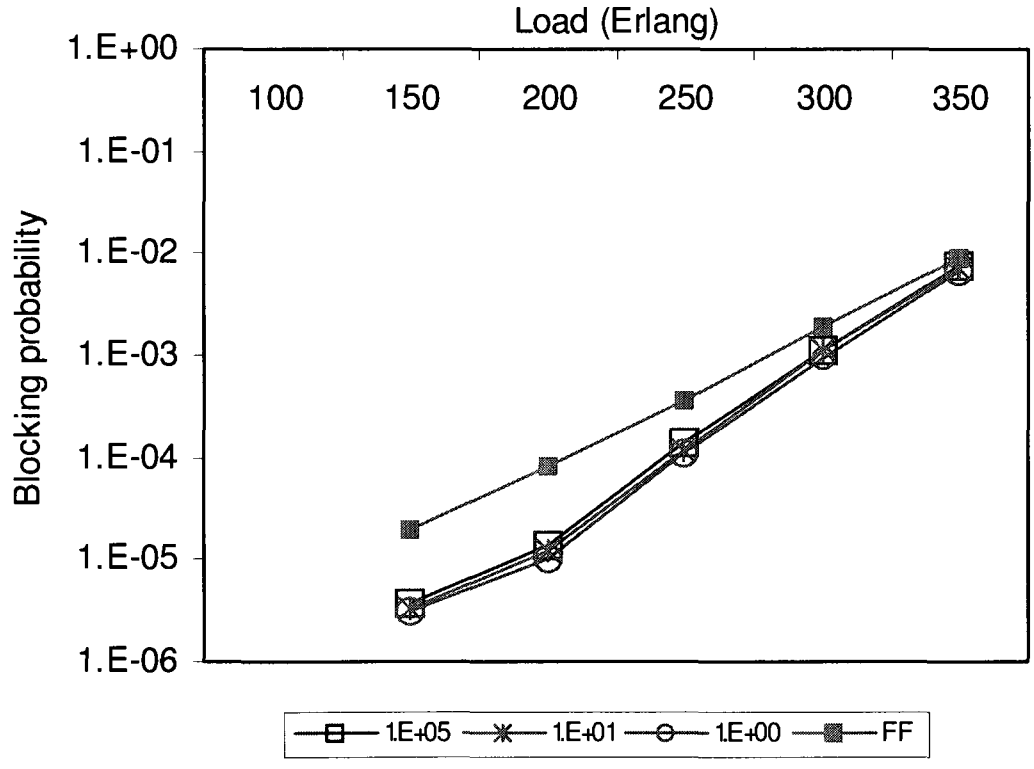

Figure 4.8: LC performance for different update rates (once per 1E+x calls) in a 3-fibers network

4.4. Analytical Discussion

In this section, we analyze the effect of stopping the resource updates, and understand the transition period shown in Figure (4.3). Based on this analysis, we gain a better insight on the discrepancy in performance trend between the single and multi-fiber cases. The transition period from best to degraded performance is related to the probability of changing the output of function $Low(SD, \omega_t)$ on a given route SD; we refer to this probability as $P_{(Low(SD,\omega_t) \neq Low(SD,\omega_{t+1}))}$.

With any arrival in the network, $P_{(Low(SD,\omega_t) \neq Low(SD,\omega_{t+1}))}$ can be described as a product of several probabilities listed in Table (4.1):

Probability Symbol	Description
$P_{(C_{(\overline{SD_i},\tau+1)} < C_{(\overline{SD_i},t)})}$	*Probability that a route-slot constraint is reduced after an arrival at time* τ
$P_{(A_{\overline{SD_i}} > 0)}$	*Probability that route-slot* $\overline{SD_i}$ *is available*
$P_{(Low(SD,\omega_\tau) \neq \overline{SD_i})}$	*Probability that route-slot* $\overline{SD_i}$ *does not have the lowest constraint at the arrival time* τ
$P_{(Low(SD,\omega_{\tau+1}) = \overline{SD_i})}$	*Probability that route-slot* $\overline{SD_i}$ *has lowest constraint as a result of the arrival at time* τ

Table 4.1: Probability Symbols

$$P_{(Low(SD,\omega_\tau) \neq Low(SD,\omega_{\tau+1}))} = t \times P_{(C_{(\overline{SD_i},\tau+1)} < C_{(\overline{SD_i}\tau)})} \times P_{(A_{\overline{SD_i}} > 0)} \times P_{(Low(SD,\omega_\tau) \neq \overline{SD_i})} \times P_{(Low(SD,\omega_{\tau+1}) = \overline{SD_i})} \quad (4.1)$$

The probability $P_{(C_{(\overline{SD}_i,\tau+l)}<C_{(\overline{SD}_i,\tau)})}$ can be described as the probability that at least one constituent link-slot constraint is reduced as a result of an arrival at time τ. The probability that a link-slot constraint is reduced as a result of an arrival is derived as follows:

$$P_{(C_{(XY_j,\tau+l)}<C_{(XY_j,\tau)})}=\frac{h^2\times r\times K}{l\times t} \tag{4.2}$$

Thus,

$$P_{(C_{(\overline{SD}_i,\tau+l)}<C_{(\overline{SD}_i,\tau)})}=\frac{h^3\times r\times K}{l\times t} \tag{4.3}$$

The probability $P_{(A_{\overline{SD}_i}>0)}$ that a route slot $\overline{SD}_i$ is available is actually equal to the odd of having all constituent link-slots available, and can be derived by:

$$P_{(A_{\overline{SD}_i}>0)}=(1-\mu)^h \tag{4.4}$$

To measure the probability $P_{(Low(SD,\omega_\tau)\neq\overline{SD}_i)}$ and $P_{(Low(SD,\omega_{\tau+l})=\overline{SD}_i)}$, we derive the probability that a route-slot has the lowest constraint among all available route-slots on the same route as follows:

$$P_{(Low(SD,\omega_\tau)=\overline{SD}_i)}=\left(P_{(C_{\overline{SD}_i}\leq C_{\overline{SD}_a})}\right)^{\alpha} \tag{4.5}$$

where,

$$\alpha = \left(P_{(A_{\overline{SD_i}} > 0)} \times t \right) - 1 = \left((1-\mu)^h \times t \right) - 1 \tag{4.6}$$

The probability $P_{(C_{\overline{SD_i}} \leq C_{\overline{SD_a}})}$ depends on the number of values that a route-slot constraint ($C_{\overline{SD_i}}$) can have. In general, it is equal to $h \times r \times f$. Assuming that a route-slot constraint can be an integer value between 0 and $h \times r \times f$ with equal probability, we derive the following equation as an approximation:

$$P_{(C_{\overline{SD_i}} \leq C_{\overline{SD_a}})} = \frac{\sum_{z=1}^{h \times r \times f} z}{(h \times r \times f)^2} = \frac{(h \times r \times f) + 1}{2(h \times r \times f)} \tag{4.7}$$

Consequently, the probability that one route-slot's constraint is not the lowest during an arrival at time τ is approximately given by:

$$P_{(Low(SD,\omega_\tau) \neq \overline{SD_i})} = 1 - \left(\frac{(h \times r \times f) + 1}{2(h \times r \times f)} \right)^{\alpha} \tag{4.8}$$

Similarly, the probability that one route-slot's constraint is the lowest after an arrival time τ is approximately:

$$P_{(Low(SD,\omega_{\tau+1}) = \overline{SD_i})} = \left(\frac{\left(\sum_{z=0}^{h \times r \times f} z \right) + (h \times r \times f \times \theta)}{(h \times r \times f)^2} \right)^{\alpha} = \left(\frac{h \times r \times f + 1}{2 \times h \times r \times f} + \varepsilon \right)^{\alpha} \tag{4.9}$$

ε is the average increase on the probability $P_{(C_{\overline{SD_i}} \le C_{\overline{SD_a}})}$ after reducing a route-slot constraint due to a reservation

$$\varepsilon = \frac{\theta \times (2 \times h \times r \times f - \theta - 1)}{2(h \times r \times f)^2} \tag{4.10}$$

θ is the average reduction on a route-slot constraint

$$\theta = t \times P_{(C_{(\overline{SD_i},\tau+1)} < C_{(\overline{SD_i},\tau)})} = \frac{h^3 \times r \times K}{l} \tag{4.11}$$

Summing it all together, we get the following approximate equation:

$$P_{(Low(SD,\omega_\tau) \neq Low(SD,\omega_{\tau+1}))} = \frac{h^3 \times r \times (f+2)^{h-1} \times (1-\mu)^h}{l \times (2 \times (f+1))^{h-1}} \times \left(1 - \left(\frac{(h \times r \times f)+1}{2(h \times r \times f)}\right)^{\alpha}\right) \times \left(\left(\frac{h \times r \times f + 1}{2 \times h \times r \times f} + \varepsilon\right)^{\alpha}\right) \tag{4.12}$$

Considering the same network adopted during our simulation with the tabulated parameters in the next table (4.2), we get the following probability values based on Equation (4.12)

Mean arrival time (λ)	Average holding time (τ)	Number of fibers (f)	$P_{(Low(SD,\omega_t)\neq Low(SD,\omega_{t+1}))}$
5	240	1	0.09
6	240	1	0.07
7	240	1	0.06
8	240	1	0.05
9	240	1	0.04
10	240	1	0.04
5	1750	3	0.03
6	1750	3	0.08
7	1750	3	0.09
8	1750	3	0.08
9	1750	3	0.06
10	1750	3	0.05

Table 4.2: Analytical results

An average of "$n \times (n-1) \times P_{(Low(SD,\omega_t)\neq Low(SD,\omega_{t+1}))}$" routes are affected per accepted arrival. It takes about $\frac{1}{P_{(Low(SD,\omega_t)\neq Low(SD,\omega_{t+1}))}}$ accepted arrivals to have a call on one of these impacted routes. According to Table (4.2), this number is between 10 and 25 arrivals. That coincides with the transition period between best and degraded performance plotted in Figure (4.5). In addition, the numbers confirm that the same phenomenon is happening in the multi-fiber case; however, there was no significant transition in performance as shown in Figure (4.8). The reason can be attributed to the multi-fiber network's ability to tolerate slight changes in the global order of route-slot constraints. Deducting couple points from a constraint value whose range is between 0 and $h \times r \times f$,

in a network of f fibers, has little impact as compared to the same deduction in a single fiber network, with a constraint range between 0 and $h \times r$.

4.5. Conclusion

In this chapter, we designed a distributed LC scheme in an attempt to make it applicable to GMPLS networks. After specifying the node database, we defined new parameters that need to be added to the RSVP-TE or CR-LDP messages. In addition, we developed two different resource status update schemes: immediate and periodic. The major challenge was to incorporate the LC resource status update into GMPLS, which relies on OSPF or IS-IS link state update mechanisms. Since GMPLS' updates happen once every 30 min for each link in the network, we have to skip a number of calls before invoking the LC resource updates. We showed by simulation and analytical methods that an update rate greater than or equal to $\frac{1}{P_{(Low(SD,\omega_t) \neq Low(SD,\omega_{t+1}))}}$ maintains close to optimal performance; where $P_{(Low(SD,\omega_t) \neq Low(SD,\omega_{t+1}))}$ is the probability that the least-constraining route-slot on route SD changes after an accepted call arrival. For lower update rates, performance degrades to a fixed level but does not converge to the worst performance level reported with the First Fit (FF) approach; hence, stopping all subsequent updates throughout the network lifetime after a brief period of immediate updates produces a performance level as good as any update rate less than $\frac{1}{P_{(Low(SD,\omega_t) \neq Low(SD,\omega_{t+1}))}}$. In multi-fiber environments, the update reduction has no significant effect on performance regardless of the rate. In this case, stopping the immediate updates at an early stage of the network operation does not affect performance, and hence the associated signaling bandwidth is spared. As a general conclusion, the distributed LC scheme produces a close to optimal performance in a GMPLS optical TDM network. It requires a slightly extended reservation protocol and need not change the rate of link state updates.

5. Variations of the Least Constraining Slot Allocation Scheme

5.1. Problem Definition

In the previous chapter, we showed that the least constraining slot allocation scheme enhanced performance to a close to optimum level in single and multi-fiber networks. In this chapter, we study some variations of the LC scheme aiming to find a solution that achieve a closer to optimum performance. In addition, we investigate the effect of these variations to obtain a clear understanding on their merits and demerits.

In a single fiber environment, the availability of a link-slot, defined in Equation (3.2) becomes a binary variable showing whether the link-slot is available (1) or not (0); and hence, C_{XY_j} defined in Equation (3.8) would reflect the number of available route-slots containing XY_j. In other words, C_{XY_j} indicates the number of routes that will be blocked if the designated link-slot is entirely used. In addition, if the Availability A_{XY_j} is equal to 1, then the set Ω'_{XY_j} defined in (3.5) includes all available route-slots that contain XY_j. Hence the constraint C_{XY_j} is nothing but the cardinality of Ω'_{XY_j}. This observation does not apply in a multi-fiber environment since the availability is not binary but has values ranging from *zero* to f where f is the number of fibers per link. We believe that if the definition of a resource constraint is modified to be equal to the cardinality of set Ω'_{XY_j}, we might see different results in the multi-fiber case. With this variation, the constraint is a count of

intersecting route-slots rather than a sum of intersecting route-slot availabilities as in the original LC approach. Thus, we will refer to this variation as the LC slot allocation approach based on route-slot count, or LC variation 1 (LCv1).

In addition, the link-slot constraint defined in Equation (3.8) also reflects the number of available transmission channels on intersecting route-slots that could use the link-slot at any point in time. We believe if we change the constraint definition to be the ratio of available transmission channels on intersecting route-slots with respect to the link-slot availability, we could achieve better performance. For instance, a link-slot whose sum of available transmission channels on intersecting route-slots and availability are 20 and 5, respectively, is less constraining than a link-slot whose sum of intersecting available route-slots and availability are 10 and 1. Hence, dividing the sum of available transmission channels on intersecting route-slots by the link-slot availability produces a better indication of the actual constraint. If the availability is zero, the constraint is set to *infinity*. Note that in the single fiber case, this division is not necessary since the availability cannot be higher than 1. However, if this division is applied in the multi-fiber case, we could see improved results. With this variation, the constraint is rather a ratio than a sum of route-slots availability. Thus, we will refer to this variation as the LC slot allocation approach based on availability ratio, or LC variation 2 (LCv2).

As noted above, the minimal difference between the new variations and the original LC approach is just the definition of the resource constraint. All the other original LC basic concepts and definitions apply under these variations. As the constraint definition changes, the centralized and distributed constraint update schemes must change accordingly. In the following sections, we explain the slight modifications required to adjust the original update scheme to work with the new variations. In addition, we compare the performance of the LC approach with the new variations.

5.2. Resource Constraint Definition Variations

5.2.1. Constraint Definition for LC Based on Route-Slot Count (LCv1)

As discussed earlier, we designate the constraint of link-slot XY_i to be the cardinality of the set Ω'_{XY_j}, denoted by $\left|\Omega'_{XY_j}\right|$. In this case, the constraint of a link-slot would consistently reflect the number of route-slots whose availabilities decrease when reserving XY_j. In other words, it indicates the number of routes whose capacity is reduced if the designated link-slot is reserved regardless of the number of fibers per link.

$$C_{XY_j} = \left|\Omega'_{XY_j}\right|. \tag{5.1}$$

Consequently, we redefine the constraint of a route-slot as follows:

$$C_{\overline{SD_i}} = \sum_{XY_j \, in \, SD_i} \left|\Omega'_{XY_j}\right|. \tag{5.2}$$

Equation 5.2 shows that the constraint of a route-slot reflects the number of routes whose availabilities are reduced if the designated link-slot is reserved. It is evident that reserving a route-slot which impacts the availabilities of the least number of available route-slots keeps the highest number of resources available for subsequent communication requests, hence improving the blocking rate. Thus, the route-slot that has the lowest constraint $C_{\overline{SD_i}}$ would be the best choice on a given route between S and D. In this case, the minimum number of route-slots in the network would become unavailable when serving a given call. As a

comparison, the allocation principle of the original LC approach only guarantees that a close to minimum number of routes-slots in the network could become unavailable when serving a call.

5.2.2. Constraint Definition for LC Based on Availability Ratio (LCv2)

To realize the second variation of the LC approach, we designate the constraint of link-slot XY_i to be a ratio equal to the sum of the availabilities of all route-slots belonging to Ω_{XY_j} divided by the availability of XY_i:

$$C_{XY_j} = \frac{\sum_{\overline{SD_i} \in \Omega_{XY_j}} A_{\overline{SD_i}}}{A_{XY_j}}. \tag{5.3}$$

Consequently, the constraint of a route-slot becomes a sum of ratios defined as follows:

$$C_{\overline{SD_i}} = \sum_{XY_j \text{ in } \overline{SD_i}} \frac{\sum_{\overline{SD_i} \in \Omega_{XY_j}} A_{\overline{SD_i}}}{A_{XY_j}}. \tag{5.4}$$

With the original LC approach, the constraint of a route-slot reflects the total availability of all route-slots that intersects with it in one of its links as shown in Equation (3.7). Based on this proposed variation, we have a paradigm shift in the allocation principle. The number of available route-slots intersecting in a link-slot is not the sole factor in defining the constraint. The link-slot availability is now a decisive factor. Thus, in principle, the reservation procedure would reserve a route-slot that has the lowest sum of availability ratios rather than the lowest number of available transmission channels on intersecting route-slots. I.e., the route-slot's constraint is not anymore an indicator of the number of

available transmission channels on intersecting route-slots that could use one of the constituent link-slots.

5.2.3. Illustrative Example

In Figure (5.1), we show one link-slot and the containment relationship with its 5 intersected route-slots. Each route-slot is represented with a diamond box labeled by its availability; and, the intersection link-slot is shown as a circle also labeled by its availability. The same figure is sketched in two different scenarios, a) multi-fibers and b) single fiber. Based on the resource availabilities shown in the multi-fiber case (Figure 5.1.a), the constraint of the link-slot is 11 based on the original LC approach, and 2 based on the LC approach with variation 1 (LCv1). On the other hand, the constraint is consistently equal to 2 in the single fiber case (Figure 5.1.b) regardless of the variation.

Referring to the same figure, we calculate the link-slot constraints using the definition in variation 2. The results are shown in the following table:

Constraint of the intersection link-slot		
	3 fibers	1 fiber
LC	12	2
LCv1	2	2
LCv2	4	2

Table 5.1: Results from Figure 5.1

Based on the resource availabilities shown in the multi-fiber case (Figure 5.1.a), the constraint of the link-slot is 12/3 = 4 based the LC approach with variation 2 (LCv2). On the other hand, the constraint is consistently equal to 2 in the single fiber case (Figure 5.1.b) regardless of the variation.

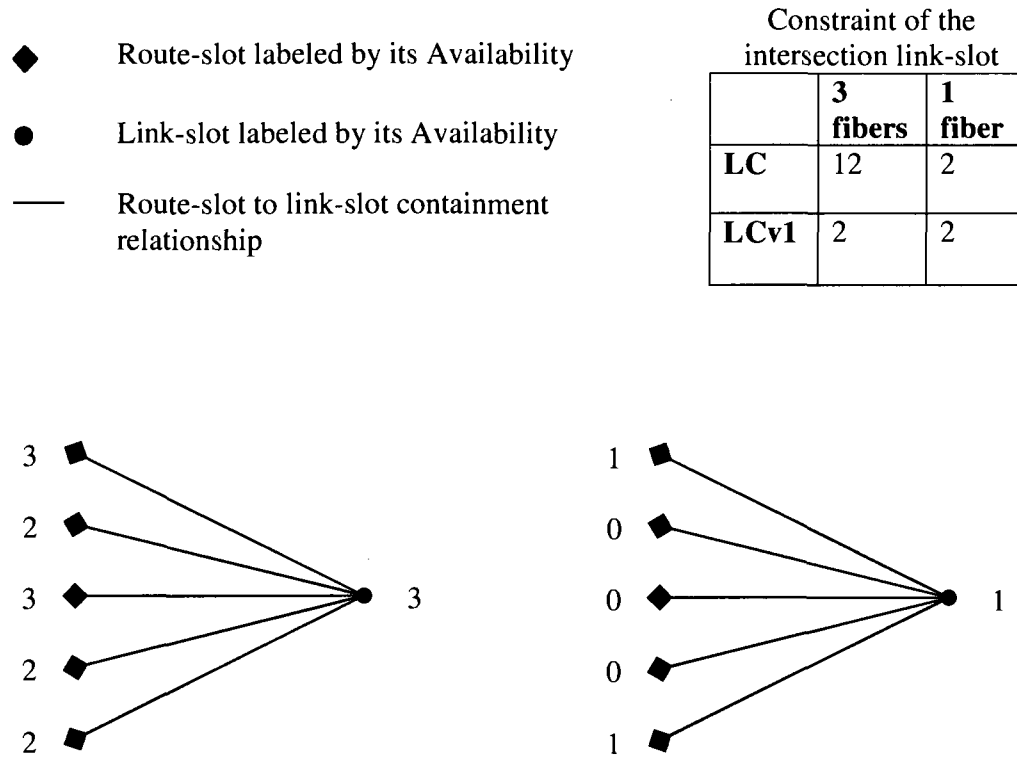

a) Relationship of five route-slots intersecting in a common link-slot in a 3 fibers network

b) Relationship of five route-slots intersecting in a common link-slot in a single fiber network

Figure 5.1: Example of the constraint calculation for LCv1 and LCv2

5.2. Essential Changes to the Resource Constraint Update Module

Two resource constraint update procedures were defined for the original LC approach, centralized and distributed. These procedures need to be slightly modified to conform to the new constraint definition in each variation.

5.2.1. Constraint Update Change for LCv1

5.2.1.1. Centralized Approach

Based on the new definition of the link-slot constraint in Equation (5.1), we need to slightly modify the associated constraint update algorithm. During the reservation phase for each link-slot XY_j in route-slot $\overline{SD_i}$, the following algorithm is used to update the constraint of each link-slot in each route-slot in Ω'_{XY_i}:

```
foreach XY_j in SD_i do
{
    foreach RT_n ∈ Ω'_{XY_j} do
        foreach UV_k in RT_n do
            if A_{UV_k} = A_{RT_n} do
                C_{UV_k} := C_{UV_k} - 1
    ReserveLinkSlot(XY_j)
    C_{XY_j} := |Ω'_{XY_j}|
}
```

Figure 5.2: Constraint update algorithm after reservation of a call

By definition, Ω'_{XY_j} contains all route-slots whose availabilities are decremented due to a reservation of XY_j. Consequently, the constraints of some constituent link-slots in these route-slots need to be updated accordingly. Only the constraint of the link-slots whose availabilities match the availability of the containing route-slot should be decreased by 1. That is because they lost one route-slot from Ω'_{XY_j}. In the release phase, the following algorithm is used:

```
foreach XY_j in SD_i do
{
    foreach RT_n ∈ Ω''_XYj do
        foreach UV_k in RT_n do
            if A_UVk − A_RTn = 1 do
                C_UVk := C_UVk + 1
    FreeLinkSlot(XYj)
    C_XYj = |Ω'_XYj|
}
```

Figure 5.3: Constraint update algorithm after release of a call

By definition, Ω''_{XY_j} contains all route-slots whose availabilities are incremented due to a release of XY_j. Consequently, the constraints of some constituent link-slots in these route-slots need to be updated accordingly. Only the constraint of the link-slots whose availabilities match the new availability of the containing route-slot should be increased by 1. That is because they gain one new route-slot in Ω'_{XY_j}.

5.2.1.2. Distributed Approach

The nodal database and reservation scheme described in the original LC approach are applicable for this variation. However, the resource status update procedure is different due to the change in the definition of the resource constraint, as explained below.

Immediate Resource Status Update

The same steps of the original LC immediate update procedure are adopted with the LCv1 approach, except for the last step (2.iv), where the appropriate resource constraints are updated. Instead, the following needs to be executed depending on the notification type:

a. *Reservation Notification*: Indentify the route-slot availability $A_{\overline{SD_k}}$ which would be the minimum availability in the LSAL of the corresponding CRSL entry. First, if $A_{\overline{SD_k}}$ is equal to A_{XY_i} and also equal to A_{UV_j}, deduct 1 from the constraint of the corresponding local link-slot UV_j. Second, deduct 1 from the availability of XY_i in the CRSL LSAL. Note that the source node that sends the notification should update the availability of XY_i, and its constraint by counting the number of intersecting route-slots that matches its new availability.

b. *Release Notification*: Indentify the route-slot availability $A_{\overline{SD_k}}$ which would be the minimum availability in the LSAL of the corresponding CRSL entry. If $A_{\overline{SD_k}}$ is equal to A_{XY_i}, check the CRSL LSAL for other link-slots that has the same availability. First, if no link-slots other than XY_i are identified and $A_{XY_i} + 1 = A_{UV_j}$, then add 1 to the constraint of the corresponding local link-slot UV_j. Second, add 1 to the availability of XY_i in the CRSL LSAL. Note that the source node that sends the notification should update the availability of XY_i, and its constraint by counting the number of intersecting route-slots that matches its new availability.

Periodic Resource Status Update

The same steps of the original LC periodic update procedure are adopted with the LCv1 approach, except for the last step (3.ii), where the appropriate resource constraints are updated. Instead, the following step needs to be processed for every link-slot that is included in the received notification:

- Set the corresponding link-slot availability in the CRSL LSAL to the availability of the considered link-slot XY_i. Identify the new route-slot availability $A_{\overline{SD_k}}$ which would be the minimum availability in the LSAL of the corresponding CRSL entry. Calculate the constraint of the corresponding local link-slot UV_j by counting the number of intersecting route-slots that have the same availability.

5.2.2. LCv2 Update Module change

5.2.2.1. Centralized Approach

Based on the new definition of the link-slot constraint in Equation (5.3), we need to redesign the associated constraint update algorithm. To simplify the notation, we define a variable recording the sum of intersecting route-slot availabilities as follows: $\tau_{XY_j} = \sum_{\overline{SD_i} \in \Omega_{XY_j}} A_{\overline{SD_i}}$. During the reservation phase for each link-slot XY_j in route-slot $\overline{SD_i}$, the following algorithm is used to update the constraint of each link-slot in each route-slot in Ω'_{XY_i}:

foreach XY_j *in* $\overline{SD_i}$ ***do*** {

$$C_{XY_j} := \frac{\tau_{XY_j} - 1}{A_{XY_j} - 1}$$

foreach $\overline{RT_n} \in \Omega'_{XY_j}$ ***do***

if $\overline{RT_n} \neq \overline{SD_i}$

foreach UV_k *in* $\overline{RT_n}$ ***do***

$$C_{UV_k} := \frac{\tau_{UV_k} - 1}{A_{UV_k}}$$

ReserveLinkSlot(XY_j)

}

Figure 5.4: Constraint update algorithm after reservation of a call

An algorithm similar to what is used in the original LC approach is adopted for this variation. The difference is in calculating the constraint where the ratio defined in Equation (5.3) is introduced. Similarly, the following algorithm is used in the release phase:

```
foreach XY_j in SD_i do {
    C_XYj := (τ_XYj + 1) / (A_XYj + 1)
    foreach RT_n ∈ Ω''_XYj do
        if RT_n ≠ SD_i
            foreach UV_k in RT_n do
                C_UVk := (τ_UVk + 1) / A_UVk
    FreeLinkSlot(XY_j)
}
```

Figure 5.5: Constraint update algorithm

5.2.2.2. Distributed Approach

The same concepts described in the original distributed LC approach are applicable with variation 2. The only difference is in the method used at each node in calculating the constraints of its local link-slots according to Equation (5.3). The constraint here is equal to the recorded number of available intersecting route-slots divided by the link-slot availability. Note that the link-slot availability here is always up to date since it is a local variable that does not depend on external parameters. However, the recorded number of available intersecting route-slots would most likely be outdated since it depends on external parameters that get reconciled at every update.

5.3. Simulation Results

In this section, we compare the performance of the LC approach variations in single and multi-fibre environments. Our observations are based on simulations using the simulation parameters described in Chapter 3. We focus on the multi-fibre case since all the described variations become identical when calculating the constraint of a resource in a single-fibre

network. In a single fibre network, $A_{XY_j} = 1 \Rightarrow A_{\overline{SD_i}} = 1 \quad \forall \overline{SD_i} \in \Omega'_{XY_j} \Rightarrow \left|\Omega'_{XY_j}\right| = \sum_{\overline{SD_i} \in \Omega_{XY_j}} A_{\overline{SD_i}}$. Thus, the behavior of LCv1 approach is identical to the original LC approach in a single fiber environment. Similarly, $A_{XY_j} = 1 \Rightarrow \frac{\sum_{\overline{SD_i} \in \Omega_{XY_j}} A_{\overline{SD_i}}}{A_{XY_j}} = \sum_{\overline{SD_i} \in \Omega_{XY_j}} A_{\overline{SD_i}}$ confirming that the behavior of LCv2 approach and the original LC approach are identical in a single fiber environment. Thus, the performance of original LC, LCv1, and LCv2 approaches should converge in single fiber networks. Figure (5.6) showing the performance of all LC approach variations in a single-fibre environment confirms this observation.

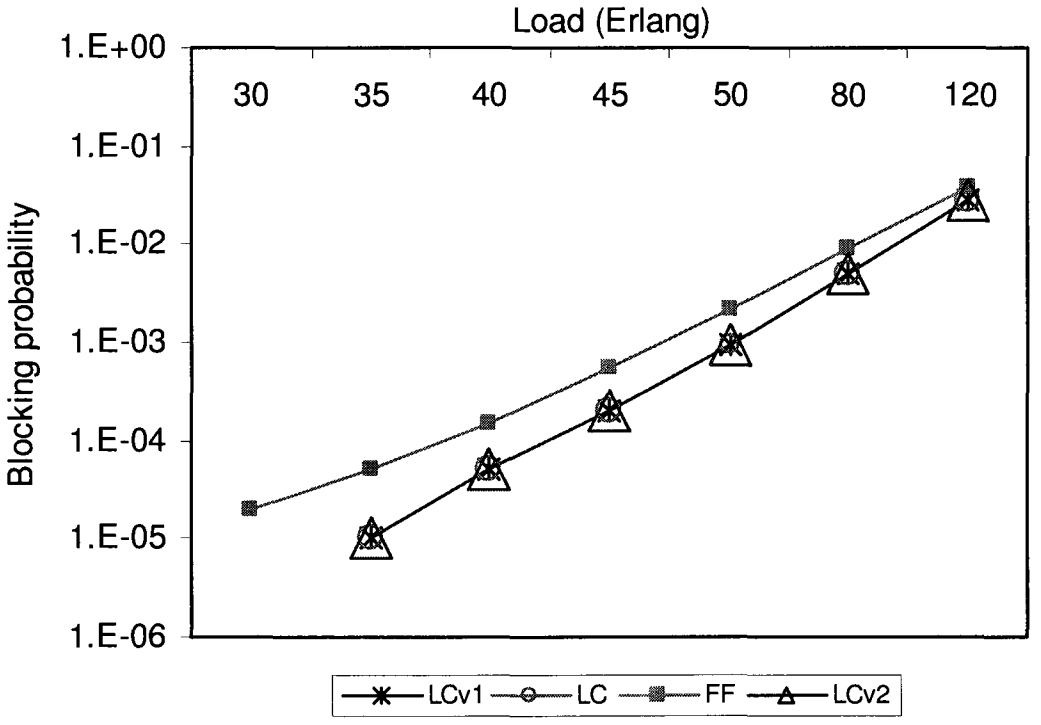

Figure 5.6: Performance of all LC approach variations in a single-fibre environment

Figure (5.7) compares the performance of the LC approach variations in a multi-fiber network. It shows that the different variations of the LC approach produced a slightly better performance which is closer to the optimum level than the original LC approach. Note that the optimum performance level is achieved by the First Fit approach with OTSI.

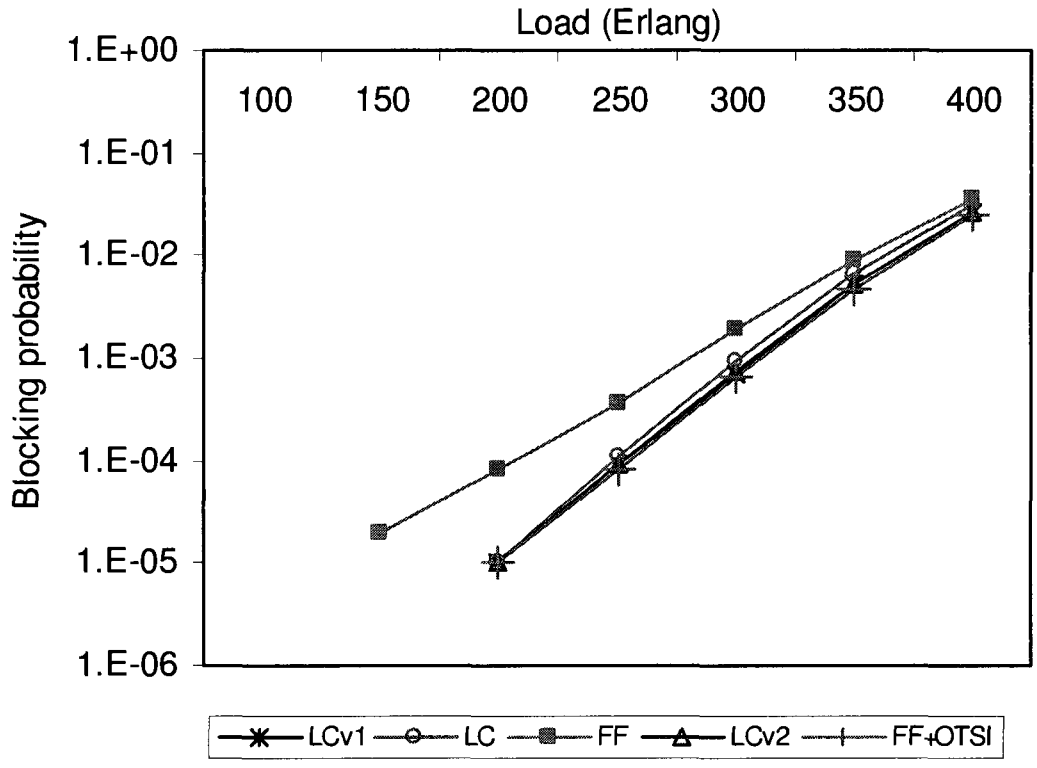

Figure 5.7: Performance of the LC approach variations in a multi-fiber network

Figure (5.8) compares the performance of the distributed LC approach with different variations in a multi-fiber network where no status update is applied after a brief initial period (not included in the chart). It shows that the variation of the LCv2 approach produces the closest performance to the optimal case of the FF approach with OTSI. The resulting performance is slightly better than what is achieved with the original LC approach. The LCv1 approach produces the worst performance which is close to the worst case scenario of the FF approach without OTSI. The results are slightly better at low loads

and converge to the results of the FF approach without OTSI at medium and high loads. Figure (5.9) shows the same performance trend when the status update rate is 1 per 10^3 calls.

The difference in performance stems from the resource constraint definitions of the LCv1 approaches. In a multi-fiber network, a link-slot constraint based on the LCv1 approach tends to be significantly less than its constraint based on the original LC approach. In principle, $\left|\Omega'_{XY_j}\right| \leq \sum_{\overline{SD_i} \in \Omega_{XY_j}} A_{\overline{SD_i}}$ since $\Omega'_{XY_j} \subseteq \Omega_{XY_j}$. However, the inequality is more likely than the equality. Equality is possible only when $\Omega'_{XY_j} = \Omega_{XY_j}$ and $A_{SD_i} = 1 \quad \forall \overline{SD_i} \in \Omega_{XY_j}$ which is a rare case in a multi fibers system. Thus, the constraint is a route-slots counter with a range between 0 and *r*, where *r* is the average number of routes intersecting on a given link; it reflects the number of route-slots whose availabilities are reduced when the link-slot is reserved. It does not reflect the total number of available route-slots that could use the link-slot as defined in the original LC approach. Therefore, the resulting order from the outdated ω_t (defined in Chapter 4) is not based on the status of all route-slots in the network. It is rather a partial order based on route-slot counters rather than the availabilities of all route-slots. The resulting priorities of the route-slots in all routes according to the constraints collected by the last update are not accurately synchronized. Back to the traffic lights system analogy, an order organizing traffic based on a very limited view of the map cannot reduce traffic jams.

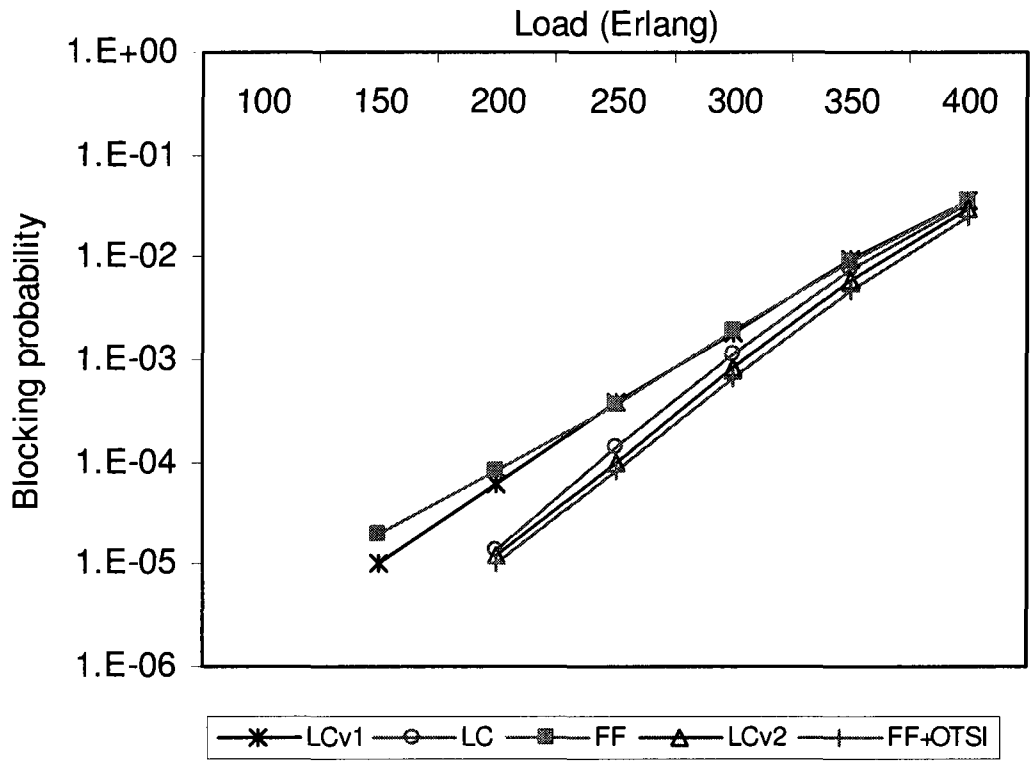

Figure 5.8: Performance of the distributed LC approach with different variations in a multi-fiber network (with no updates)

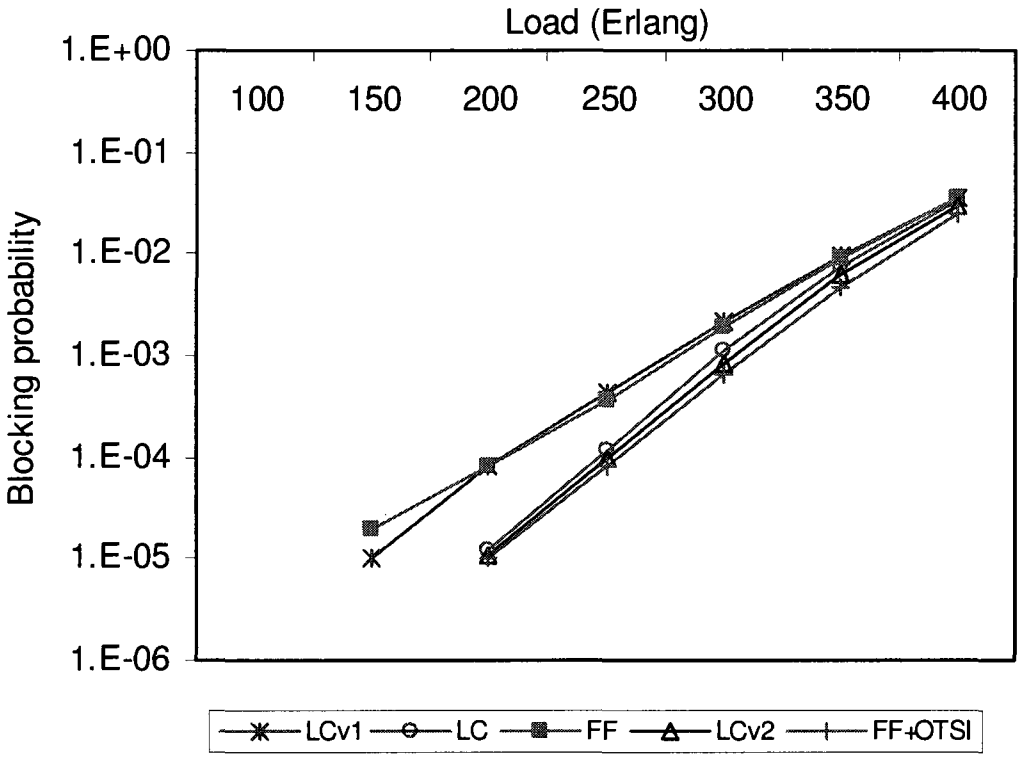

Figure 5.9: Performance of the distributed LC approach with different variations in a multi-fiber network (with update rate of 1 per 10^3 calls)

5.4. Conclusion

In this chapter, we identified two variations of the original LC approach, LC Approach based on Route-Slot Count (LCv1), and LC Approach based on Availability Ratio (LCv2). Both variations slightly enhance network performance in the multi-fiber case reaching the optimum performance level of the FF approach with OTSI. However, the performance of all considered LC approaches converge in the single-fiber case as it is expected. The LCv2 approach produced the best results in the case of periodic or no status updates as compared to the LCv1 and the original LC approaches. On the other hand, the performance of the LCv1 approach exceeded the worst performance level of the FF approach in the cases of

periodic or no status updates. As a conclusion, the LCv2 approach outperformed the LCv1 and the original LC approaches and should be adopted as the standard LC approach.

6. Optimized Passive Optical Time-Slot Interchanger

6.1. Introduction

A major concern with the POTSI architecture that we proposed in [Maach2004] is its bulky size and the insertion loss caused by the coupling of optical signals at each delay unit. Although a POTSI has the smallest size in terms of fiber length as compared to other OTSI architectures which we described in the background chapter, it is still considered bulky. It takes about 2 km of fiber lines to delay a traffic segment by 10 μs. If an OTDM frame of 64 time slots (10 μs each) is adopted, we need 128 km of fiber lines to build a POTSI. In addition, the passive signal flow inside a POTSI comes at the cost of insertion loss. As the signal propagates from one FDL to another, it loses some of its power at the joint point. To mitigate the insertion loss factor, we need to interleave a few amplifiers among the FDLs depending on the loss ratio of employed optical couplers and fiber lines inside the POTSI. The more and longer the FDLs used inside a POTSI, the more amplifiers are required to restore the fading signal, which increases the overall equipment cost. Based on these limitations, we propose in this chapter a new optimized form of POTSI, the Limited Range POTSI (POTSI-LR). We reduce the number of FDLs to a fraction of the number of time slots in the frame (N), which will consequently reduces the POTSI's bulkiness, the crossbar size and the number of required amplifiers. It was proven in the literature that a limited range wavelength converter, having a 30 percent conversion range, achieves the same network performance as a full-range converter [Zeineddine1998]. Similarly, we believe that the same conclusion, if not better, can be applied in the case of POTSI-LR. In addition, we propose the sharing of POTSIs amongst the output links of a switch as opposed to using dedicated POTSI per link. We also propose and investigate the effect of

interleaving POTSIs among network nodes as opposed to deploying a POTSI in each node. Before discussing the simulation results, we briefly define the use of the POTSI architecture as an efficient tool for time slot synchronization between two adjacent nodes. Finally, due to the apparent functional similarity between OTSI and optical wavelength converter, we dedicate a section summarizing the similarity and differences between the two devices.

6.2. Limited-Range POTSI (POTSI-LR)

A POTSI as defined in [Maach2004] has N FDLs, equal to the number of time slots in a TDM frame, and is said to be of size N. We define the POTSI-LR to be a POTSI of size M, where $M < N$. A POTSI-LR has an interchanging-range of $\frac{M}{N}$ and is capable of delaying a time slot i to a time slot j if $i < j < i + M < N$, or $0 < j < (i + M) mod N$, where i and j are slot positions in a TDM frame of size N. Table (6.1) compares the characteristic of POTSI-LR versus regular POTSI. It clearly shows the reduction in fibre length and crossbar size achieved by POTSI-LR. Figure (6.1) describes the high level architecture of a POTSI-LR. It is quite similar to the POTSI in Figure (2.7), but with less FDLs.

Delay Lines per OTSI	Crossbar Size	Fiber Length	Switching operations
POTSI	1 × N-1	N	1
POTSI-LR size M (1 < M < N)	1 × M	M	1

Table 6.1: OTSI Architecture Comparison

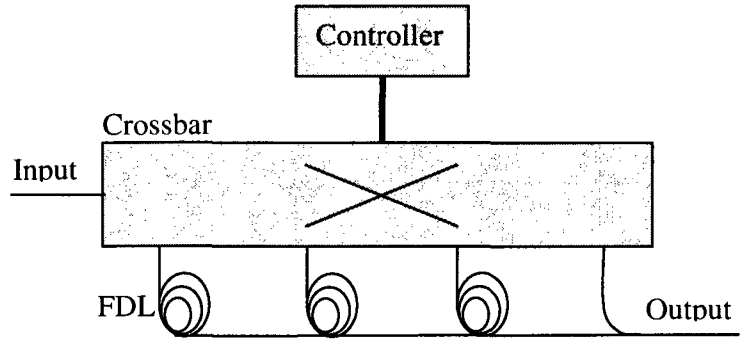

Figure 6.1: A limited Range POTSI with 3 FDLs instead of N-1

6.3. Shared Switch Architecture

In [Maach2004], we introduced a switch architecture having one POTSI of size N per output line, as opposed to the known architecture of one OTSI per input line [Ramamirtham2003]. The rational behind relocating the POTSI from the input to the output side of a switch is to avoid potential blocking on the input side. Blocking can occur when two time slots arriving on the same input are to be switched to the same time slot but on two different outputs. The POTSI on the input side cannot switch two time slots to the same time slot position. Thus, placing the POTSI on the output side of the switch eliminates this problem. In this section, we propose a shared POTSI architecture as shown in Figure (6.3) instead of dedicating one PTOSI per output line as shown in Figure (6.2). Each node has a pool of POTSIs to share amongst its output lines when needed. We define the sharing-percentage, as $\frac{Number\ of\ shared\ POTSI}{Nodal\ Degree}$.

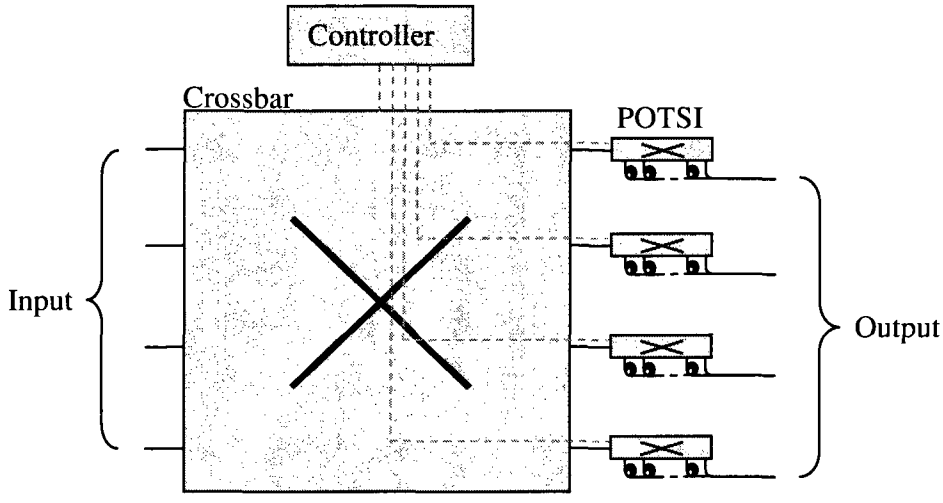

Figure 6.2: Dedicated POTSI Architecture of a 4 x 4 switch

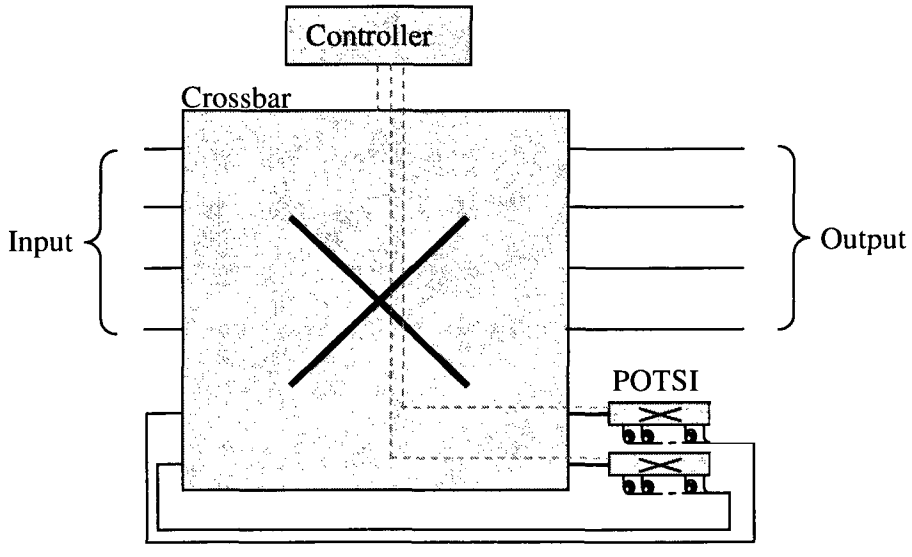

Figure 6.3: Shared OTSI Architecture of a 4 x 4 switch having 2 POTSIs

6.4. OTSI Vs Wavelength Converter

By definition, an all-optical wavelength converter (OWC) converts wavelength λ_x to λ_y by pure optical means without opto-electronic processing. Similarly, OTSI converts between time slots instead of wavelengths. At this point, many researchers concluded that both devices would yield similar results in terms of network performance. In fact, this conclusion is not very precise. An OWC can serve only one call, riding on a wavelength, during a given period; on the other hand, an OTSI can serve multiple concurrent calls, riding on different time slots during the same period. Thus, it is closer to the truth to say that an OTSI, in an OTDM node, achieves similar performance improvement to a bank of N OWCs in a Wavelength Routed Optical Network (WRON) node, where N is the number of time slots per frame in the network.

We say that the above conclusion is very close to the truth, and not completely true, because of a little discrepancy when considering limited-range conversion. A full range converter covers the whole spectrum of wavelengths in a WDM system. A limited range converter covers a subset of the WDM spectrum; the covered spectrum is relative to the input wavelength, and is between $-k$ and $+k$ from that wavelength. A wavelength within a distance j from the boundaries of the WDM spectrum, where $j < k$, cannot take full conversion advantage of the limited range converter. In contrast, thinking of a limited range OTSI, we see that this limitation does not exist. An interchanger has the capability of delaying one time slot beyond its frame boundaries to another time slot in the next frame.

One final discrepancy is the size. Wavelength converters are tiny in size as compared to the bulky nature of the OTSI. As defined, an OTSI is made of a number of FDLs each having a delay capacity equal to one time slot. By a quick calculation, we derive that 2 km of fiber is needed to form one FDL that delays a time slot equal to 10 μs. Given that the diameter of a single mode fiber is around 150 μm, the volume of one FDL cable is close to 45 cm^3.

6.5. POTSI Based Synchronizers

In the background chapter, we reviewed the usage of delay lines as synchronizers that realign incoming frames to the local switch's time slot boundaries [Bononi1999, Liew2003]. We also learned that the internal architecture of a synchronizer resembles the architecture of an OTSI. In this section, we propose a POTSI-based synchronizer hoping to introduce a more feasible solution to the synchronization problem. The POTSI-based synchronizer is made of k FDLs, each having a delay duration g. The duration g is equal to the guard time separating each pair of adjacent time slots in the TDM frame. The number of FDLs k is equal to the slot time μ divided by g (i.e. $\frac{\mu}{g}$), assuming that $\mu > g$. The time slot can be considered as a series of k mini-time-slots of size g, labelled from *0* to *k-1*. If the propagation delay and the clock difference between two adjacent switches are equal to d and c respectively, the time slot shift with respect to the receiving switch is $(d+c) \, mod \, (\mu + g)$. In this case, the signal has to be adjusted in the synchronizer by passing through $\frac{(d+c) \, mod \, (\mu+g)}{g}$ FDLS. Note that the remainder of this division is less than g, and hence is covered by the guard time. To know the time slot shift between two adjacent nodes, a predetermined probe signal equal to one time slot must be sent occasionally from the upstream to the downstream node. The downstream node should keep sensing for the signal at every time slot. Upon receipt, the downstream node measures the un-received portion of the signal which would basically be the time slot shift with the upstream node. The signalling operation between adjacent nodes can be performed over a dedicated wavelength, or over any idle one for an efficient bandwidth usage. Figure (6.4) is a schematic representation of a POTSI-based synchronizer and the essential parameters.

As an elaborative example, if the guard time is 2 and the time slot is 10, the synchronizer should have 5 FDLs of size 2. If the propagation delay and clock difference between two nodes are 47 and 4 respectively, the signal has to be adjusted by hopping through

$\frac{51 \bmod 12}{2} = \frac{3}{2} = 1$ FDLs. We should not be concerned about the remainder value ($3 \bmod 2 = 1$) since it will always be covered by the guard time 2.

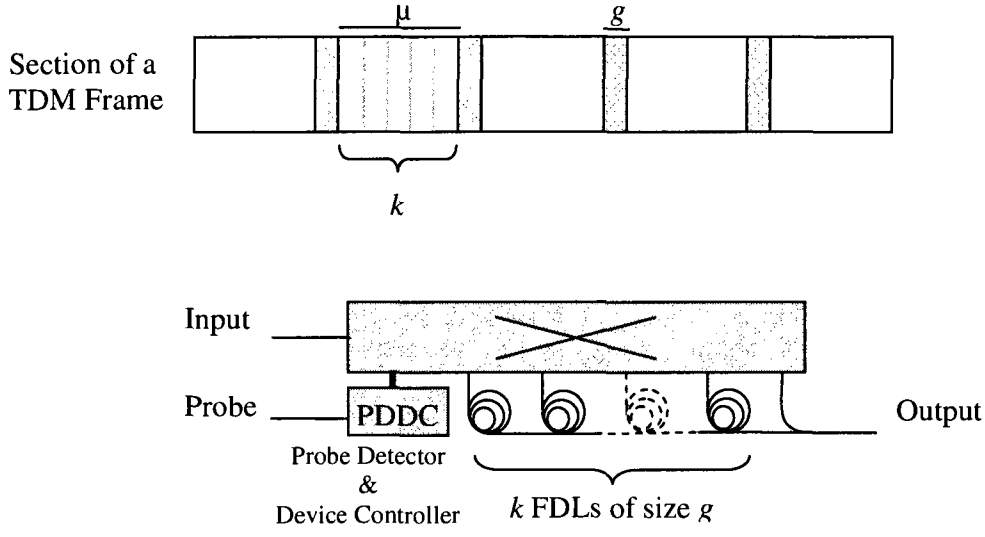

Figure 6.4: Schematic representation of a POTSI-based synchronizer

6.6. Bandwidth allocation with shared limited-range POTSIs

In this section, we study the optimization of two key POTSI configuration parameters, i.e. the sharing-percentage, interchanging-range and interleaving-rate, through simulation results. We use the same simulation parameters described in Chapter 3.

Figure (6.5) shows the network performance under different combinations of POTSI sharing percentages and interchange ranges. Beside the no POTSI and the regular dedicated full-range POTSI cases, we present three other cases: (1) 30% sharing percentage and 30% interchange range, (2) 20% sharing percentage and 20% interchange range, and (3) 10% sharing percentage and 10% interchange range. The chart shows that

30% sharing percentage and 30 percentage interchange range should be enough to yield the same performance gain resulting from the dedicated full POTSI case.

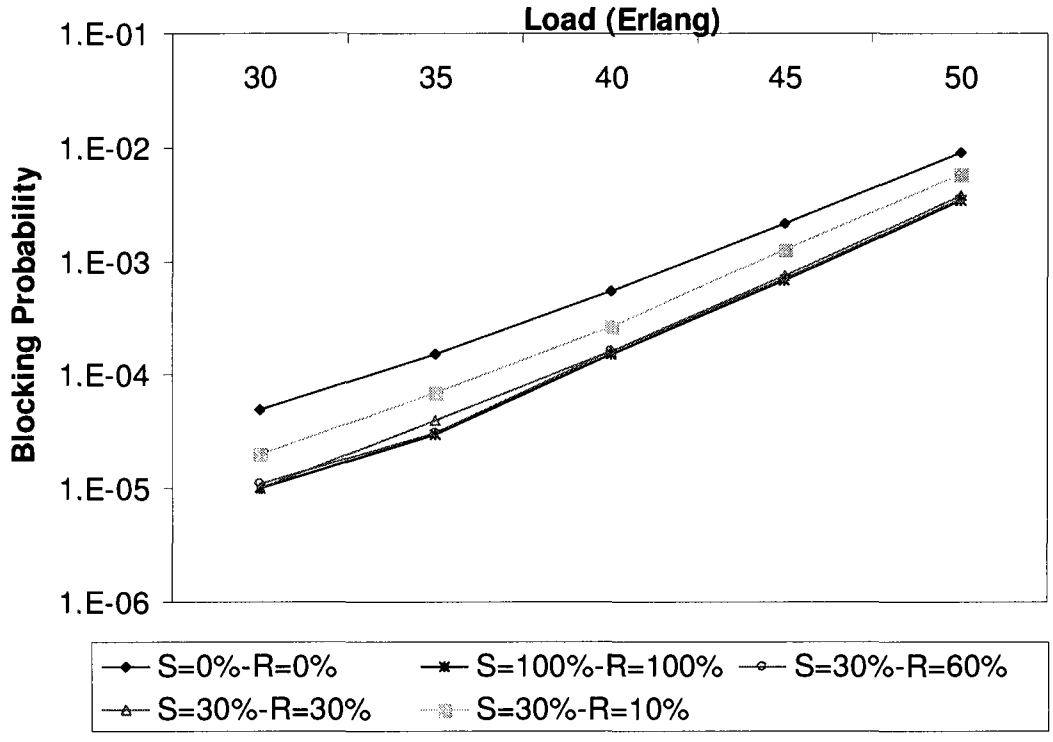

Figure 6.5: The effects of varying the POTSI's sharing-percentages (S%) and interchanging ranges (R%) in NSF network

Since the charts in Figure (6.5) are generated based on the NSFNET topology where the average nodal degree is close to 3, we do not have data for cases where the POTSI's sharing is below 30%. To bypass this limitation, we employ a star topology of 20 edge nodes with a POTSI-equipped core. The results of varying the POTSI sharing percentage in the core node are plotted in Figure (6.6). The charts show that when the interchange range is at 30% or above, varying the sharing percentage has no substantial impact on performance. However, performance degrades slightly when the sharing percentage is 10%. On the other hand, if the interchange range is below 30%, any reduction on the sharing percentage clearly degrades network performance. The worst case scenario is noticed when both the sharing percentage and interchange range are at 10%. On the other

hand, when both parameters are 30%, the network produced a performance close to the optimum case of dedicated full-range POTSIs.

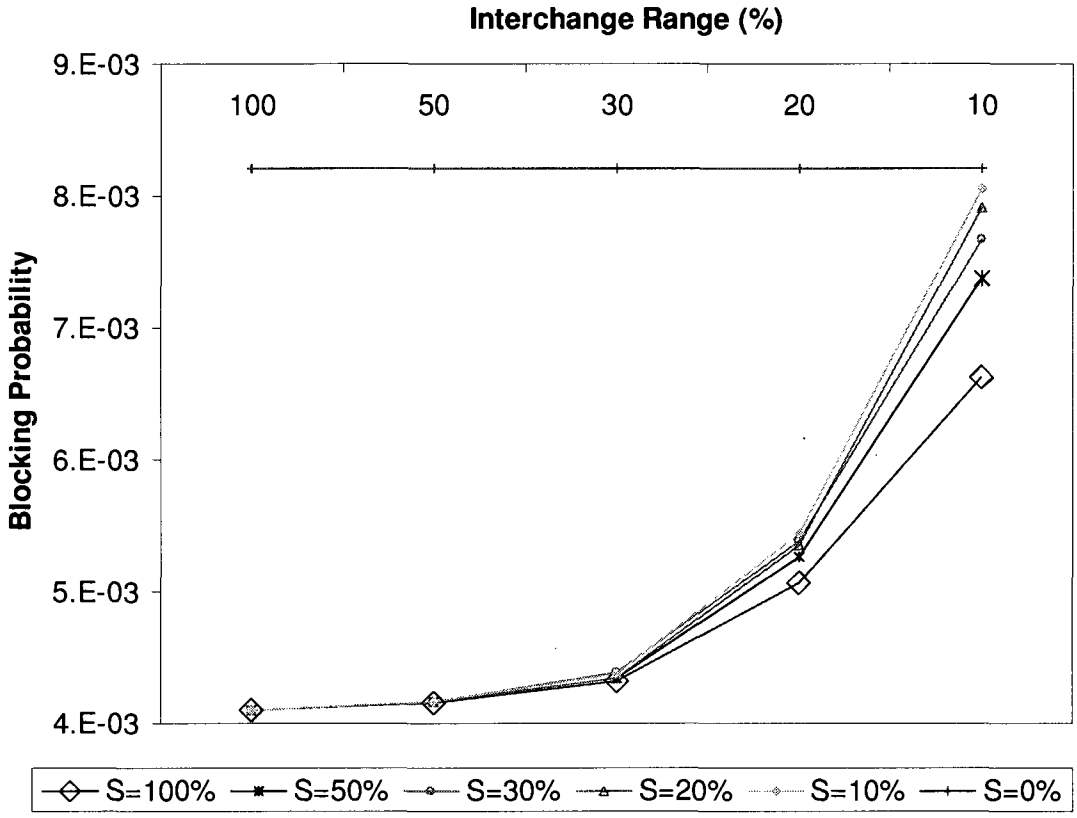

Figure 6.6: The effects of varying POTSI's sharing-percentage (S%) and interchanging range in a star network of 20 edge nodes, with load 60 Erlang

The charts in Figure (6.7) and (6.8) are generated based on a 14 nodes ring topology. They are meant to study the effect of interleaving POTSIs among nodes instead of using these devices at each node. Some nodes are equipped with POTSI and others have none. The interleaving rate reflects the number of POTSI-equipped nodes with respects to the total number of nodes. In addition, the distribution of POTSI-equipped nodes is uniform; i.e., if the interleaving rate is *1/x*, we know that there should be a PTOSI-equipped node every *x* nodes on the ring. For both charts, the number of POTSIs inside the POTSI-equipped nodes is 1, or 50% of the nodal degree in a bidirectional ring. It is not possible to go lower

than 50%; and, going higher is proven to yield the same performance. Figure (6.7) shows that as the POTSI's interleaving rate gets smaller, the network performance degrades substantially. An interleaving rate of 0.5, one POTSI at every second node, produces a performance very close to the dedicated full-range POTSI. The most interesting result shown on the chart is when the interleaving rate is 0.75, i.e. one non-POTSI-equipped node every 4 nodes.

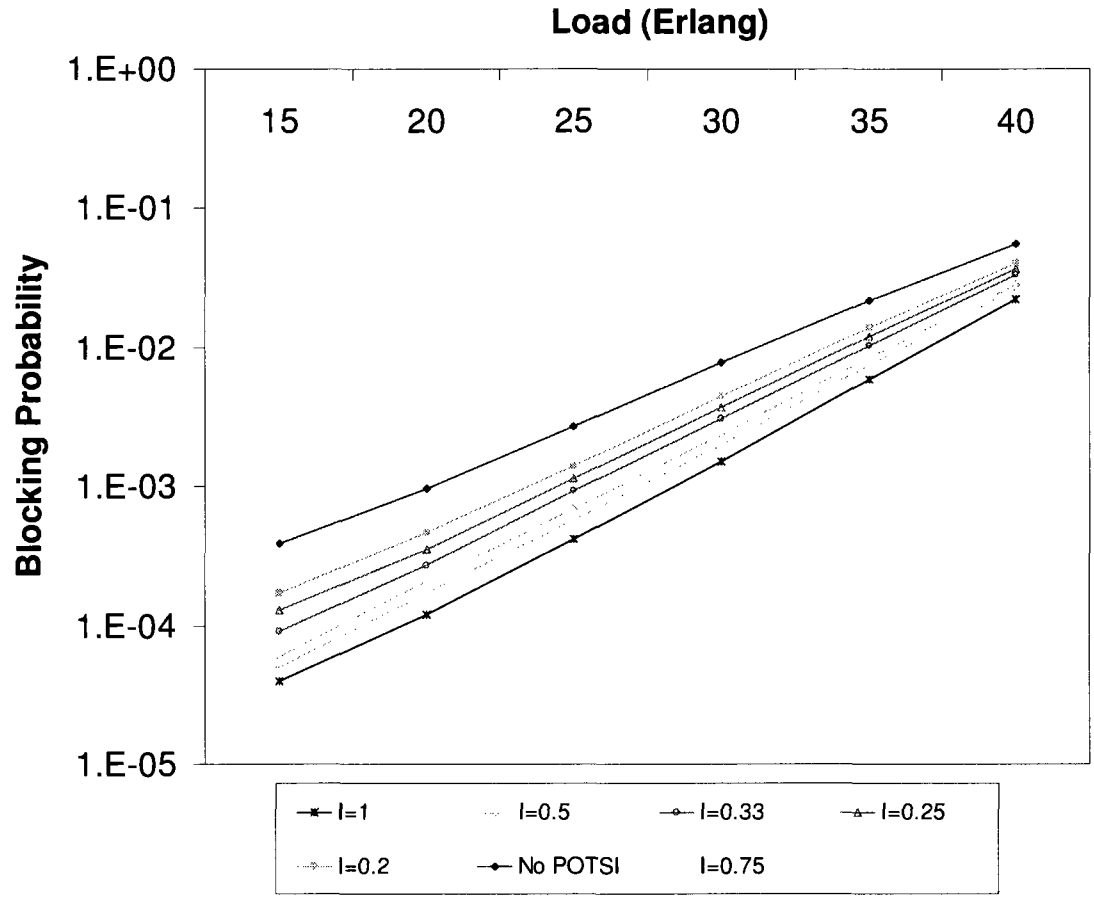

Figure 6. 7: Blocking probability in a 14-Nodes Ring topology, when interleaving POTSIs amongst nodes at different rate (I)

Figure (6.8) shows the effect of varying the OTSI interleaving rate on a 14-nodes ring network loaded at 35 Erlang. The chart shows that when the rate is less than 0.5, the network performance degrades at a steeper rate. On the other hand, performance

degradation is less steep when the rate is above 0.5. An interleave rate of 0.5 seems to offer an acceptable performance level with a decent saving in the number of deployed POTSIs.

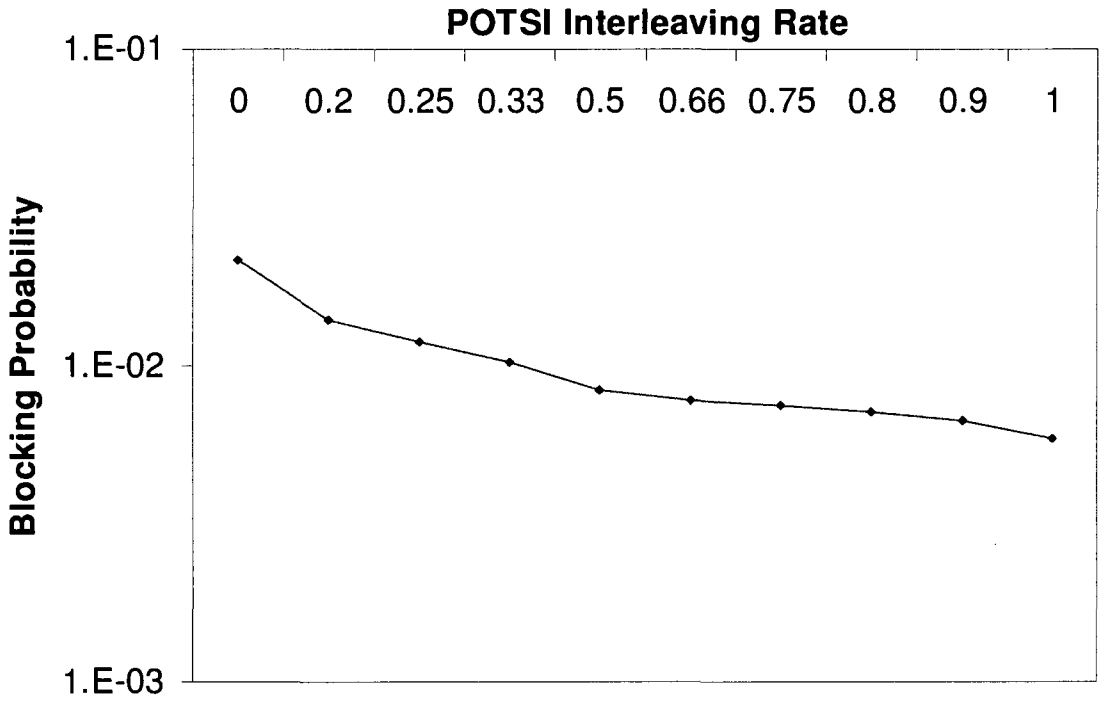

Figure 6.8: Blocking probability in a 14-Nodes Ring topology, when varying the POTSIs Interleaving Rate between 0 and 1, at a fixed load of 35 Erlang

Figure (6.9) shows the effect of varying the interchanging range in the case where the interleaving rate is 0.5. When the interchanging range is 30% or 50%, the network performance remains close to the case where the range is 100%. Lowering the interchanging range to 10% degrades performance drastically. Thus, based on the information reported in charts (6.7), (6.8) and (6.9), we say that interleaving POTSIs in a ring network at a 0.5 rate, where each POTSI-equipped node has a POTSI sharing percentage and interchange range of 50%, respectively, yields a performance improvement close to the optimum level which is reported for the dedicated full-range POTSI case.

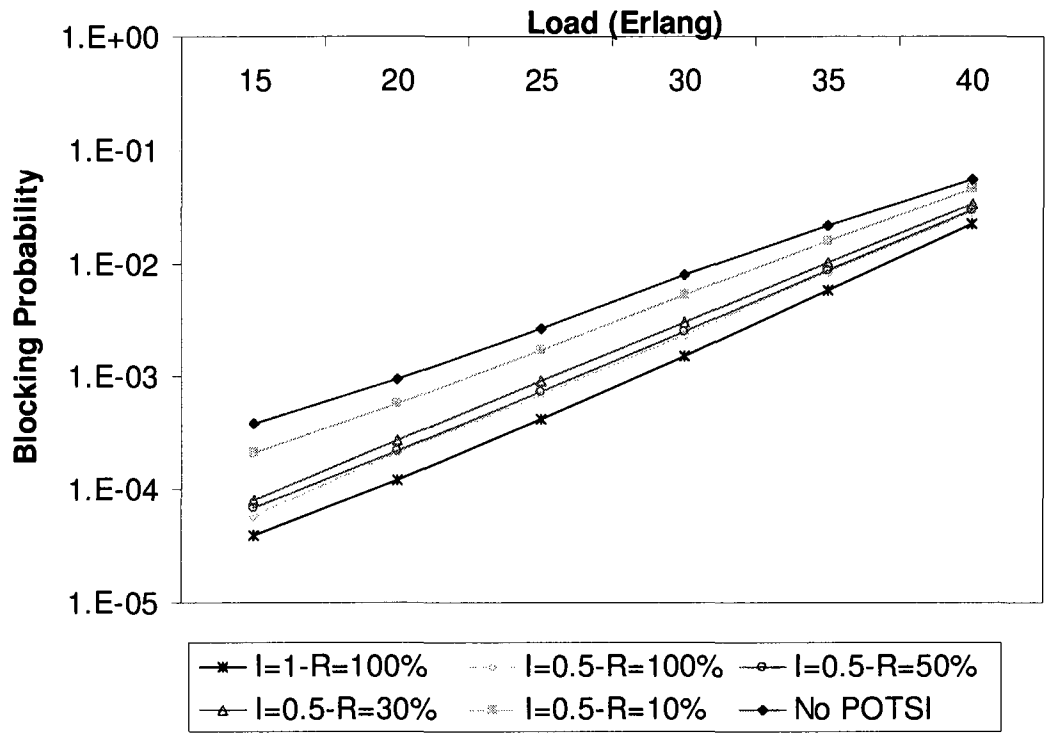

Figure 6.9: Blocking probability in a 14-node ring topology, with POTSI's interleaving rate (I) 0.5, and various percentages of interchanging ranges (R%)

6.7. Conclusion

Compared to the family of optical time slot interchangers noted in the literature, the passive optical time slot interchanger (POTSI), proposed in an earlier work [Maach2004], has the best number of switching operations, crossbar size and total fibre length. In this chapter, we proposed an optimized form of POTSI, Limited-Range POTSI (POTSI-LR), whose capability is limited to switching a time slot to a subset of nearby time slots in the frame instead of all possible time slots. In addition, we investigated the sharing and interleaving of POTSI-LR as opposed to dedicating one POTSI to each ongoing link. Relying on simulation results, we showed that deploying shared limited-range POTSIs can achieve blocking probabilities very close to those of dedicated full-range POTSIs. In fact, the POTSI sharing-percentage can be as small as 20% of the nodal degree together with an interchanging-range as small as 30%. Thus, the overall cost and crossbar complexity can

be substantially reduced while still maintaining close to optimal performance gains. In addition, we showed that POTSIs can be interleaved at a 0.5 rate and still produces a close to optimum performance, even with a sharing percentage and interchange rate of 50%. Finally, we discussed in this chapter the use of POTSIs to build efficient time slot synchronizers between adjacent nodes.

7. Conclusions

7.1. Summary

In Optical TDM (OTDM) networks, transmission between two adjacent nodes must be synchronized to ensure proper data processing and avoid loss. Synchronization in an OTDM network is the process of ensuring that each OTDM switch receives a time sliced traffic segment right at the start of a time slot based on its local clock. If the same time slot (in a TDM frame) must be maintained throughout a communication channel between a source-destination pair, **frame** boundary synchronization is required among all network nodes. On the other hand, **slot** boundary synchronization should be adequate if maintaining the same slot location over a communication channel is not essential. Several papers in the literature assumed frame boundary synchronization, and hence treated a time slot as a small communication channel that is continuous from source to destination. This assumption helped the authors to employ wavelength allocation schemes to solve the slot reservation problem since a communication channel, based on the same time slot across a route, can be seen as a subdivision of a wavelength. On the other hand, if assuming slot boundary synchronization, the wavelength allocation schemes cannot solve the slot reservation question since the time slot continuity is not maintained for a communication channel. Slot reservation schemes that reserve a series of time slot across a given route are required in this case. Some papers considered the First Fit (FF), Random Fit (RF) and Least Loaded (LL) schemes to handle slot reservation in OTDM networks synchronized on slot boundary. None of these schemes, under fixed routing algorithms, comes close to optimum in terms of network performance. The optimum OTDM network performance, under fixed routing algorithms, can be identified by assuming unlimited optical interchanging capacity at each node which allows the interchange from any slot to any other slot. In our thesis, we used the FF scheme with full optical time slot interchangers (OTSI) as an optimal benchmark against which we measured our results. Aiming to avoid

optical buffering or slot interchanging and still maintain close to optimal performance, we proposed the Least Constraining (LC) Slot Allocation scheme as a novel bandwidth reservation method for all-optical TDM networks without buffering. The link-slot constraint is measured by the sum of availabilities of the route-slots on the intersecting routes that can use the link-slot at a given point in time. In addition, the route-slot constraint is equal to the sum of all constituent link-slot constraints. The LC schemes allocate the least constraining route-slot. After several simulation runs based on uniform and non-uniform traffic, backed by an analytical discussion based on uniform traffic only, we proved that the LC schemes provide close to optimum performance in OTDM networks without buffering. The results are consistent under uniform and non-uniform traffic, mesh and ring topology, single and multi-fiber, and fixed and alternate fixed routing.

Aiming to apply the LC approach in GMPLS networks, we designed a distributed LC scheme. We defined the essential nodal database and basic parameters that should be added to the RSVP-TE or CR-LDP signaling messages used in GMPLS networks. In the proposed distributed scheme, resource status update may be immediate or periodic. Immediate updates are broadcasted for each reserved or released resource immediately after the reservation or release operation. On the other hand, periodic updates are exchanged among all nodes in the network at a fixed time interval, reporting status changes in their managed resources since the last status update. The periodic update approach is essential to incorporate the LC resource status update into GMPLS, which relies on global periodic updates using OSPF or IS-IS link state update mechanisms. In this case, the LC approach must maintain its proven performance gain under this limitation. We proved that an update rate greater than or equal to $\frac{1}{\alpha}$ maintains close to optimal performance, where α is the probability that the least-constraining route-slot on a route changes after an accepted call arrival. Reducing the update rate to any value below $\frac{1}{\alpha}$, the network performance degrades to a fixed level but still better than the worst performance of the FF approach. Thus, after an initial period of immediate updates, we can stop all subsequent updates and still get a performance level as good as obtained by update rates lower than $\frac{1}{\alpha}$. On the

other hand, when varying the status update rate in multi-fiber environments, the performance remains stable at the improved level achieved by the immediate update approach. In this case, it is possible to stop resource updates after a brief period of immediate updates and still achieve close to optimal performance. That would substantially save the signaling bandwidth for status updates and the associated processing power, in addition to facilitating the deployment in a GMPLS network.

Interested in investigating the performance of the LC scheme when varying the definition of a resource constraint, we proposed two variations. As a first variation of the LC scheme, we modified the definition of a link-slot constraint to be the number of intersecting route-slots that might use the slot at a given point in time, instead of the sum of availabilities of these route-slots. As a second variation, we changed the link-slot constraint definition to be the sum of intersecting route-slots availabilities divided by the link-slot availability. Both variations slightly enhanced network performance in the multi-fiber case, reaching the optimum performance level of the FF approach with OTSI. However, the performance of all LC variations converged in the single-fiber. The second variation produced the best results in the case of periodic or no status updates as compared to the first variation and the original LC approaches. On the other hand, the performance of the first variation exceeded the worst performance level of the FF approach in the cases of periodic or no status updates. As a conclusion, the second variation outperformed the other variations and should be adopted as the standard LC approach.

Although the LC scheme eliminates the need for Optical Time-Slot Interchangers (OTSI) to improve network performance, we proposed in this thesis an enhancement to the Passive OTSI (POTSI), which was introduced in a separate joint work with Dr. Abdul Maach. Compared to the family of optical time slot interchangers noted in the literature, a POTSI has the best number of switching operations, crossbar size and total fibre length. The enhanced version of POTSI is limited to switching a time slot to a subset of nearby time slots in the frame instead of all possible time slots. We called it Limited-Range POTSI (POTSI-LR). To further optimize the usage of POTSIs in a network, we investigated the sharing and interleaving of POTSI-LR as opposed to dedicating one POTSI to each

ongoing link. The sharing of limited-range POTSIs achieved a network performance close to the case of dedicated full-interchanging-range POTSIs. We proved that a sharing-percentage equal to 20% of the nodal degree and an interchanging-range equal to 30% of the frame size maintained essentially the same performance achieved by dedicated full-interchanging-range POTSIs. This approach reduces the overall cost and crossbar complexity. In addition, we showed that POTSIs can be interleaved at a 0.5 rate and still produces a close to optimum performance, even with a sharing percentage and interchange rate of 50% respectively. Although, OTSIs are not needed with the LC scheme, we still need optical buffering to build synchronizers at the end of each fiber link in order to adjust the propagation delay of the link to a multiple of the slot time. Therefore, we proposed the use of the POTSI architecture as an efficient solution to construct synchronizers between adjacent nodes.

7.2. Overview of Contributions

Over the course of developing our thesis, we made the following contributions:

- **The Least Constraining (LC) slot allocation scheme:** We proposed the LC slot allocation scheme as the main contribution in this thesis. It is designed to provide close to optimal performance in all-optical TDM networks, synchronized on slot boundaries and with no buffering. The optimal performance is measured by the employment of full-range dedicated OTSIs along with the FF allocation scheme. The LC scheme proved its superiority over other optical time-slot allocation schemes in single or multi-fiber environments, fixed or alternative routing schemes, uniform or non-uniform traffic, and mesh or ring topologies [Zeineddine2007].
- **A distributed approach to the LC scheme in GMPLS network:** We proposed a distributed approach to the LC scheme in an attempt to make it deployable in a GMPLS network. Beside defining the nodal database and essential messaging, the main challenge was to reduce the associated link-state signalling overhead. In addition, GMPLS relies on periodic link-state updates. We proved that the distributed LC scheme in a multi-fiber environment does not require any update after an initial period

of immediate updates to maintain close to optimal performance. On the other hand, if stopping the updates in a single-fiber environment, performance degrades to a fixed level but does not converge to the worst performance level reported with the FF approach [Zeineddine2009].

- **Variations of the LC scheme:** We proposed two variations of the original LC scheme aiming to improve performance to a level closer to optimum. The variations are based on modifying the definition of the resource constraint. Both variations showed slight performance improvement over the original LC scheme in a multi-fiber environment and converged to the same performance level in the single fiber case.
- **Limited-Range Passive Optical Time-Slot Interchanger (POTSI-LR):** We proposed an enhancement to the Passive OTSI architecture by reducing the number of the constituent fiber delay lines to a fraction of N, where N is the number of time-slots in a TDM frame. The main goal was to reduce the device size and overall cost and still maintain the same performance achieved by a full range POTSI, which has N fiber delay lines. We showed that an interchange range equal to 30% of N achieves practically the same performance gain as a full interchange range [Zeineddine2006].
- **Shared OTSI:** We proposed a shared OTSI architecture for an optical TDM switch instead of a dedicated OTSI per output line. The aim is to reduce the number of utilized OTSIs per node and still maintain the same performance achieved by the dedicated OTSI architecture. We showed that an OTSI sharing percentage equal to 20 % of the nodal degree is enough to maintain practically the same performance gain as the dedicated OTSI approach [Zeineddine2006].
- **Interleaved OTSI:** We proposed the interleaving of OTSIs among network nodes instead of equipping every node with these devices. The aim is to reduce the number of utilized OTSIs in the global network and still maintain the performance achieved by the regular OTSI approach. We showed that an OTSI interleaving rate of 0.5 yields a performance level close to what is achieved with the case of having OTSIs at every node.
- **Using POTSI as synchronizers:** We proposed the usage of POTSI as an effective solution to the synchronization problem along the link between two adjacent nodes.

Over the years of graduate studies and work toward this thesis, we participated in the following projects:

- **A bandwidth allocation scheme in Optical TDM network:** Dr. Abdul Maach and I proposed a new scheme to share network resources using Time Division Multiplexing (TDM) instead of the statistical multiplexing employed in optical burst switching. To avoid contention and improve bandwidth utilization, we defined a simple reservation scheme that guarantees time slot deliveries as far as the bandwidth is available. In addition, we proposed the POTSI architecture as a simplified form of OTSI. The POTSI was used to solve the contention problem, and improve performance. The proposed scheme can simultaneously serve many classes of traffic by adjusting some bandwidth allocation parameters [Maach2004].
- **Deploying AAPN in legacy networks:** Dr. Sofia Parades and I proposed deployment approaches for the Agile All-Photonic Network (AAPN) project over legacy networks. The legacy systems are assumed to be made of IP routers connected to a network of Reconfigurable Add-Drop Multiplexers (ROADM) and Wavelength Selective Switches (WSS). In our solutions, we proposed the partitioning of the mesh network into intersected rings, each forming an autonomous domain. ROADMs are used to bridge traffic between two intersected rings. Another solution was to use static wavelength allocation to exclusively assign at least one wavelength to each node. The wavelengths assigned to a node are the only communication channels through which it receives traffic from other nodes. The project was under the AAPN umbrella and partially funded by JDSU.

7.3. Future Work

For further expansions of the work described in our thesis, we list the following topics of future work:

- Investigate solutions to employ the LC scheme along with dynamic routing protocols instead of fixed routing. We proved the efficiency of the LC scheme with fixed and

alternative routing schemes; however, we did not consider dynamic routing since the definition of link-slot constraints is based on the assumption of predetermined routes.

- Study the scalability problem of the distributed LC scheme in terms of nodal database size and messaging volume; investigate solutions to reduce the amount of saved and exchanged information. In the thesis, we focused on the signalling problem and paid little attention to the scalability concerns related to the size of the managed and exchanged information.
- Study the technological and economical constraints for the realization of POTSI-LR. Although we proposed the POTSI and POTSI-LR architecture, we did not investigate the technological limits of a feasible POTSI. A PTOSI is made of series of individual fiber delay lines and a switch fabric, patched together via passive couplers. Therefore, a signal passing through a POTSI would loose a fair amount of its signal as it passes from one fiber delay line to another. Some of the important questions are: how can signal amplification help in this case? - And, how many amplifiers do we need and where should they be deployed?

References

[Banerjee2001] A. Banerjee et al, "Generalized Multiprotocol Label Switching: An Overview of Routing and Management Enhancements," IEEE Commun. Mag., vol. 39, no. 1, Jan. 2001.

[Blumenthal1994] D. Blumenthal, P. Prucnal, and J. Sauer, "Photonic packet switches: architectures and experimental implementations," Proc. IEEE, Vol. 82, pp. 1650–1667, November 1994.

[Bochmann2004] G. Bochmann, T. Hall, O. Yang, M. Coates, L. Mason, and R. Vickers, "The Agile All Photonic Network: An Architectural Outile," Queen's Biennial Conference on Communications, February 2004.

[Bononi1999] A. Bononi, Optical Networking (Ref to Synchornizer), Published by Springer, 1999.

[Chen2004] A. Chen, A. Wong, and C. Lea, "Routing and Time-Slot Assignment in Optical TDM Networks," IEEE Journal on Selected Areas in Communications, Vol. 22, No. 9, November 2004.

[Colle2003] D. Colle, J. Cheyns, C. Develder, E. Van Breusegem, A. Ackaert, M. Pickavet, and P. Demeester, "GMPLS extensions for supporting advanced optical networking technologies," 5th International Conference on Transparent Optical Networks, Vol. 1, pp. 170 – 173, June 2003.

[Hafid2005a] A. Hafid and A. Maach, "A Novel Resources Provisioning Scheme in Time Slotted Optical Networks," IEEE International Conference on Communications, 2005, Vol. 3, pp. 1641-1645, May 2005.

[Hafid2005b] A. Hafid, A. Maach, J. Drissi, "DARISON: A Distributed Advance Reservation System for Interconnected Optical Networks," Conference on Optical Network Design and Modeling, pp. 85-92, February 2005.

[Helsinki2004] J. Helsinki, "OSPF and IS-IS Evolution," The Pennsylvania State University CiteSeer Archives, 2004.

[Huang2000] N. Huang, G. Liaw, and C. Wang, "A Novel All-Optical Transport Network with Time-Shared Wavelength Channels," IEEE Journal on Selected Areas in Communications, Vol. 18, No. 10, October 2000.

[Lang2004] J. P. Lang, Y. Rekter, and D. Papadimitriou, "RSVP-TE Extensions in Support of End-to-End Generalized Multiprotocol Label Switching (GMPLS)-Based Recovery," Internet draft, draft-ietf-ccamp-gmpls-recovery-e2e-signaling-02.txt, 2004.

[Liew2003] S. Liew and H. Chao, "On Slotted WDM Switching in Buffereless All-Optical Networks," Proc. IEEE High Performance Interconnects '03, 11th Symposium, pp. 96 -101, August 2003.

[Liu2005a] X. Liu, A. VinoKurov, and L. Mason, "Performance Comparison of OTDM and OBS Scheduling for Agile All-Photonic Network," Proc. IFIP Metropolitan Area Network Conference, Ho Chi Minh City, Vietnam, April 2005.

[Liu2005b] X. Liu, N. Saberi, M. Coates and L. Mason, "A Comparison between Time-slot Scheduling Approaches for All-Photonic Networks," Proc. IEEE ICICS, Bangkok , Thailand , December 2005.

[Maach2004] A. Maach, H. Zeineddine and G. Bochmann, "A bandwidth Allocation Scheme in Optical TDM Network," Proc. IEEE International Conference on High Speed

Networks and Multimedia Communications (HSNMC), Toulouse, Springer LNCS, pp. 801-812, July 2004.

[Mei1997] Y. Mei and C. Qiao, "Efficient Distributed Control Protocols for WDM All-Optical Networks," Proc. 6th International Conference on Computer Communications and Networks, p. 150, 1997.

[Nuzman2006] C. Nuzman and I. Widjaja, "Time-domain Wavelength Interleaved Networking with Wavelength Reuse," Proc. IEEE INFOCOM 2006.

[Pattayina2000] A. Pattavina, M. Martinelli, and G. Maier, "Techniques and Technologies towards All-Optical Switching," Optical Networking Magazine, pp.75-93, Apr. 2000.

[Peng2006] C. Peng, G. Bochmann and T. Hall, "Quick Birkhoff-von Neumann Decomposition Algorithm for Agile All-Photonic Network Cores," IEEE International Conference on Communications, Istanbul Turkey, Vol. 6, pp. 2593-2598, June 2006.

[Qiao1997] C. Qiao and R. Melhem, "Reducing Communication Latency with Path Multiplexing in Optically Interconnected Multiprocessor Systems," IEEE Transactions on Parallel and Distributed Systems, Vol. 8, pp. 97-108, February 1997.

[Qiao1999] C. Qiao and M. Yoo, "Optical burst switching (OBS)–a new paradigm for an optical Internet," Journal of High Speed Networks, Vol. 8, no. 1, pp. 69–84, 1999.

[Ramakrishna2005] Bo Wen, Ramakrishna, and Krishna Sivalingam, "Routing, Wavelength and Time-Slot-Assignment Algorithm for Wavelength-Routed Optical WDM/TDM Networks," Journal of Lightwave Technology, vol. 23, No. 9, September 2005.

[Ramamirtham2003] J. Ramamirtham and J. Turner, "Time Sliced Optical Burst Switching," Proc. IEEE INFOCOM 2003, San Francisco, California, April 2003.

[Ramaswami2002] R. Ramaswami, K.N., Sivarajan, "Optical Networks, A Practical Perspective," 2nd ed. Published by Morgan Kaufmann Publishers, 2002.

[RFC1629] R. Colella et al, Guidelines for OSI NSAP Allocation in the Internet, May 1994.

[RFC2205] E. Braden et al, Resource Reservation Protocol (RSVP), September 1997.

[RFC2328] J. Moy, OSPF Version 2, April 1998.

[RFC3031] E. Rosen et al, Multiprotocol Label Switching Architecture, January 2001.

[RFC3036] L. Anderson et al, LDP Specification, October 2001. (obsoleted by RFC5036, October 2007).

[RFC3209] D. Awduche et al, RSVP-TE: Extensions to RSVP for LSP Tunnels, December 2001.

[RFC3212] B. Jamoussi et al, Constraint-Based LSP Setup using LDP. Network Working Group, January 2002.

[RFC3471] P. Ashwood-Smith et al, "Generalized MPLS — Signaling Functional Description," April 2001.

[RFC3472] P. Ashwood-Smith et al, "Generalized MPLS Signaling—CR-LDP Extensions," Internet draft, draft-ietf-mplsgeneralized-cr-ldp-02.txt, Apr. 2001, work in progress.

[RFC3630] D. Katz et al, Traffic Engineering (TE) Extensions to OSPF Version 2, September 2003.

[RFC3945] E Mannie, Generalized Multi-Protocol Label Switching (GMPLS) Architecture, October 2004.

[RFC4136] P. Pillay-Esnault, OSPF Refresh and Flooding Reduction in Stable Topologies, July 2005.

[RFC4203] K. Kompella et al, "OSPF Extensions in Support of Generalized MPLS," March 2001.

[RFC4205] K. Kompella et al, "IS-IS Extensions in Support of Generalized MPLS," March 2001.

[RFC4974] P. Ashwood-Smith et al, "Generalized MPLS Signaling — RSVP-TE Extensions," April 2001.

[Saberi2004] N. Saberi, and M. Coates "Bandwidth Reservation in Optical WDM/TDM Star Networks," Queens Biennial Symposium on Communications, Kingston, Canada, June 2004.

[Shaikh2001] A. Shaikh, J. Rexford, and K. G. Shin, "Evaluating the impact of stale link state on quality-of-service routing," IEEE/ACM Transactions on Networking, Vol. 9, pp. 162–176, April 2001.

[Shen2004] S. Shen, G. Xiao, and T. H. Cheng, "Evaluating the impact of the link-state update period on the blocking performance of wavelength-routed networks," Proc. Optical Fiber Communication Conference (OFC), February 2004.

[Shen2006] S. Shen, G. Xiao, and T. Cheng, "The Performance of Periodic Link-State Update in Wavelength-Routed Networks," 3rd International Conference on Broadband Communications, Networks and Systems, San Jose, CA, pp. 1-10, October 2006.

[Siew2006] C. Siew, D. Xue, Y. Qin, and J. Schmitt "Providing Deterministic Quality of Service in Slotted Optical Networks," Optics Express, Vol. 14, Issue 26, pp. 12679-12692, December 2006.

[Srinivasan2002] R. Srinivasan, A. Somani, "A Generalized Framework for Analyzing Time-Space Switched Optical Networks," IEEE Journal on Selected Areas in Communications, Vol. 20, No. 1, January 2002.

[Subramaniam2000] S. Subramaniam, J. Harder, and H. Choi, "Scheduling Multirate Sessions in Time Division Multiplexed Wavelength-Routing Networks," IEEE Journal on Selected Areas in Communications, Vol. 18, No. 10, October 2000.

[Sukhni2008] E. Sukhni, and Hussein T. Mouftah: Parallel Fixed-Alternative-Routing Based Provisioning Framework for Distributed Controlled Survivable WDM Mesh Networks. 6th Annual Communication Networks and Services Research Conference (CNSR), Halifax, Canada, pp. 287-294, May 2008.

[Turner1999] J. Turner, "Terabit Burst Switching," Journal of High Speed Networks, Vol. 8, pp 3-16, March 1999.

[Vinokurov2005] A. Vinokurov, X. Liu, and L. Mason, "Resource sharing for QoS in Agile All Photonic Networks", OPNETWORK 2005, Washington D.C., August 2005.

[Vokkarane2003] V. Vokkarane and J. Jue, "Segmentation-based non-preemptive scheduling algorithms for optical burstswitched networks," Proc. First International Workshop on Optical Burst Switching (WOBS), October 2003.

[Wang2006] Z. Wang, N. Chi, and S. Yu, "Time-Slot Assignment Using Optical Buffer With a Large Variable Delay Range Based on AVC Crosspoint Switch," J. Lightwave Technol. 24, 2994- (2006).

[Widjaja2004] I. Widjaja and I. Saniee, "Simplified Layering and Flexible Bandwidth with TWIN," Proc. SIGCOMM FDNA Workshop, Portland August 2004

[Yang2007a] W. Yang, S. Paredes, T. Hall, "A Study of the Impact of Stale Information on the Blocking Performance of Dynamic Routing, Wavelength and Timeslot Assignment Scheme for Bandwidth on Demand in Metro Agile All-Optical Networks," Photonics North 2007, Ottawa, Canada, June 2007.

[Yang2007b] W. Yang, S. Paredes, T. Hall, "A Study of Fast Flexible Bandwidth Assignment Methods and their Blocking Probabilities for Metro Agile All-optical Ring Networks," IEEE International Conference on Communications (ICC-2007), Glasgow, Scotland, 24-28 June 2007.

[Yao2000] S. Yao, B. Mukherjee, S. Yoo, and S. Dixit, "All-Optical Packet-Switched Networks: A Study of Contention Resolution Schemes in an Irregular Mesh Network with Variable-Sized Packets," Proceedings of SPIE OptiComm 2000.

[Yates1999] J. M. Yates, J. Lacey, and D. Everitt, "Blocking in multiwavelength TDM networks," Telecommunication Systems Journal, vol. 12, no. 1, pp. 1-19, August 1999.

[Yuan1996] X. Yuan, R. Gupta, and R. Melhem, "Distributed Control in Optical WDM Networks," IEEE Conf. on Military Communications, McLean, VA , October 1996.

[Yuan1997] X. Yuan, R. Gupta, and R. Melhem, "Distributed Path Reservation Algorithms for Multiplexed All-Optical Interconnection Networks," International Symposium on High Performance Computer Architecture - HPCA-3, 1997.

[Zang1999] H. Zang, J. Jue, and B. Mukherjee, "Photonic Slot Routing in All-Optical WDM Mesh Networks," Proc. IEEE Globecom '99, Rio de Janeiro, Brazil, December 1999.

[Zang2000] H. Zang, J. Jue, and B. Mukherjee, "Capacity Allocation and Contention Resolution in a Photonic Slot Routing All-optical WDM Mesh Network," Journal of Lightwave Technology, Vol. 18, No. 12, December 2000.

[Zeineddine1998] H. Zeineddine, A. Jakel, S. Bandyopadhayay, A. Sengupta "Efficacy of Wavelength Translation in all-Optical Networks," Proc. International Conference on Computing and Information (ICCI), pp. 43-50, June 1998.

[Zeineddine2006] H. Zeineddine, P. He, and G. Bochmann, "Optimization Analysis of Optical Time Slot Interchanges in All-Optical Network," Proc. IASTED Wireless and Optical Communications, Banf Alberta, pp. 207-212, July 2006.

[Zeineddine2007] H. Zeineddine and G. Bochmann, "Least Constrained Slot Allocation in Optical TDM Networks," Proc. asdxczIEEE International Conference on Wireless and Optical Communications Networks, Singapore, pp. 1 – 5, July 2007.

[Zeineddine2009] H. Zeineddine and G. Bochmann, "A Distributed Algorithm for the Least Constraining Slot Allocation in MPLS Optical Networks," IEEE International Conference on Communications, Dresden, Germany, June 2009.